EUROPEAN ORGANISATION FOR NUCLEAR RESEARCH (CERN)

Submitted to: EPJC

CERN-EP-2025-283
23rd December 2025

Measurement of inclusive dijet cross-sections in proton–proton collisions at $\sqrt{s}$ = 13 TeV with the ATLAS detector

The ATLAS Collaboration

Inclusive dijet cross-sections have been measured in proton–proton collisions at a centre-of-mass energy of 13 TeV using data with an integrated luminosity of 140 fb^{-1}, recorded by the ATLAS detector at the Large Hadron Collider during 2015–2018. Jets are identified using the anti-k_t algorithm with a radius parameter of $R = 0.4$. The inclusive dijet double-differential cross-sections are measured first as a function of the invariant dijet mass and the half absolute rapidity separation between the two leading jets, (m_{jj}, y^*), and second as a function of the invariant dijet mass and the total longitudinal boost of the dijet system, (m_{jj}, y_{boost}). The measured dijet system covers the invariant mass range from 240 GeV to almost 10 TeV, with dijet separation $y^* < 3.0$ and dijet boost $y_{\mathrm{boost}} < 3.0$. The results are unfolded to the particle level and compared with state-of-the-art next-to-next-to-leading-order full colour perturbative QCD calculations, corrected for non-perturbative and electroweak effects.

Contents

1 Introduction

Dijet cross-section measurements provide a fundamental test of Quantum Chromodynamics (QCD), in particular its perturbative regime (pQCD), by probing the dynamics of hard parton–parton scattering. Using data collected with the ATLAS detector [1] at the Large Hadron Collider (LHC) [2] at a centre-of-mass energy of 13 TeV, a measurement of the inclusive dijet double-differential cross-section is presented as a function of key kinematic observables. This analysis offers detailed insights into parton distribution functions (PDFs) and higher-order QCD effects, providing robust constraints on theoretical predictions.

In this context, the dijet final state provides a particularly suitable environment, benefiting from the copious production of jets in hadron-induced processes over a broad phase space. Several measurements were already performed at the LHC: by CMS at centre-of-mass energies of 7, 8, and 13 TeV [3–5] and by ATLAS at 7 and 13 TeV [6, 7]. The most recent 13 TeV ATLAS (CMS) measurements were based on partial LHC Run-2 data samples corresponding to 3.2 fb^{-1} (36.3 fb^{-1}).

In this article, measurements of the dijet cross-section in proton–proton (pp) collisions at $\sqrt{s} = 13$ TeV using anti-k_t [8] jets with a radius parameter $R = 0.4$ are presented. The double-differential cross-sections are measured as functions of the invariant dijet mass, m_{jj}, and one of two angular variables, y^* or y_{boost}, defined as

$$m_{\text{jj}} = \sqrt{(p_1 + p_2)^2}, \quad y^* = \frac{1}{2}|y_1 - y_2|, \quad y_{\text{boost}} = \frac{1}{2}|y_1 + y_2|,$$

using the jet four-momenta, p_1, p_2, and the rapidities, y_1, y_2, of the p_{T}-ordered leading and subleading jets. The invariant mass m_{jj} provides a direct handle on the energy scale of the hard interaction, while the angular variables offer insight into the dynamics of the dijet system.

The variable y^* is directly related to the scattering angle θ^* in the partonic centre-of-mass frame through $\tanh(y^*) = \cos(\theta^*)$, and the commonly used dijet angular variable χ defined as $\chi = e^{2y^*} = \frac{1+\cos(\theta^*)}{1-\cos(\theta^*)}$. The variable y_{boost} characterises the overall rapidity of the dijet system in the laboratory frame. Both angular variables are directly related to the longitudinal momentum fractions of the incoming partons $x_{1,2} = \frac{m_{\text{jj}}}{\sqrt{s}} e^{\pm y_{\text{boost}}}$ with $m_{\text{jj}} = 2p_{\text{T,avg}} \cosh(y^*)$, where the formulas are derived for back-to-back jets at the Born level. The positive (negative) sign corresponds to the leading (subleading) parton, and $p_{\text{T,avg}}$ denotes their average transverse momentum. Small y_{boost} values correspond to $x_1 \approx x_2$, whereas large y_{boost} selects strongly asymmetric momentum fractions. All three variables, m_{jj}, y^*, and y_{boost} provide sensitivity to the parton momentum fractions $x_{1,2}$ and, consequently, to the PDFs [9].

This measurement builds on previous dijet cross-section results by using a significantly larger data sample collected by ATLAS with an integrated luminosity of 140 fb^{-1}. The y_{boost} variable is used for the first time in the dijet cross-section measurement by ATLAS. The increased data sample enhances statistical precision, particularly in high-mass and forward regions where earlier measurements were limited by the sample size. Additionally, an improved jet energy calibration is implemented, incorporating updated systematic uncertainties [10, 11]. These updates reduce the experimental uncertainties in the jet energy scale by a factor of two to three for m_{jj} above a few hundred GeV, enabling more precise constraints on theoretical predictions. The phase space of the measurement extends from $m_{\text{jj}} = 240$ GeV to 10 TeV, covering a wide kinematic range where the two highest-p_{T} jets are required to be within $|y| < 3.0$. This broad coverage allows stringent tests of pQCD across a wide range of the relevant hard-scattering scale, including regions where higher-order effects and the running of the strong coupling become increasingly significant.

To fully exploit these improvements, the results of this measurement are compared with state-of-the-art theoretical predictions, including next-to-next-to-leading-order (NNLO) QCD calculations with full colour for jet production [12] and the most recent PDFs [13–17]. These comparisons highlight the sensitivity to NNLO pQCD corrections, particularly in kinematic regions where higher-order corrections could become increasingly relevant.

Recently, α_s was extracted from dijet cross-section measurements [18], using the invariant dijet mass as the characteristic energy scale. This approach extends renormalisation group evolution (RGE) studies up to scales of approximately 7 TeV, probing the running of α_s at an unprecedented energy. The present measurement, with its extended m_{jj} range and reduced experimental uncertainties, provides an opportunity to further test the validity of this scale choice and its implications for high-energy QCD dynamics.

After the introduction and a brief description of the ATLAS detector in Section 2, the definition of the cross-sections is given in Section 3. Data and Monte Carlo (MC) samples, event selection, trigger strategy, and jet calibration are described in Section 4. The unfolding procedure is explained in Section 5. In Section 6, sources of experimental uncertainties are presented. Section 7 describes the details and settings of the calculation of the pQCD prediction, the non-perturbative corrections and electroweak corrections. In Section 8, the final results and theory are compared and interpreted using statistical χ^2 tests.

2 ATLAS detector

The ATLAS detector [1] at the LHC covers nearly the entire solid angle around the collision point.[1] It consists of an inner tracking detector surrounded by a thin superconducting solenoid, electromagnetic and hadronic calorimeters, and a muon spectrometer incorporating three large superconducting air-core toroidal magnets.

The inner-detector system (ID) is immersed in a 2 T axial magnetic field and provides charged-particle tracking in the range $|\eta| < 2.5$. The high-granularity silicon pixel detector covers the vertex region and typically provides four measurements per track, the first hit generally being in the insertable B-layer (IBL) installed before Run 2 [19, 20]. It is followed by the SemiConductor Tracker (SCT), which usually provides eight measurements per track. These silicon detectors are complemented by the transition radiation tracker (TRT), which enables radially extended track reconstruction up to $|\eta| = 2.0$. The TRT also provides electron identification information based on the fraction of hits (typically 30 in total) above a higher energy-deposit threshold corresponding to transition radiation.

The calorimeter system covers the pseudorapidity range $|\eta| < 4.9$. Within the region $|\eta| < 3.2$, electromagnetic calorimetry is provided by barrel and endcap high-granularity lead/liquid-argon (LAr) calorimeters, with an additional thin LAr presampler covering $|\eta| < 1.8$ to correct for energy loss in material upstream of the calorimeters. Hadronic calorimetry is provided by the steel/scintillator-tile calorimeter, segmented into three barrel structures within $|\eta| < 1.7$, and two copper/LAr hadronic endcap calorimeters. The solid angle coverage is completed by forward copper/LAr and tungsten/LAr calorimeter modules optimised for electromagnetic and hadronic energy measurements, respectively.

[1] ATLAS uses a right-handed coordinate system with its origin at the nominal interaction point (IP) in the centre of the detector and the z-axis along the beam pipe. The x-axis points from the IP to the centre of the LHC ring, and the y-axis points upwards. Polar coordinates (r, ϕ) are used in the transverse plane, ϕ being the azimuthal angle around the z-axis. The pseudorapidity is defined in terms of the polar angle θ as $\eta = -\ln\tan(\theta/2)$ and is equal to the rapidity $y = \frac{1}{2}\ln\left(\frac{E+p_z}{E-p_z}\right)$ in the relativistic limit. Angular distance is measured in units of $\Delta R \equiv \sqrt{(\Delta y)^2 + (\Delta\phi)^2}$.

The muon spectrometer (MS) comprises separate trigger and high-precision tracking chambers measuring the deflection of muons in a magnetic field generated by the superconducting air-core toroidal magnets. The field integral of the toroids ranges between 2.0 and 6.0 T m across most of the detector. Three layers of precision chambers, each consisting of layers of monitored drift tubes, cover the region $|\eta| < 2.7$, complemented by cathode-strip chambers in the forward region, where the background is highest. The muon trigger system covers the range $|\eta| < 2.4$ with resistive-plate chambers in the barrel, and thin-gap chambers in the endcap regions.

The luminosity is measured mainly by the LUCID–2 [21] detector that records Cherenkov light produced in the quartz windows of photomultipliers located close to the beampipe.

Events were selected by the first-level trigger system implemented in custom hardware, followed by selections made by algorithms implemented in software in the high-level trigger [22]. The first-level trigger accepted events from the 40 MHz bunch crossings at a rate close to 100 kHz, which the high-level trigger further reduced in order to record complete events to disk at about 1.25 kHz.

A software suite [23] is used in data simulation, in the reconstruction and analysis of real and simulated data, in detector operations, and in the trigger and data acquisition systems of the experiment.

3 Dijet cross-section definition

The measured cross-section is corrected to particle level using simulated samples with jets constructed directly from generated stable particles with lifetimes satisfying $c\tau > 10$ mm, excluding muons and neutrinos. The jets are clustered using the collinear and infrared-safe anti-k_t algorithm [8] with a radius parameter of $R = 0.4$, as implemented in the FastJet [24] package.

The event selection requires at least two jets with transverse momentum $p_{\mathrm{T}} > 75$ GeV and rapidity $|y| < 3.0$. Additionally, the scalar sum of the two leading jet p_{T}, $H_{\mathrm{T},2} = p_{\mathrm{T},1} + p_{\mathrm{T},2}$, is required to be above 200 GeV, ensuring the stability of the pQCD calculations [25, 26].

The inclusive dijet double-differential cross-section is calculated for (m_{jj}, y^*) and (m_{jj}, y_{boost}) at the particle level as a ratio of dijet event yields N^{part} to the integrated luminosity $\mathcal{L}_{\mathrm{int}}$ and the bin widths of Δm_{jj}, and Δy^* or $\Delta y_{\mathrm{boost}}$, respectively,

$$\frac{\mathrm{d}^2\sigma}{\mathrm{d}m_{\mathrm{jj}}\mathrm{d}y^*} = \frac{1}{\mathcal{L}_{\mathrm{int}}}\frac{N^{\mathrm{part}}}{\Delta m_{\mathrm{jj}}\Delta y^*},$$

$$\frac{\mathrm{d}^2\sigma}{\mathrm{d}m_{\mathrm{jj}}\mathrm{d}y_{\mathrm{boost}}} = \frac{1}{\mathcal{L}_{\mathrm{int}}}\frac{N^{\mathrm{part}}}{\Delta m_{\mathrm{jj}}\Delta y_{\mathrm{boost}}}.$$

The dijet event topologies in corresponding analysis bins of y^* and y_{boost} are illustrated in Figure 1. The y^* and y_{boost} equidistant binning from 0.0 to 3.0 and the 0.5 bin width are chosen for two reasons: first, to ensure consistency with the previous ATLAS dijet cross-section measurement [7] performed in y^* bins; and second, to satisfy the kinematic constraints between y^* and y_{boost} variables.

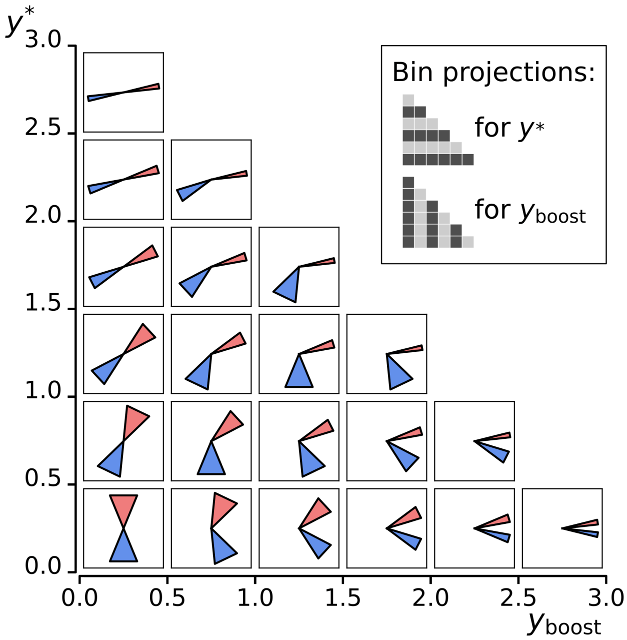

Figure 1: An illustration of the dijet event topology in the laboratory frame as a function of the $y^* = |y_1 - y_2|/2$ and $y_{\text{boost}} = |y_1 + y_2|/2$ observables, with y_1 and y_2 being the rapidities of the leading and subleading jets. Projections of individual rows (columns) to the y^* (y_{boost}) axis correspond to the bin configurations of the measurement. In each subfigure, the horizontal axis corresponds to the beam direction, while the vertical axis represents the x–y plane.

The invariant dijet mass binning of m_{jj} is optimised to obtain a uniform purity[2] of 50% and a corresponding stability[3] above 50% derived from MC simulations. Additionally, the m_{jj} binning guarantees at least 10 events in the reconstructed ATLAS data and maintains reasonable statistical uncertainty in ATLAS MC simulations.

4 Data, simulation, and event selection

This measurement uses the complete LHC Run-2 data sample collected between 2015 and 2018, satisfying the ATLAS data quality requirements, ensuring that all relevant detector subsystems were fully operational [27]. The integrated luminosity reached 140 fb^{-1} with a corresponding uncertainty of 0.83% [28], determined with the van der Meer beam separation scan method using the LUCID-2 sub-detector [21] and a set of complementary measurements using the inner detector and the calorimeter.

The data events are selected with a set of single-jet triggers [29–31] with p_{T} thresholds ranging from 60 GeV to 420 GeV and a detector acceptance of $|\eta| < 3.2$. The lower threshold single-jet triggers are prescaled to reduce high trigger rates and record only a fraction of events for online processing and data storage at an acceptable level. Only the highest p_{T} threshold single-jet triggers are unprescaled to record

[2] Purity represents the conditional probability of observing a particle-level dijet (T) for a given reconstructed-level dijet (R) entering the response matrix, expressed as $P(T|R) = P(T \cap R)/P(R)$.

[3] Stability represents the conditional probability of observing a reconstructed-level dijet (R) from a given particle-level dijet (T) entering the response matrix, expressed as $P(R|T) = P(T \cap R)/P(T)$.

each observed event with high-p_T jets. A leading-jet trigger strategy [32] is employed, where the trigger is accepted only if the leading jet fell within a predefined p_T range, achieving an efficiency of 99.5%. To obtain a smooth m_{jj} spectrum at the reconstructed level, events are weighted according to the trigger prescale.

The event reconstruction includes particle flow jets [33], which combine topological clusters [34] in the calorimeter system with tracks from the inner detector to improve the jet energy resolution and the reconstruction efficiency at low p_T. The jet energy calibration begins by mitigating pile-up effects through a data-driven event-by-event pile-up p_T-density and jet–area subtraction, followed by residual pile-up MC-based corrections for the dependence on the number of interactions per bunch crossing and the number of primary vertices. An absolute MC-based calibration is then applied to restore the jet four-momentum to the particle level in bins of η and p_T. The global sequential calibration is subsequently applied to reduce flavour- and topology-dependence. Finally, residual data-to-MC differences are corrected using in-situ techniques in γ+jet, Z+jet, dijet, and multijet events. The resulting jet energy scale reaches per-cent precision for central jets with $p_T > 100$ GeV, with uncertainties reduced by a factor of two to three compared with early Run 2 [10, 11].

The simulated events are generated using Pythia 8.230 [35] with leading-order (LO) matrix elements for $2 \to 2$ dijet production, including the default Pythia Lund string hadronisation model [36, 37], transverse momentum ordering [38] parton showers, and the A14 [39] set of tuned parameters. The renormalisation and factorisation scales are set to the geometric mean of the squared transverse masses of the two outgoing particles, $m_{T,1}, m_{T,2}$, in the matrix element, $\sqrt{m_{T,1}^2 \cdot m_{T,2}^2} = \sqrt{(p_{T,1}^2 + m_1^2)(p_{T,2}^2 + m_2^2)}$. The NNPDF2.3lo PDF set [40] is used in the matrix element generation, the parton shower, and in the simulation of the multi-parton interactions. For the modelling of heavy hadron decays, EvtGen [41] is used.

The simulated events are propagated through the full detector simulation [42] of the ATLAS detector using Geant4 [43] and overlaid with inelastic minimum-bias interactions generated using Pythia 8.1 [44] to simulate pile-up interactions. The simulated events are re-weighted according to the normalised distribution of an actual number of pile-up interactions to match the measured data precisely. The simulated particles are reconstructed with the same software [23] as the ATLAS data.

The jet cleaning requirements are applied to both data and simulated events [45], which suppress background from coherent noise, pathological calorimeter cells, and beam-induced effects. Additionally, events must contain at least one well-reconstructed primary vertex built from at least two associated inner detector tracks with $p_T > 500$ MeV.

5 Unfolding of detector effects

To obtain the final dijet cross-sections at particle level, the reconstructed data distributions are corrected for detector inefficiencies and resolution effects using a modified Bayesian technique, the iterative, dynamically stabilised (IDS) method of data unfolding [46].

Migrations of dijet events across analysis bins between the particle and reconstructed levels are described with a response matrix built using MC-simulated dijet events.[4] The particle-level and reconstructed-level jets are geometrically matched according to their angular distance. Two jets are considered to be matched

[4] Migrations in both (m_{jj}, y^*) are simultaneously accounted for in the unfolding, as the response matrix is constructed to include all m_{jj} bins across the six y^* intervals. The same approach is applied for (m_{jj}, y_{boost}).

if they are closer to each other than to any other jet and lie within a radius of $\Delta R = 0.3$. The leading and subleading reconstructed jets must be matched to the leading and subleading particle jets.[5] The response matrix is filled with dijet masses calculated using particle-level and reconstructed-level dijet events that simultaneously satisfy the analysis selection criteria described in Section 4 and that are geometrically matched between the two levels. Events passing the selection on the reconstructed (particle) level that either fail to satisfy the selection on the particle (reconstructed) level or do not pass the matching procedure are used for impurity (inefficiency) corrections during the unfolding.

Reconstructed data are unfolded to the particle level using a three-step procedure, which corrects for the matching impurity at the reconstructed level, migrations of dijet events between analysis bins, and matching inefficiency at the particle level. The number of dijet events, N_i^{part}, at the particle level in bin i is calculated from the number of events, N_k^{reco}, at the reconstructed level in bin k, according to

$$N_i^{\text{part}} = \sum_k N_k^{\text{reco}} \cdot \mathcal{P}_k \cdot \mathcal{U}_{ik} / \mathcal{E}_i,$$

where $\mathcal{P}_k$ and $\mathcal{E}_i$ denote matching purity and matching efficiency, respectively, in corresponding bins. The matching purity, $\mathcal{P}_k$, is defined using the previously described matching procedure as the fraction of reconstructed-level dijet events matched to corresponding particle-level events in the reconstructed bin k. Similarly, the matching efficiency, $\mathcal{E}_i$, is defined as a fraction of particle-level dijet events matched to corresponding reconstructed-level events in the particle bin i. Elements of the unfolding matrix, $\mathcal{U}_{ik}$, are calculated from the response matrix and describe the probability of a dijet event reconstructed in a bin k to originate from a particle-level bin i.

The particle-level MC-simulated spectrum and, therefore, the unfolding matrix, $\mathcal{U}$, are iteratively improved in the IDS unfolding method. The residual shape uncertainty of the unfolded spectrum is evaluated using a data-driven closure test [46]. The particle-level MC-simulated spectrum is reweighted so that the agreement at the reconstructed level between the data and MC simulation is improved. The relative difference between the reweighted reconstructed-level MC spectrum unfolded by the nominal response matrix and the reweighted particle-level MC spectrum is interpreted as a bias of the unfolding procedure. The number of iterations of the IDS method is chosen such that the residual bias in each analysis bin is smaller than the respective statistical uncertainty, considering both data and MC contributions. One iteration is chosen for y^*-binned cross-section and two iterations are chosen in the case of y_{boost}.

6 Experimental uncertainties

The total experimental uncertainty in the cross-sections, combining effects of statistical fluctuations of data and MC simulation and various sources of systematic uncertainties, is shown in Figure 2.

The statistical uncertainty in the measurement consists of data and MC simulation contributions, which are propagated through the unfolding procedure using a set of 1000 pseudo experiments. Each pseudo experiment is created by fluctuating weights of the dijet events according to a Poisson distribution with a mean equal to one, producing varied data spectra and MC-simulated response matrices. The data contribution to the total statistical uncertainty is evaluated by unfolding the fluctuated data spectra using the nominal response matrix, whereas the MC contribution is propagated by unfolding the nominal data

[5] The order of the two jets can be swapped between the reconstructed and particle levels due to the resolution effects, allowing for leading-to-subleading and subleading-to-leading matches.

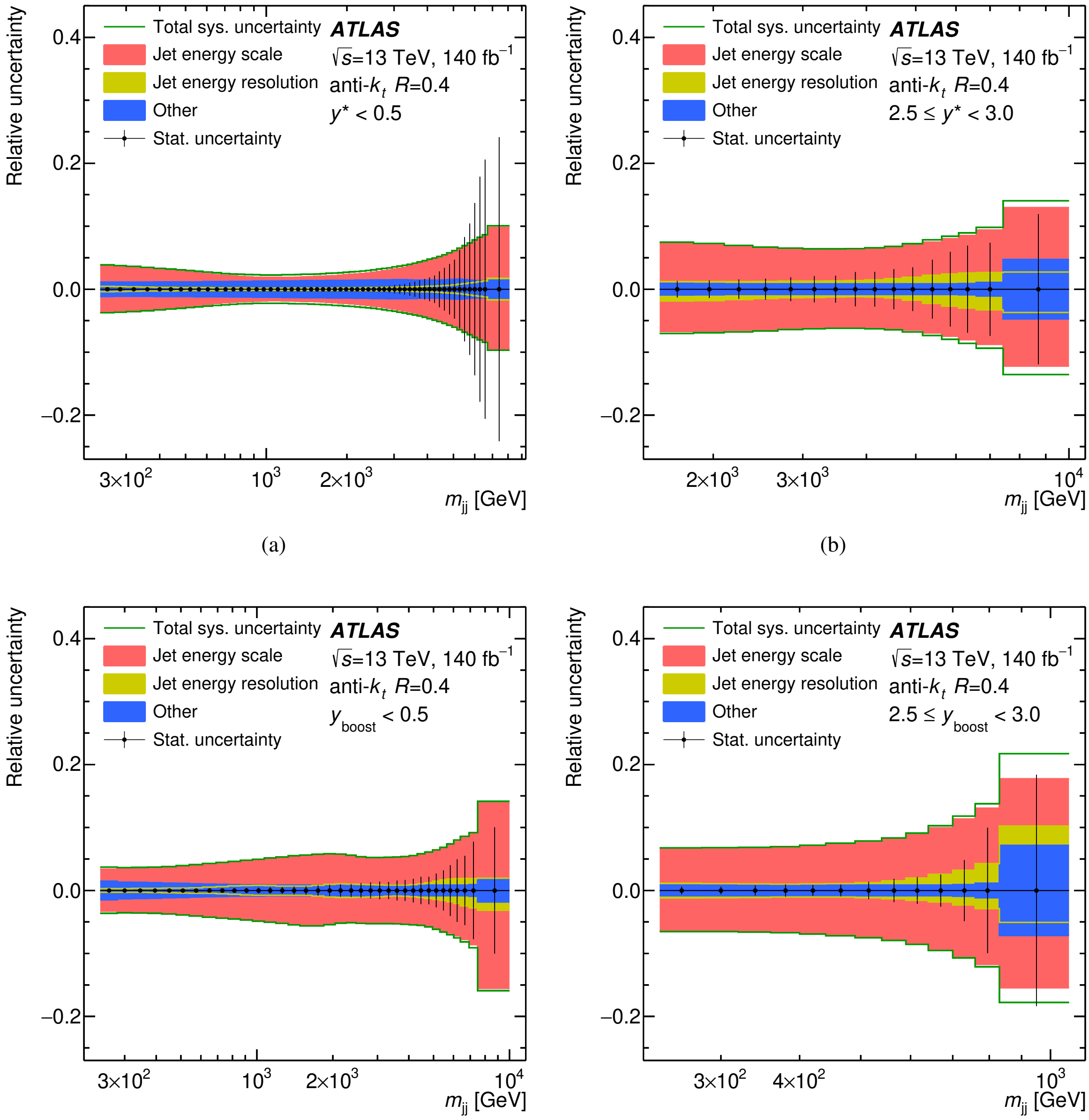

Figure 2: Relative systematic uncertainty in the dijet cross-section as a function of m_{jj} in the first and last y^* (a, b) and y_{boost} (c, d) analysis bins. The components of the uncertainty are displayed as colour bands—Jet energy scale, Jet energy resolution, and Other (combining the residual unfolding bias, the effect of disabled Tile calorimeter modules, and the luminosity uncertainty). The total systematic uncertainty is obtained as a quadrature sum of the components and is compared with the statistical component.

spectrum using the fluctuated response matrices. The corresponding statistical uncertainties are calculated as the root mean square error from the resulting distributions. Bootstrap replicas are also used to produce a covariance matrix describing correlations between the analysis bins.

The total statistical uncertainty of the measurement is calculated as a quadrature sum of the data and MC contributions. In the first y^* analysis bin, the uncertainty is about 0.1% at lower m_{jj} values and increases up to 24% at higher m_{jj}. In the last y^* bin, the uncertainty is about 1% at lower m_{jj} values and increases up to 12% at higher m_{jj}. Similarly, in the first y_{boost} bin, the uncertainty is about 0.2% at lower m_{jj} values and increases up to 10% at higher m_{jj}. In the last y_{boost} bin, the uncertainty is about 0.5% at lower m_{jj} values and increases up to 18% at higher m_{jj}.

The jet energy scale (JES) uncertainty is the dominant systematic uncertainty of this measurement. It is evaluated using various simulation-based techniques and in-situ measurements described in Refs. [10, 11]. The full JES uncertainty set of 1172 individual components, including the latest improvements[6] discussed in Ref. [11], is used. All components of the JES uncertainty are propagated through the unfolding procedure using an MC simulation. Each reconstructed jet p_{T} is scaled up and down by one standard deviation of a given component. The m_{jj} spectra produced using the varied jets are unfolded with the nominal response matrix. The relative difference to the nominal unfolded MC spectrum is taken as a corresponding systematic uncertainty, which is applied to the unfolded data.

At higher m_{jj} values, the η intercalibration method uncertainty (described in Ref. [10]) is the dominant JES uncertainty component in all y_{boost} and high-y^* bins. In low-y^* bins, the uncertainty in the energy response to isolated hadrons (described in Refs. [11, 47]) is the most significant component. At lower m_{jj} values, the pile-up uncertainty is the dominant component in low-y^* and low-y_{boost} bins, being overtaken by the η intercalibration method uncertainty for higher y^* and y_{boost} values.

The jet energy resolution (JER) is measured using various techniques described in Ref. [10]. The JER systematic uncertainty is split into 34 individual components. Each component is propagated through the unfolding procedure using an MC simulation by smearing the jet p_{T} according to a Gaussian function with a width σ_{smear},

$$\sigma_{\mathrm{smear}}^2 = (\sigma_{\mathrm{nom}} + |\sigma_{\mathrm{NP}}|)^2 - \sigma_{\mathrm{nom}}^2,$$

where σ_{nom} is the nominal resolution in the MC sample and σ_{NP} is a one-standard-deviation variation of a given uncertainty component [10]. Components of the JER uncertainty can involve JER improvement in part of the phase space, but JER degradation in another, relative to the nominal resolution σ_{nom}. To preserve anti-correlations in such cases, the JER improvement and degradation are treated differently. The effect of JER degradation is propagated by smearing the p_{T} of MC-simulated jets filled into the reconstructed spectrum. In contrast, the effective JER improvement is realised by smearing the p_{T} of MC jets used for the response matrix construction. The relative difference between the varied reconstructed spectrum unfolded by the varied response matrix and the nominal reconstructed spectrum unfolded by the nominal response matrix is taken as the corresponding systematic uncertainty.

The relative residual unfolding bias described in Section 5 is applied to the unfolded data as a source of systematic uncertainty. It stays mostly below one per mil and reaches up to a few per cent for large values of m_{jj}.

The effect of certain Tile calorimeter modules being disabled due to technical problems during the Run 2 data taking [48] is evaluated by comparing the nominal cross-section and one produced while removing

[6] Jet energy scale uncertainty improvements come mainly from reduced jet flavour response and single-particle deconvolution uncertainties [11].

dijet events with jets pointing to the disabled modules in both the data and MC simulations. The difference, reaching up to approximately one per cent in some m_{jj} bins, is taken as a systematic uncertainty.

The relative luminosity uncertainty of 0.83% [28] is applied across all m_{jj} bins.

No additional sources of the experimental systematic uncertainty are considered. For particle flow jets, the effect of the jet angular resolution is negligible relative to the other sources of the uncertainty. There is no uncertainty associated with the jet quality selection.

To mitigate the effects of statistical fluctuations of the systematic uncertainty estimates, a smoothing procedure is applied to the JES and JER components, the effect of disabled Tile modules, and to the unfolding bias. First, statistical uncertainties in the uncertainty components are estimated by using pseudo experiments (100 for each component). Second, neighbouring m_{jj} bins are combined until the statistical significance in each bin is larger than two standard deviations. Last, a Gaussian kernel smoothing [49] is applied, restoring the original, fine binning.

The total systematic uncertainty on the dijet cross-section measurement is calculated as a quadrature sum of the components. In the first y^* analysis bin, the uncertainty is about 2% at medium m_{jj}, increasing to 4% at low m_{jj} and up to 10% at high m_{jj}. In the last y^* bin, the uncertainty is higher: about 6% at medium m_{jj}, increasing to 7% at low m_{jj} and up to 14% at high m_{jj}. Similarly, in the first y_{boost} bin, the uncertainty is below 4% at low m_{jj} and rises to 16% at high m_{jj}. In the last y_{boost} bin, it increases from below 7% at low m_{jj} to 22% at high m_{jj}.

7 Theoretical prediction

Theoretical predictions of the dijet cross-sections are obtained using pQCD, supplemented by corrections for non-perturbative and electroweak effects. While the previous ATLAS dijet publication [7] relied on next-to-leading-order (NLO) leading colour pQCD predictions from NLOJET++ [50, 51], the theoretical precision is now improved by employing NNLO predictions with full colour information, obtained using NNLOJET [12, 52–54] interfaced to PINEAPPL [55] and APPLGRID [56] for fast convolutions with varied input parameters (PDFs, renormalisation and factorisation scales and the strong coupling constant). The predictions are calculated using several recent PDF sets provided by the LHAPDF6 [57] library: CT18 [13], MSHT2020 [14], NNPDF3.1 [15], NNPDF4.0 [16] and ATLASPDF21 [17]. The corresponding NNLO sets are used with the value of the strong coupling constant taken from the corresponding PDF set. The applied renormalisation and factorisation scale of dijet invariant mass, $\mu_R = \mu_F = m_{jj}$, is the one proposed in Ref. [53].

The uncertainties in the theoretical predictions come from the uncertainties on the PDFs, the renormalisation and factorisation scales, and the uncertainty in the value of the strong coupling constant. The PDF uncertainties are defined at 68% confidence level (CL) and propagated through the calculation following the recommendation of each PDF set. The scale uncertainty is estimated as the envelope obtained by varying the renormalisation and factorisation scales up and down by a factor of 2 from the nominal values, excluding the opposite variations in the two scales. The uncertainty in the value of the strong coupling constant is estimated by varying its value by 0.001 from the nominal value $\alpha_s(m_Z) = 0.118$ in the matrix element and applying the corresponding shifted PDF sets.

The representative uncertainties in the theoretical predictions from the NNLO calculation using the CT18NNLO (NNPDF4.0) PDF sets are shown in Figure 3 (Figure 4). At the highest m_{jj}, CT18NNLO has

PDF uncertainties of up to 15–22%, whereas NNPDF4.0 reaches about 2% (except in the highest m_{jj} region of the highest y_{boost} bin, where it can reach about 6%), consistent with the 1–2% precision[7] quoted by the NNPDF Collaboration [16]. For NNPDF4.0, the PDF uncertainty is comparable to the α_s and statistical components, while the scale uncertainty becomes the dominant contribution.

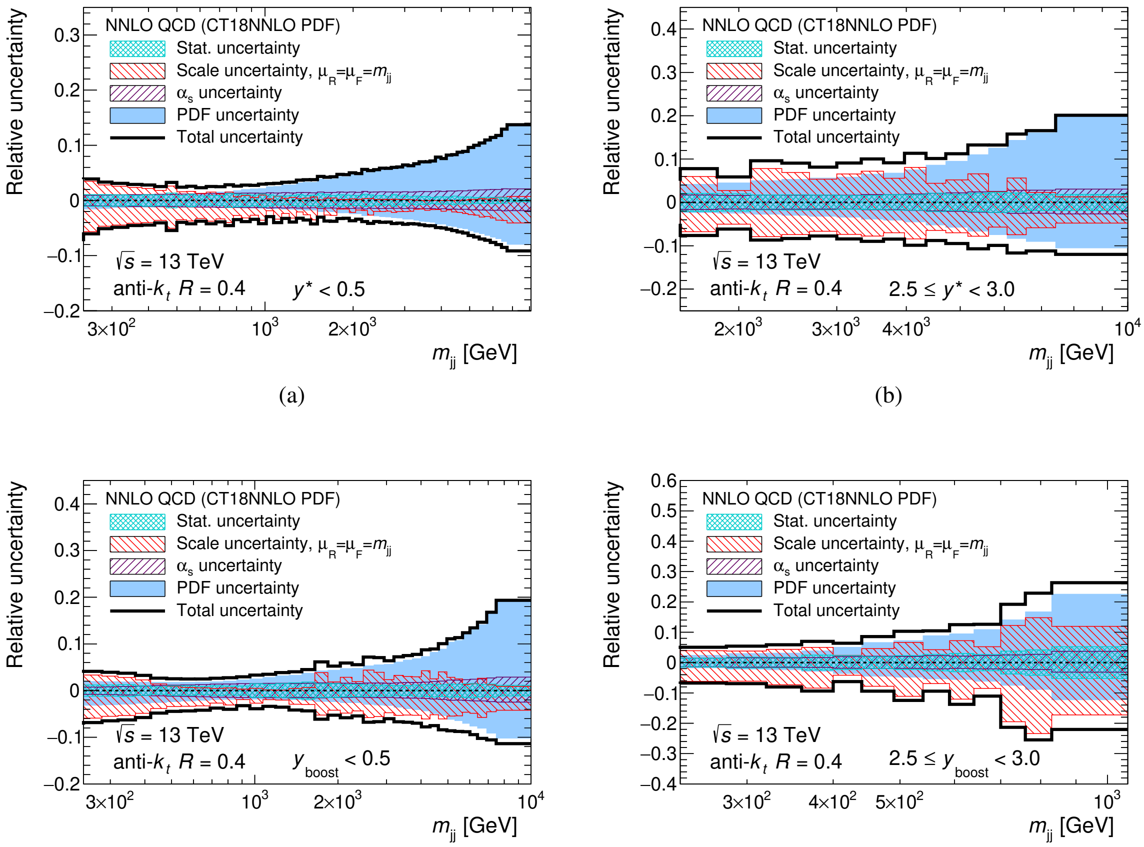

(c) (d)

Figure 3: Relative NNLO pQCD theoretical uncertainties for dijet cross-section predictions for the CT18NNLO PDF set. Panels a, b (c, d) correspond to the first and last y^* (y_{boost}) analysis bins. The uncertainties due to the renormalisation and factorisation scales, the value of α_s, the choice of particular PDF, the statistical uncertainty on the calculation and the total uncertainty are shown. The total uncertainty is calculated by adding the individual uncertainties in quadrature.

To obtain the predicted cross-section at the particle level, non-perturbative (NP) corrections are applied to the parton-level pQCD predictions. These corrections are obtained using LO MC generators, as the bin-by-bin ratios of the nominal particle-level MC prediction to the prediction from the partons remaining after showering (PS), but with hadronisation (HAD) and multi-parton interactions (MPI) modelling

[7] Each PDF set employs different input data samples and methodologies. The 1–2% level of precision achieved by NNPDF4.0 is widely recognised within the PDF community and is confirmed in several benchmarking studies [16]. Despite this, CT18NNLO is adopted as the default PDF set in this measurement because its PDF uncertainty is comparable to that of other modern global fits (e.g. MSHT2020, ATLASpdf21). The choice is consistent with the most recent dijet CMS measurement [5].

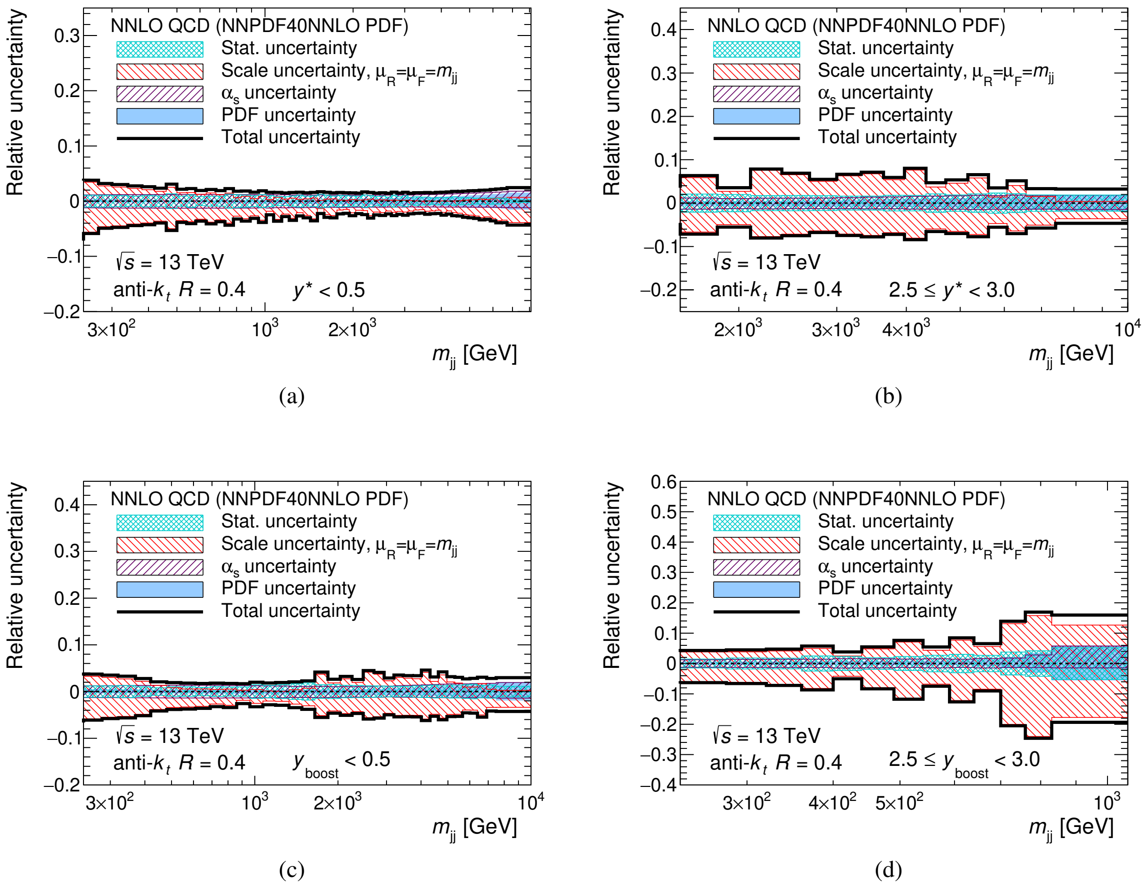

Figure 4: Relative NNLO pQCD theoretical uncertainties for dijet cross-section predictions for the NNPDF4.0 PDF set. Panels a, b (c, d) correspond to the first and last y^* (y_{boost}) analysis bins. The uncertainties due to the renormalisation and factorisation scales, the value of α_s, the choice of particular PDF, the statistical uncertainty on the calculation and the total uncertainty are shown. The total uncertainty is calculated by adding the individual uncertainties in quadrature.

switched off, according to

$$\text{NP corrections} = \frac{\sigma^{\text{Particle level}}}{\sigma^{\text{Parton level}}} = \frac{\sigma^{\text{PS+HAD+MPI}}}{\sigma^{\text{PS}}}.$$

In order to account for various HAD and MPI models, several MC generators with different hadronisation models, PDFs and sets of tuned parameters due to the underlying events[8] are considered as shown in Table 1.

Table 1: List of MC generators, hadronisation models, PDF sets, and tuned parameters due to underlying event used for the determination of the NP corrections.

MC generator	Hadronisation	PDF	Tuned parameters
Pythia 8.210 [35]	Lund String model [36, 37]	CTEQ6L1 [58]	C4 [59]
Pythia 8.210	Lund String model	CTEQ6L1	AU2 [60]
Pythia 8.210	Lund String model	CT10 [61]	AU2
Pythia 8.210	Lund String model	NNPDF2.3 [40]	A14 [39]
Herwig 7.2.3p2 [62]	Cluster model [63]	NNPDF2.3	H7.1-Default [64]
Herwig 7.2.3p2	Cluster model	NNPDF2.3	H7.1-BaryonicReconnection [65]
Herwig 7.2.3p2	Cluster model	NNPDF2.3	H7.1-Soft

The final NP corrections (NPC) are evaluated as the envelope of all sets of the tuned parameters around the nominal prediction from Pythia 8.210 with NNPDF2.3 and the A14 tuned parameters. The nominal central values are applied as multiplicative correction factors to the theory, while the envelope defines an additional systematic uncertainty. The smoothed out representative NPC factors are shown in Figure 5. The NP corrections reach 5% at low dijet mass region and decrease at high dijet mass in all y^* bins. In contrast, the NPC factors stand approximately constant as a function of m_{jj} in the lower y_{boost} bins, whereas a decreasing trend is observed in high y_{boost} bins.

The pQCD predictions are subsequently corrected for electroweak (EW) effects calculated for $2 \to 2$ processes up to NLO order using a tree and one-loop correction factors:

$$\text{EW corrections} = 1 + \delta^{\text{tree}} + \delta^{\text{1-loop}}. \tag{1}$$

The individual terms δ^{tree} and $\delta^{\text{1-loop}}$ are defined as ratios relative to the LO pQCD cross-section. The contribution proportional to δ^{tree} accounts for tree-level effects of order α^2 (pure EW), and $\alpha_s\alpha$ (QCD–EW interference). The $\delta^{\text{1-loop}}$ term includes one-loop virtual corrections of order $\alpha_s^2\alpha$ at NLO. These correction factors, computed within the same phase space as the measurement, are provided by the authors of Ref. [66]. No uncertainty associated with these corrections is presently estimated.

The electroweak corrections are shown in Figure 6. Their impact is negligible at low m_{jj} but increases with dijet mass, reaching up to +10% in the lowest y^* bins, then it suddenly drops up to −5% with increasing y^*. In the y_{boost} bins, the corrections reach up to −3% in the high m_{jj} region.

A strong dependence of the electroweak corrections is observed in the (m_{jj}, y^*) phase space, particularly across the transition between the first and second y^* bins. The competition between the two contributions

[8] The Herwig7.1 tuned parameters are fitted to LHC data at 900 GeV, 7 TeV, and 13 TeV, with Tevatron measurements used only for validation. The Pythia AU2 tuned parameters are primarily based on ATLAS minimum-bias and underlying-event data at 7 TeV and 900 GeV, with Tevatron (CDF) underlying-event observables included only with small weights to guide the energy extrapolation. The later A14 tuned parameters are derived solely from LHC Run-1 data. For the non-perturbative correction, the A14 tuned parameters are used with the NNPDF2.3 PDF as nominal, and the others are used to evaluate the uncertainty.

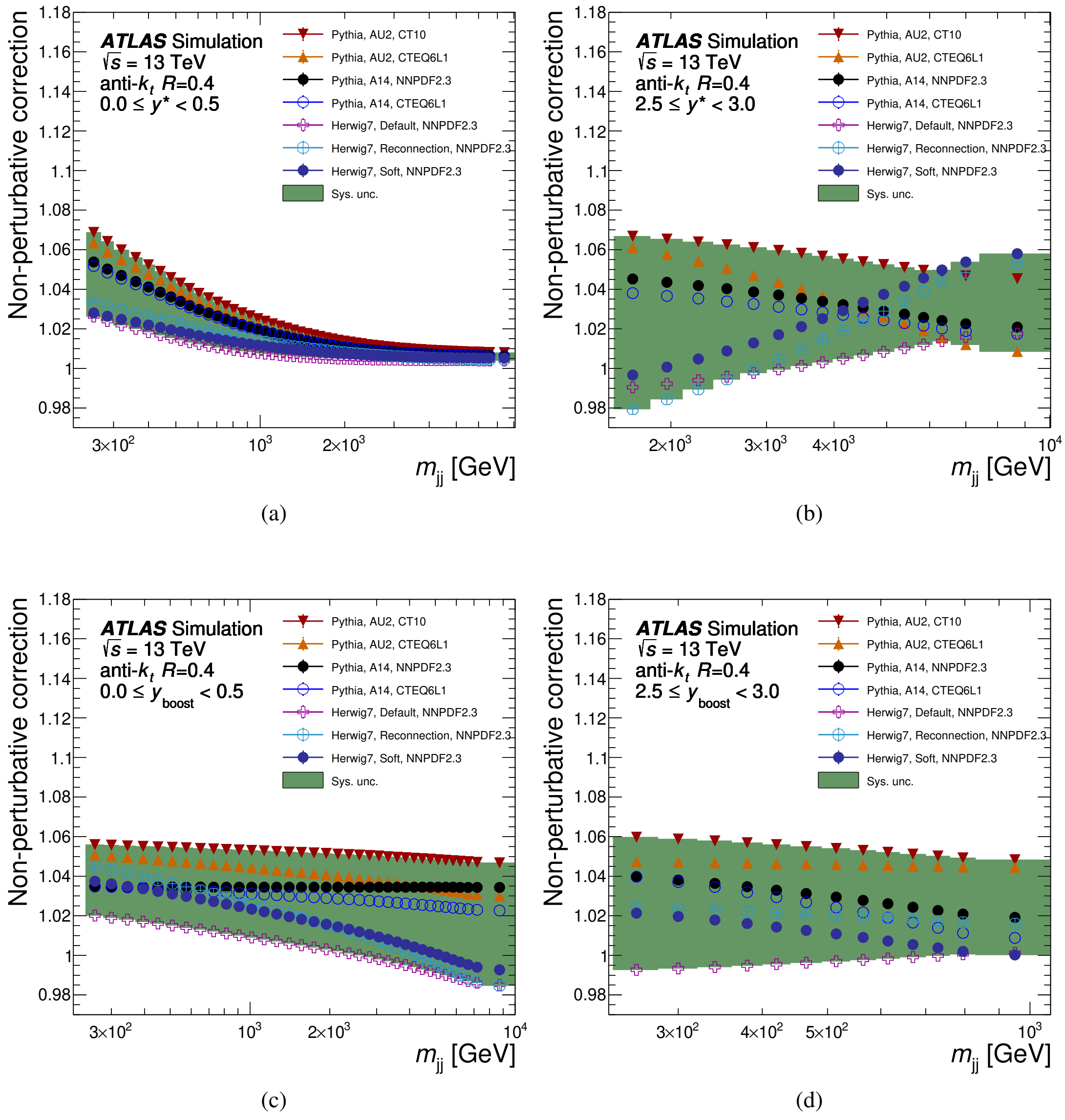

Figure 5: The non-perturbative correction factors in the first and last y^* (a, b) and y_{boost} bins (c, d). The nominal non-perturbative correction factors are derived using Pythia 8.210, NNPDF2.3 PDF set, and A14 tuned parameters, while the envelope defines the associated uncertainty applied to the theory.

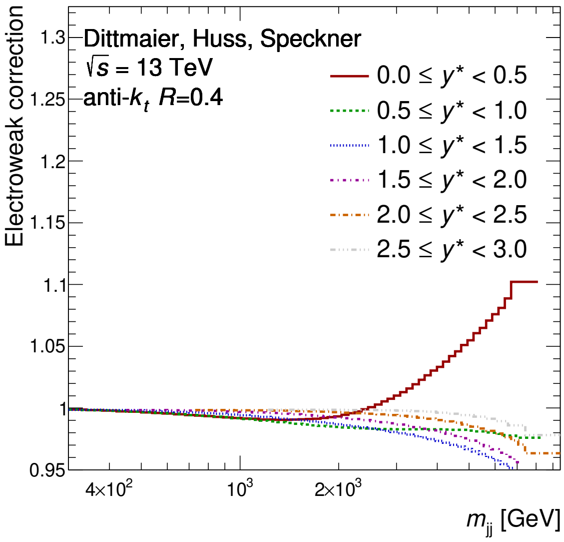

(a)

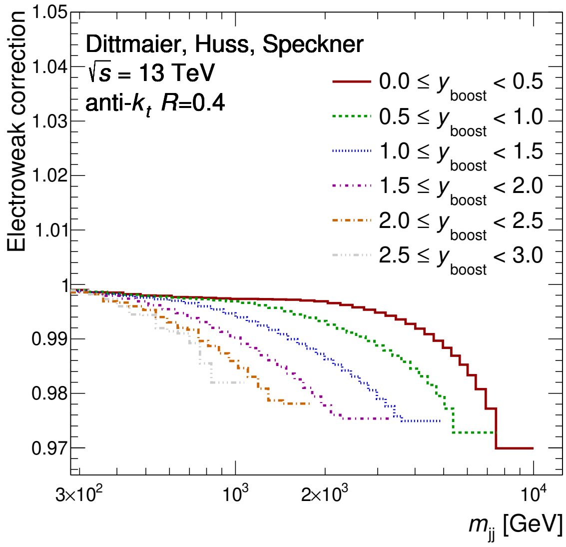

(b)

Figure 6: Electroweak correction factors for the dijet double-differential cross-section as a function of the invariant dijet mass m_{jj} in (a) six y^* bins and (b) six y_{boost} bins. The calculation follows the methodology of Ref. [66].

δ^{tree} and $\delta^{\text{1-loop}}$ drives this behaviour: the positive and rapidly decreasing tree-level term, δ^{tree}, and the negative and slowly decreasing one-loop level term, $\delta^{\text{1-loop}}$, which arises primarily from negative Sudakov logarithms. In the central region ($y^* < 0.5$), the dominant δ^{tree} contributions originate from qq-initiated tree-level processes (most notably from partonic sub-processes such as $uu \to uu$ and $ud \to ud$) in the interference between QCD and EW at order $O(\alpha_s \alpha)$, where only the interference terms of the t-, u-, and s-channels contribute, while the squared topologies vanish due to the colour structure [66]. Notably, this interference is more central in rapidity than the dominant QCD contributions, which mainly originate from squared topologies of Mandelstam variables u^2, t^2, and s^2.

8 Results

The unfolded double-differential inclusive dijet cross-sections are presented as functions of (m_{jj}, y^*) and $(m_{\mathrm{jj}}, y_{\mathrm{boost}})$ and compared with theoretical predictions based on pQCD, including electroweak and non-perturbative corrections. The measurements benefit from the full Run-2 data sample of 140 fb^{-1}, providing unprecedented statistics and substantially reduced statistical uncertainties with respect to the previous measurement. The improved jet energy calibration has also been implemented, reducing the jet energy scale uncertainty by up to a factor of three for central dijet configurations ($y^* < 0.5$) with $m_{\mathrm{jj}} > 1$ TeV. These improvements lead to a smaller total experimental uncertainty and enable more precise comparisons with theoretical predictions. The measured kinematic region covers dijets with y^*, y_{boost} between 0.0 and 3.0 and m_{jj} between 240 GeV and nearly 10 TeV, with the highest observed dijet mass reaching 9.54 TeV. Representative comparisons between data and theory are shown in Figures 7 and 8, based on nominal NNLO pQCD predictions using the CT18NNLO PDF set.

The theory-to-data comparisons using NLO and NNLO matrix elements of pQCD calculations with the nominal CT18 PDF set are presented in Figures 9 and 10. The NLO matrix elements are coupled to the NLO PDF set, while the NNLO matrix elements are coupled to the NNLO PDF. Both NLO and NNLO predictions overestimate the data on average by 15–20%.

At low y^* ($y^* < 1.5$), the theoretical predictions overestimate the data, with the theory to data ratio gradually decreasing as m_{jj} increases. At higher y^* values, the differences become more pronounced, showing a clear rise in the theory to data ratio with increasing m_{jj}. A similar trend is observed across the y_{boost} bins, where the agreement progressively worsens toward larger y_{boost} and large m_{jj}. For the (m_{jj}, y^*) measurement, the NNLO predictions provide an improved description of the shape at low y^*, which contains the majority of events in the phase space. At higher y^* values, however, the NNLO predictions remain consistently above the data, similar to the NLO predictions. In the (m_{jj}, y_{boost}) measurement, a better agreement is also observed at low m_{jj} across all y_{boost} bins. Furthermore, the NNLO predictions lead to an improved agreement with the data for all m_{jj} bins at higher y_{boost} values above 1.5. This behaviour is expected since each y_{boost} bin is dominated by contributions from low-y^* events, as illustrated in Figure 1.

These observations might be attributed to the limitations of fixed-order pQCD calculations, including the residual dependence on the unphysical renormalisation and factorisation scales, which affect both the shape and normalisation of the predictions. The conventional prescriptions for estimating theory uncertainties—based on seven-point scale variations and PDF uncertainties—do not necessarily capture the differences between central values obtained with all possible scale choices or between different PDF sets [67, 68]. Additional limitations may arise from the absence of resummation effects, which are still under development [69]. Another difference may arise from the choice of jet radius R. Small-R jets, including the ATLAS standard jets with $R = 0.4$, might have an additional perturbative uncertainty[9] [70]. Larger radii might also be preferred at LHC energies, where gluon-initiated jets dominate.

The complementary comparison for the alternative PDF sets (CT18, NNPDF3.1, NNPDF4.0, MSHT2020, and ATLASpdf21T3 using fixed NNLO matrix elements) are available in Figures 11 to 14 showing an almost constant offset between each of them, all being above the unfolded data. Focusing on the central values, the NNPDF4.0 PDF set shows the best overall agreement with the unfolded data—even in the high-m_{jj} region with a boosted topology (large y_{boost}), where most predictions tend to overestimate the data more steeply due to resummation effects. Since the NNPDF4.0 set provides significantly smaller PDF uncertainties—up to 2% level precision—it may lead to higher χ^2 values compared with other PDF sets, whose broader uncertainty bands can result in better quantitative agreement to data.

[9] For small jet radii, perturbative emissions outside the jet lead to a logarithmic R-dependent shift in the jet momentum, $\frac{\langle \delta p_T \rangle}{p_T} \sim \frac{\alpha_s}{\pi} L_i \ln(R)$, where L_i encodes a dependence on the colour factor of the initiating parton. For $R < 1.0$, the effect increases in magnitude with decreasing R [70].

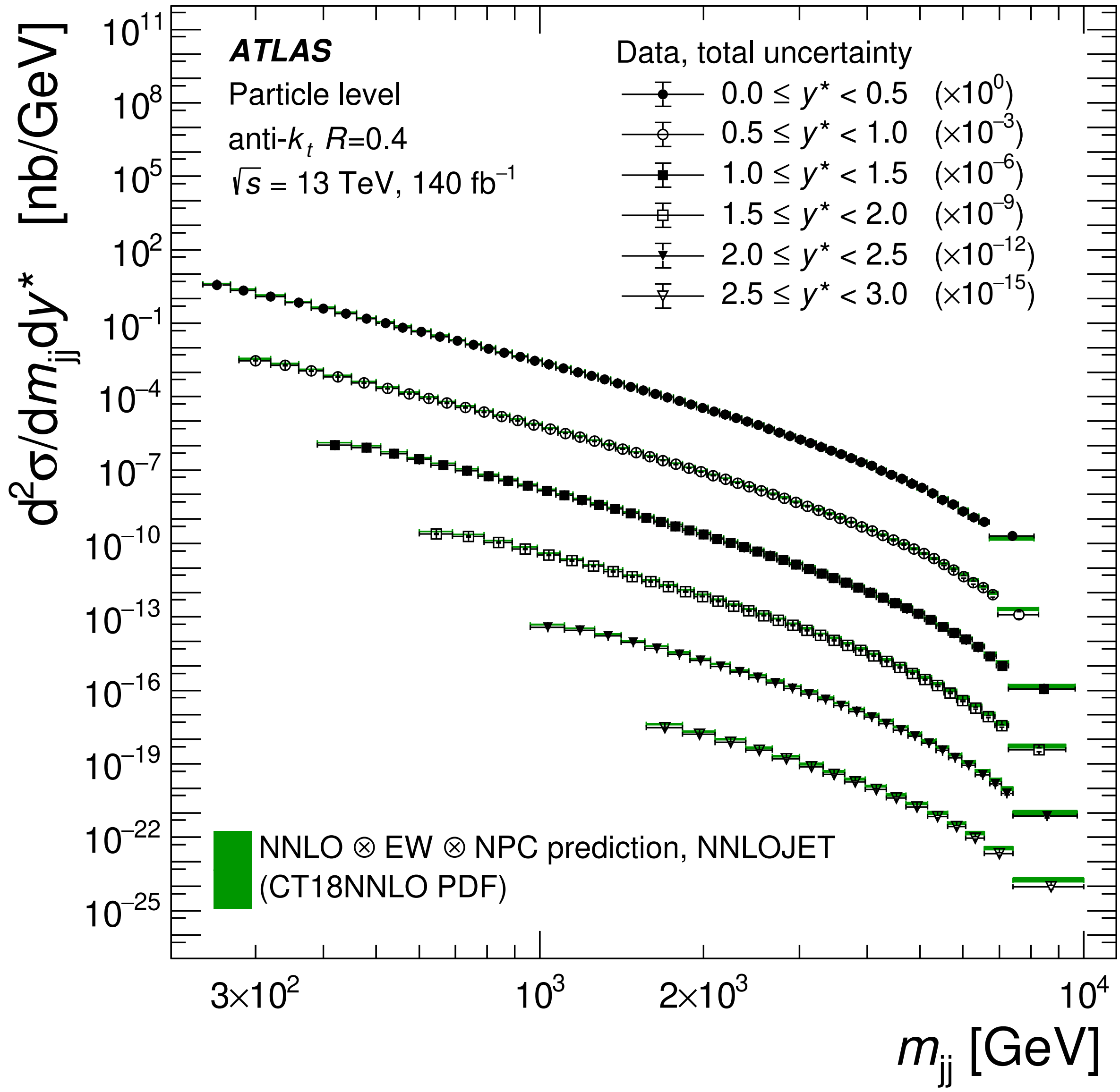

Figure 7: Double-differential cross-section as a function of the invariant dijet mass m_{jj} in six equidistant y^* bins. Each distribution is scaled by an additional factor 10^{-n}, indicated in the legend, to improve visibility. The figure compares the ATLAS unfolded data with NNLO predictions obtained using the CT18 PDF set, with electroweak and non-perturbative corrections applied. Coloured bands represent the total theoretical uncertainties, while vertical error bars show the experimental uncertainties.

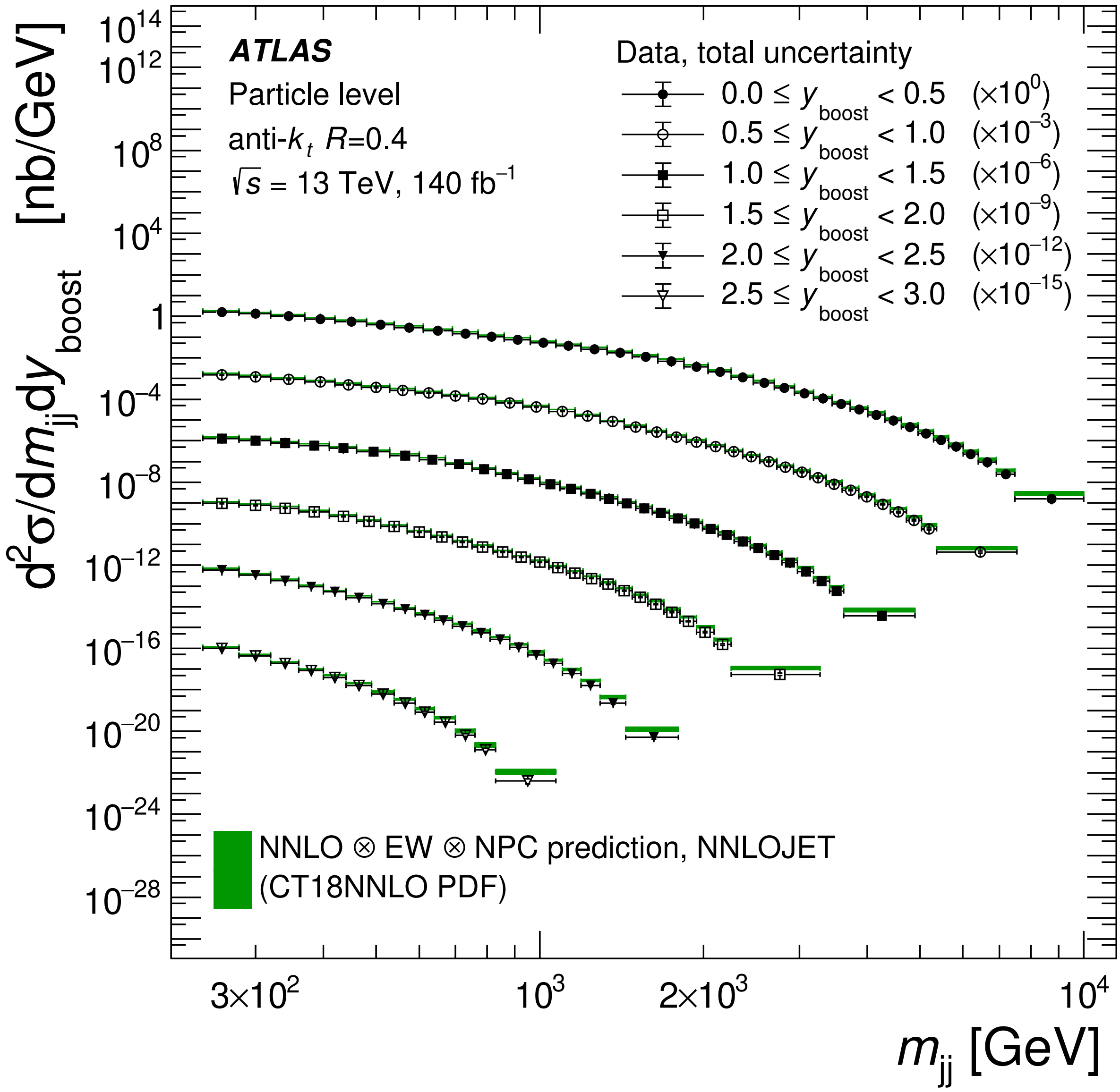

Figure 8: Double-differential cross-section as a function of the invariant dijet mass m_{jj} in six equidistant y_{boost} bins. Each distribution is scaled by an additional factor 10^{-n}, indicated in the legend, to improve visibility. The figure compares the ATLAS unfolded data with NNLO predictions obtained using the CT18 PDF set, with electroweak and non-perturbative corrections applied. Coloured bands represent the total theoretical uncertainties, while vertical error bars show the experimental uncertainties.

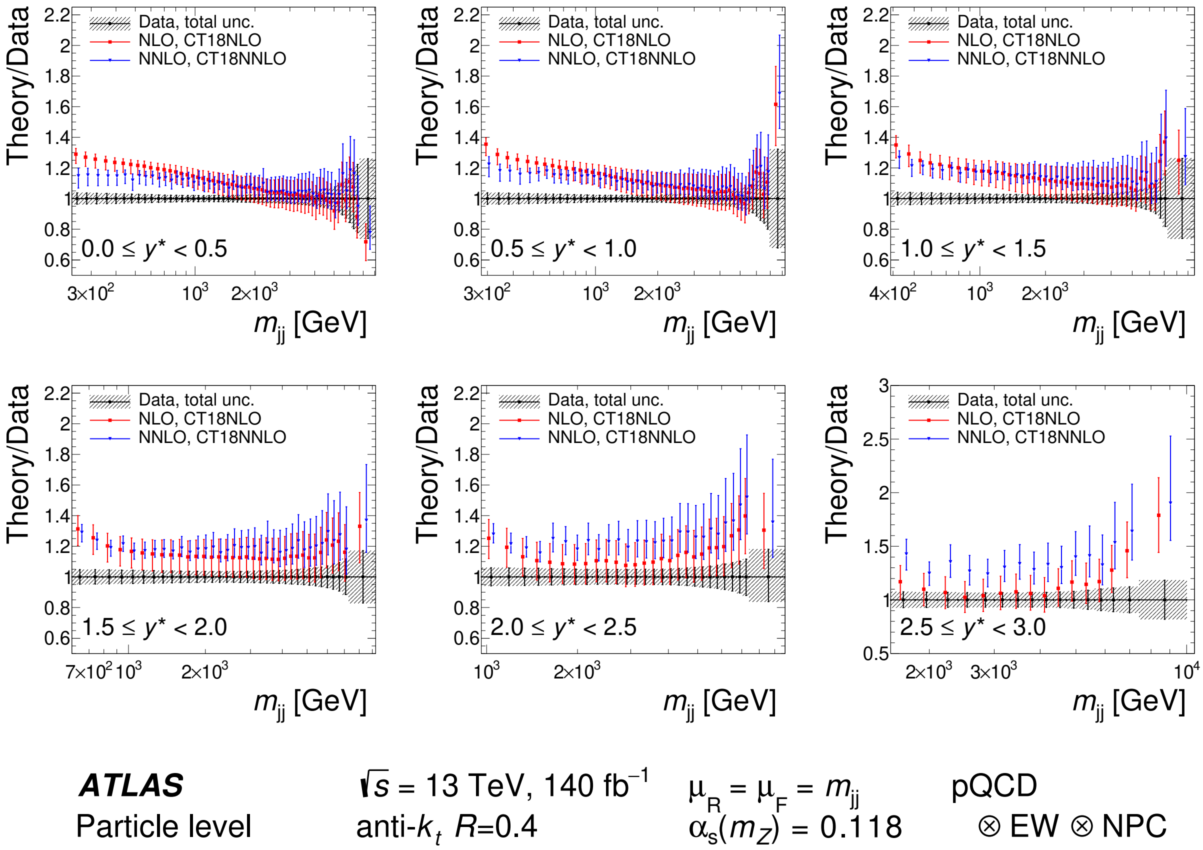

Figure 9: Theory-to-data ratio for the double-differential cross-section as a function of the invariant dijet mass m_{jj} in six equidistant y^* bins for anti-k_t $R = 0.4$ jets at the particle level. The sub-figures show different orders (NLO and NNLO) of pQCD full colour predictions via the NNLOJET programme at the parton level using the CT18 PDF set and renormalisation and factorisation scales of $\mu_{\mathrm{R}} = \mu_{\mathrm{F}} = m_{\mathrm{jj}}$. The pQCD calculations are corrected by electroweak and non-perturbative corrections to obtain the complete predictions at the particle level. The theory is compared with the data unfolded to the particle level using the IDS method with one iteration. Coloured vertical line errors indicate the total systematic uncertainties in pQCD calculations, including the effect of non-perturbative corrections. Vertical band errors around 1.0 indicate total experimental uncertainty in the data.

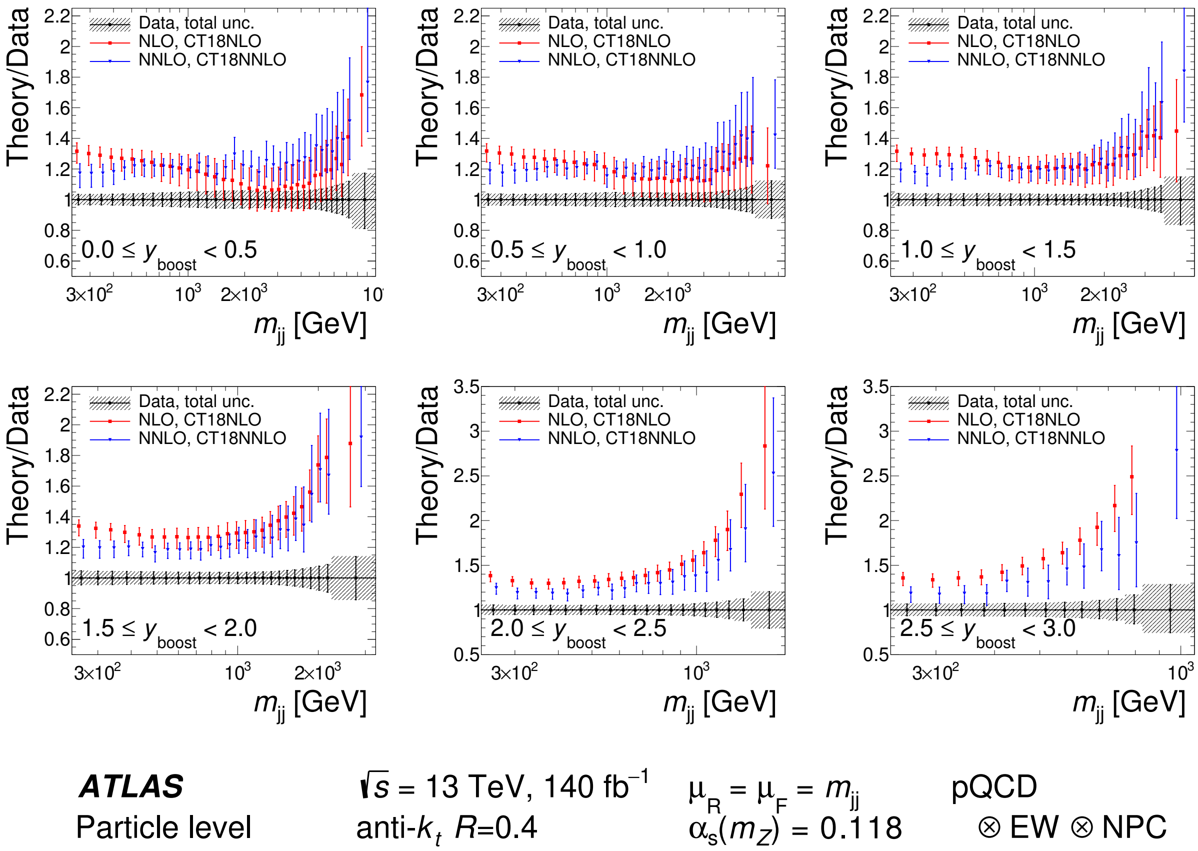

Figure 10: Theory-to-data ratio for the double-differential cross-section as a function of the invariant dijet mass m_{jj} in six equidistant y_{boost} bins for anti-k_t $R = 0.4$ jets at the particle level. The sub-figures show different orders (NLO and NNLO) of pQCD full colour predictions via the NNLOJET programme at the parton level using the CT18 PDF set and renormalisation and factorisation scales of $\mu_{\mathrm{R}} = \mu_{\mathrm{F}} = m_{\mathrm{jj}}$. The pQCD calculations are corrected by electroweak and non-perturbative corrections to obtain the complete predictions at the particle level. The theory is compared with the data unfolded to the particle level using the IDS method with two iterations. Coloured vertical line errors indicate the total systematic uncertainties in pQCD calculations, including the effect of non-perturbative corrections. Vertical band errors around 1.0 indicate total experimental uncertainty in the data.

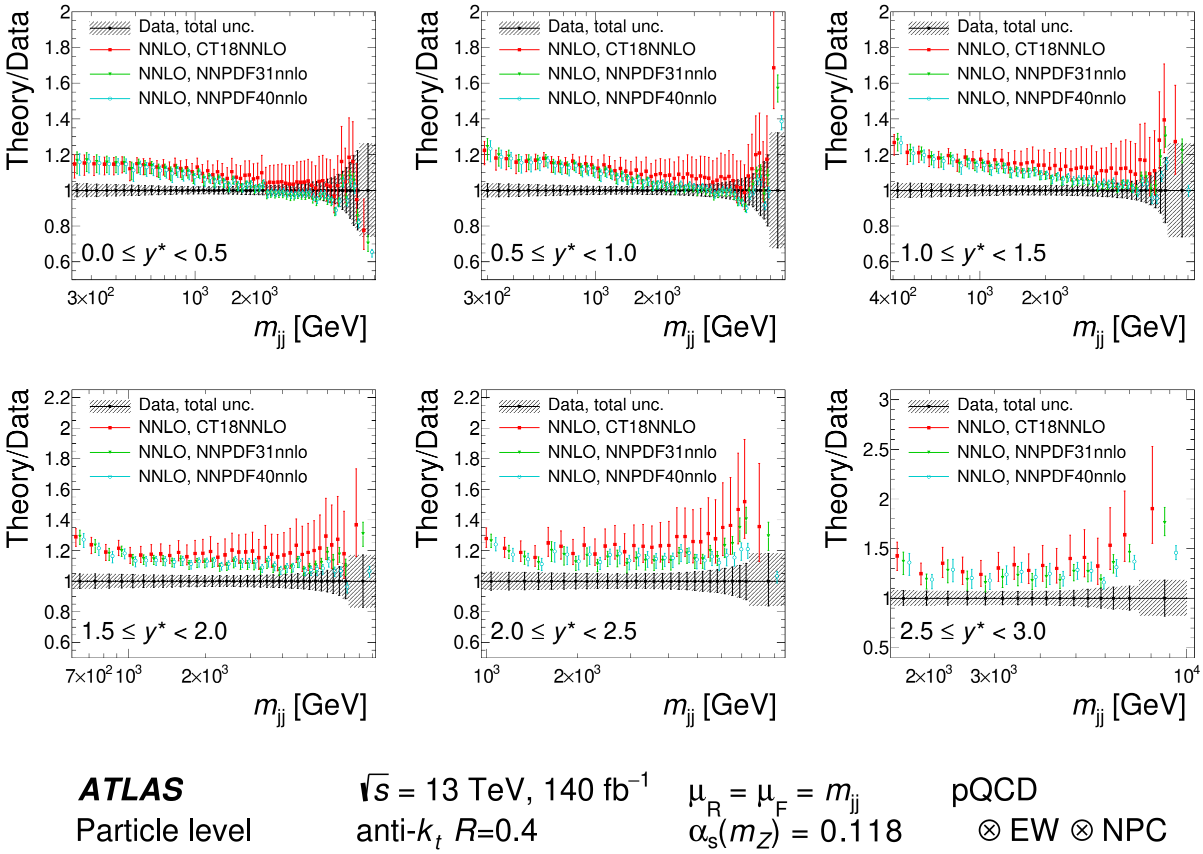

Figure 11: Theory-to-data ratio for the double-differential cross-section as a function of the invariant dijet mass m_{jj} in six equidistant y^* bins for anti-k_t $R = 0.4$ jets at the particle level. The sub-figures compare NNLO pQCD calculations with different PDF sets (CT18, NNPDF3.1, and NNPDF4.0) to the ATLAS data. The pQCD full colour predictions via the NNLOJET programme include renormalisation and factorisation scales of $\mu_{\mathrm{R}} = \mu_{\mathrm{F}} = m_{\mathrm{jj}}$. The pQCD calculations are corrected by electroweak and non-perturbative corrections to obtain the complete predictions at the particle level. The theory is compared with the data unfolded to the particle level using the IDS method with one iteration. Coloured vertical line errors indicate the total systematic uncertainties in pQCD calculations, including the effect of non-perturbative corrections. Vertical band errors around 1.0 indicate total experimental uncertainty in the data.

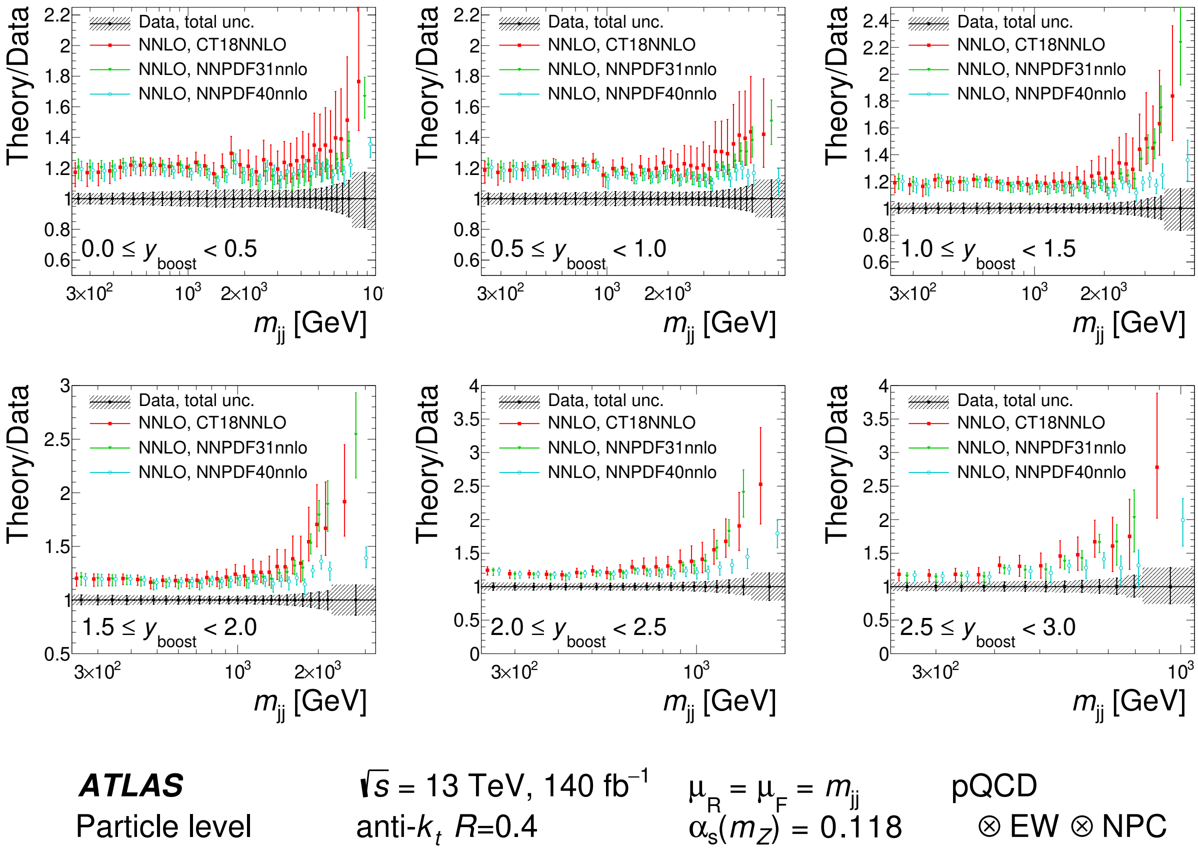

Figure 12: Theory-to-data ratio for the double-differential cross-section as a function of the invariant dijet mass m_{jj} in six equidistant y_{boost} bins for anti-k_t $R = 0.4$ jets at the particle level. The sub-figures compare NNLO pQCD calculations with different PDF sets (CT18, NNPDF3.1, and NNPDF4.0) to the ATLAS data. The pQCD full colour predictions via the NNLOJET programme include renormalisation and factorisation scales of $\mu_R = \mu_F = m_{jj}$. The pQCD calculations are corrected by electroweak and non-perturbative corrections to obtain the complete predictions at the particle level. The theory is compared with the data unfolded to the particle level using the IDS method with two iterations. Coloured vertical line errors indicate the total systematic uncertainties in pQCD calculations, including the effect of non-perturbative corrections. Vertical band errors around 1.0 indicate total experimental uncertainty in the data.

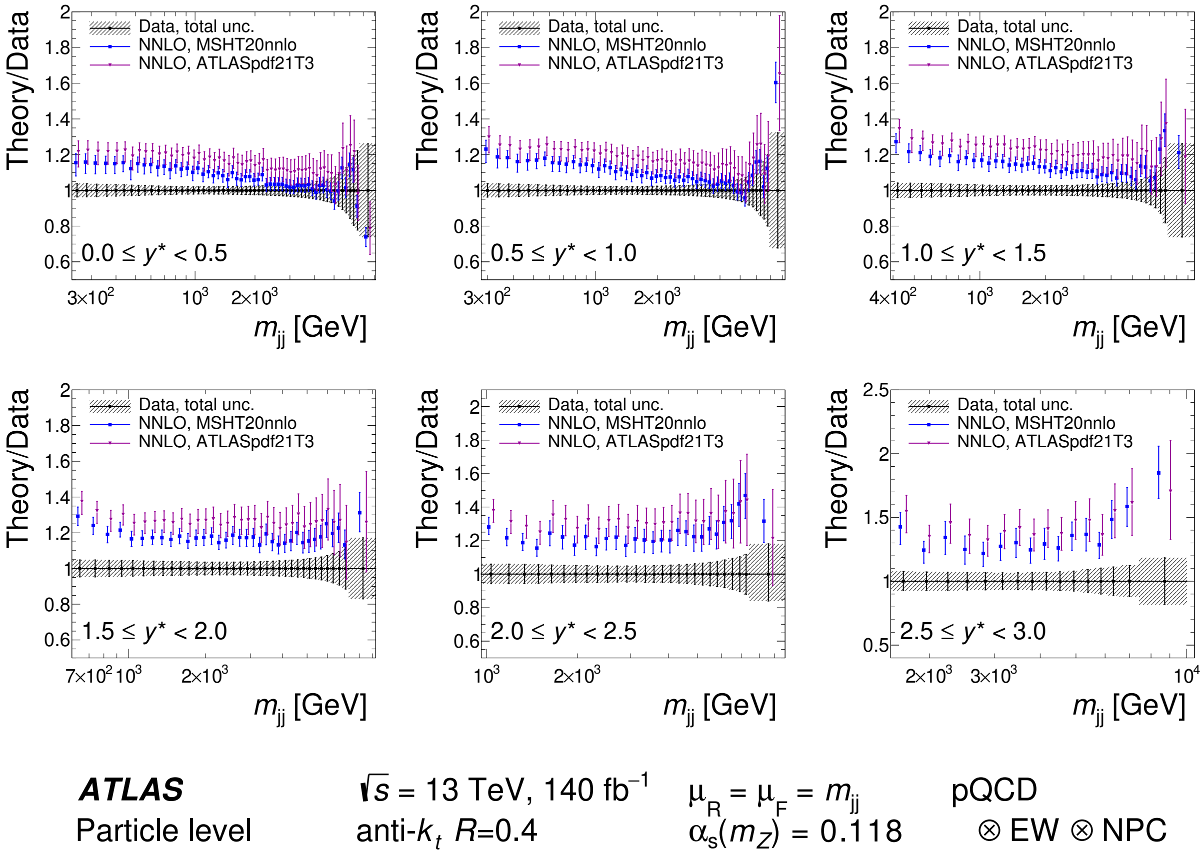

Figure 13: Theory-to-data ratio for the double-differential cross-section as a function of the invariant dijet mass m_{jj} in six equidistant y^* bins for anti-k_t $R = 0.4$ jets at the particle level. The sub-figures compare NNLO pQCD calculations with different PDF sets (MSHT2020, ATLASpdf21T3) to the ATLAS data. The pQCD full colour predictions via the NNLOJET programme include renormalisation and factorisation scales of $\mu_{\text{R}} = \mu_{\text{F}} = m_{\text{jj}}$. The pQCD calculations are corrected by electroweak and non-perturbative corrections to obtain the complete predictions at the particle level. The theory is compared with the data unfolded to the particle level using the IDS method with one iteration. Coloured vertical line errors indicate the total systematic uncertainties in pQCD calculations, including the effect of non-perturbative corrections. The prediction using the ATLASpdf21T3 PDF set does not include α_s variation as a source of theoretical systematic uncertainty. Vertical band errors around 1.0 indicate total experimental uncertainty in the data.

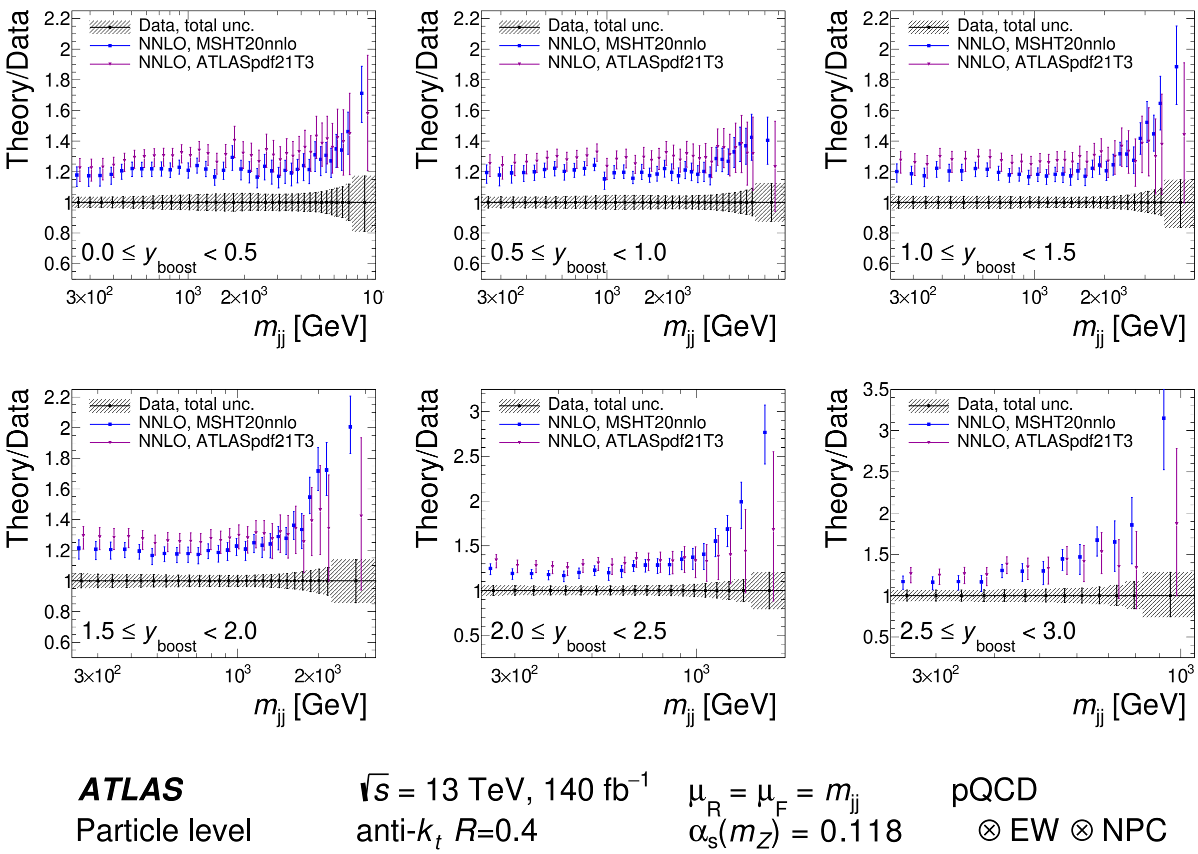

Figure 14: Theory-to-data ratio for the double-differential cross-section as a function of the invariant dijet mass m_{jj} in six equidistant y_{boost} bins for anti-k_t $R = 0.4$ jets at the particle level. The sub-figures compare NNLO pQCD calculations with different PDF sets (MSHT2020, ATLASpdf21T3) to the ATLAS data. The pQCD full colour predictions via the NNLOJET programme include renormalisation and factorisation scales of $\mu_{\mathrm{R}} = \mu_{\mathrm{F}} = m_{\mathrm{jj}}$. The pQCD calculations are corrected by electroweak and non-perturbative corrections to obtain the complete predictions at the particle level. The theory is compared with the data unfolded to the particle level using the IDS method with two iterations. Coloured vertical line errors indicate the total systematic uncertainties in pQCD calculations, including the effect of non-perturbative corrections. The prediction using the ATLASpdf21T3 PDF set does not include α_s variation as a source of theoretical systematic uncertainty. Vertical band errors around 1.0 indicate total experimental uncertainty in the data.

A quantitative assessment of the agreement between the measured dijet cross-section and theoretical predictions requires a statistical approach. To evaluate the consistency of the data with theoretical expectations, a χ^2 test is employed as described in Ref. [6].

The χ^2 test provides a measure of the overall compatibility between the experimental results and the predictions, including the correlations, accounting for statistical and (possibly asymmetric) systematic uncertainties. The individual experimental and theory uncertainty components are treated as mutually uncorrelated, while full correlation is assumed across the $(m_{\mathrm{jj}},\ y^*)$ or $(m_{\mathrm{jj}},\ y_{\mathrm{boost}})$ bins, respectively. Statistical correlations across these bins are evaluated using covariance matrices derived from 1000 pseudo experiments, in which both the data and MC simulation are fluctuated according to Poisson statistics. From the theory perspective, separate components for scale variations, PDF eigenvectors, non-perturbative corrections, and the strong coupling constant are implemented. The PDF eigenvectors for NNPDF sets are obtained from a covariance matrix derived based on the pseudo experiments.

The χ^2 tests are performed to evaluate the sensitivity of the measurement to electroweak and non-perturbative corrections using a fixed-order NNLO pQCD prediction with the CT18NNLO PDF set. For the $(m_{\mathrm{jj}},\ y^*)$ measurement, a strong sensitivity to electroweak effects is observed in global χ^2/ndf (329/237 with vs. 396/237 without). In contrast, the impact of non-perturbative corrections is small (329/237 with vs. 338/237 without). For the $(m_{\mathrm{jj}},\ y_{\mathrm{boost}})$ measurement, no sensitivity is observed to either electroweak nor non-perturbative effects, as the χ^2/ndf remains nearly unchanged (183/160 with vs. 184/160 without electroweak corrections, and 184/160 with vs. 184/160 without non-perturbative corrections).

The χ^2 tests are also used to perform quantitative comparisons between the data and different PDF sets (CT18, NNPDF3.1, NNPDF4.0, MSHT2020, and ATLASpdf21T3) across both individual and global y^* and y_{boost} bins, as shown in Tables 2 and 3. The results indicate good agreement in the individual y^* and y_{boost} bins. Overall, higher χ^2 values are observed in the $(m_{\mathrm{jj}},\ y^*)$ measurement compared with $(m_{\mathrm{jj}},\ y_{\mathrm{boost}})$; this trend is more pronounced in the global χ^2/ndf. While the global results in y_{boost} remain acceptable, the global χ^2/ndf in y^* corresponds to a low p-value of about 10^{-6}. This low p-value in $(m_{\mathrm{jj}},\ y^*)$ is primarily driven by residual bin-to-bin fluctuations in the pQCD predictions, arising from incomplete cancellations between large positive and negative integrals of the real–real and real–virtual pQCD contributions.

The lowest global χ^2/ndf is obtained with ATLASpdf21T3 in both (m_{jj}, y^*) and $(m_{\mathrm{jj}}, y_{\mathrm{boost}})$, at 288/237 and 166/160, respectively. Because ATLASpdf21T3 does not yet provide a published α_s uncertainty, this component is omitted here; its inclusion would be expected to lower the χ^2 further.

For the other PDF sets, the global χ^2/ndf values saturate at higher values—around 330/237 in (m_{jj}, y^*) and 180/160 in $(m_{\mathrm{jj}}, y_{\mathrm{boost}})$—and are mutually consistent. The second-best global χ^2 value in (m_{jj}, y^*) is found for CT18NNLO with 329/237, while in $(m_{\mathrm{jj}}, y_{\mathrm{boost}})$ it is NNPDF3.1NNLO with 178/160.

The χ^2/ndf values remain relatively good despite the observed differences between theory and data in Figures 9 to 14. This behaviour arises because the χ^2 test is largely insensitive to overall normalisation shifts, which can be absorbed due to the bin-to-bin correlations of the systematic uncertainties. Indeed, small coherent shifts of a few nuisance parameters are sufficient to account for the systematic differences observed between data and theory. The sum of the penalty terms induced in the χ^2 by these shifts remains small compared with the number of bins. Consequently, the χ^2 values are driven primarily by local bin-to-bin fluctuations rather than by global offsets.

Table 2: Evaluated χ^2/ndf for the dijet cross-section in the individual and global y^* bins taking into account NNLO pQCD predictions using CT18, NNPDF3.1, NNPDF4.0, MSHT2020, and ATLASpdf21T3 PDF sets, and $\mu_R = \mu_F = m_{jj}$ corrected for electroweak and non-perturbative corrections to the unfolded data. The ATLASpdf21T3 does not include an α_s uncertainty, as it is not published.

	χ^2/ndf				
	CT18NNLO	NNPDF3.1NNLO	NNPDF4.0NNLO	MSHT2020NNLO	ATLASpdf21T3
$y^* < 0.5$	58/58	68/58	59/58	61/58	58/58
$0.5 \leq y^* < 1.0$	62/54	70/54	63/54	67/54	59/54
$1.0 \leq y^* < 1.5$	56/45	67/45	63/45	65/45	58/45
$1.5 \leq y^* < 2.0$	51/36	59/36	57/36	54/36	63/36
$2.0 \leq y^* < 2.5$	30/28	41/28	36/28	34/28	39/28
$2.5 \leq y^* < 3.0$	17/16	21/16	17/16	21/16	19/16
$0.0 \leq y^* < 3.0$	329/237	343/237	342/237	347/237	288/237

Table 3: Evaluated χ^2/ndf for the dijet cross-section in the individual and global y_{boost} bins taking into account NNLO pQCD predictions using CT18, NNPDF3.1, NNPDF4.0, MSHT2020, and ATLASpdf21T3 PDF sets, and $\mu_R = \mu_F = m_{jj}$ corrected for electroweak and non-perturbative corrections to the unfolded data. The ATLASpdf21T3 does not include an α_s uncertainty, as it is not published.

	χ^2/ndf				
	CT18NNLO	NNPDF3.1NNLO	NNPDF4.0NNLO	MSHT2020NNLO	ATLASpdf21T3
$y_{\text{boost}} < 0.5$	33/36	48/36	37/36	43/36	44/36
$0.5 \leq y_{\text{boost}} < 1.0$	51/34	55/34	53/34	55/34	54/34
$1.0 \leq y_{\text{boost}} < 1.5$	41/31	40/31	39/31	47/31	47/31
$1.5 \leq y_{\text{boost}} < 2.0$	26/26	27/26	26/26	31/26	35/26
$2.0 \leq y_{\text{boost}} < 2.5$	24/20	24/20	21/20	28/20	31/20
$2.5 \leq y_{\text{boost}} < 3.0$	15/13	15/13	14/13	20/13	16/13
$0.0 \leq y_{\text{boost}} < 3.0$	183/160	178/160	185/160	195/160	166/160

9 Conclusion

Inclusive, double-differential dijet cross-sections have been measured as a function of (m_{jj}, y^*) and $(m_{jj}, y_{\text{boost}})$ using particle flow anti-k_t jets with a radius parameter of $R = 0.4$. The measurements were performed in pp collisions at a centre-of-mass energy of 13 TeV using the 140 fb^{-1} data collected by the ATLAS experiment during the LHC Run-2 phase between 2015 and 2018. The results incorporate the most detailed and up-to-date breakdown of systematic uncertainties currently available in the ATLAS experiment.

The measured distributions are unfolded to the particle level and compared with several theoretical predictions, including state-of-the-art full colour NNLO pQCD calculations from NNLOJET, with additional electroweak and non-perturbative corrections applied. A qualitative comparison between the measured data and the theoretical calculations is performed using both NLO and NNLO matrix elements and various PDF sets.

The NNLO theoretical predictions tend to overestimate the data by about 15–20%, with the best qualitative agreement seen for the NNPDF4.0NNLO PDF set. In contrast, the quantitative results of the χ^2 test, which accounts for correlations, show the best results (lowest global χ^2/ndf) for ATLASpdf21T3 in both (m_{jj}, y^*)

and (m_{jj}, y_{boost}). The other PDF sets give slightly higher and mutually comparable χ^2/ndf values. The second-best χ^2/ndf is obtained with CT18NNLO in (m_{jj}, y^*) and with NNPDF3.1NNLO in (m_{jj}, y_{boost}). Overall, better qualitative and quantitative results are found in (m_{jj}, y_{boost}) compared with (m_{jj}, y^*).

Acknowledgements

We thank CERN for the very successful operation of the LHC and its injectors, as well as the support staff at CERN and at our institutions worldwide without whom ATLAS could not be operated efficiently.

The crucial computing support from all WLCG partners is acknowledged gratefully, in particular from CERN, the ATLAS Tier-1 facilities at TRIUMF/SFU (Canada), NDGF (Denmark, Norway, Sweden), CC-IN2P3 (France), KIT/GridKA (Germany), INFN-CNAF (Italy), NL-T1 (Netherlands), PIC (Spain), RAL (UK) and BNL (USA), the Tier-2 facilities worldwide and large non-WLCG resource providers. Major contributors of computing resources are listed in Ref. [71].

We gratefully acknowledge the support of ANPCyT, Argentina; YerPhI, Armenia; ARC, Australia; BMWFW and FWF, Austria; ANAS, Azerbaijan; CNPq and FAPESP, Brazil; NSERC, NRC and CFI, Canada; CERN; ANID, Chile; CAS, MOST and NSFC, China; Minciencias, Colombia; MEYS CR, Czech Republic; DNRF and DNSRC, Denmark; IN2P3-CNRS and CEA-DRF/IRFU, France; SRNSFG, Georgia; BMFTR, HGF and MPG, Germany; GSRI, Greece; RGC and Hong Kong SAR, China; ICHEP and Academy of Sciences and Humanities, Israel; INFN, Italy; MEXT and JSPS, Japan; CNRST, Morocco; NWO, Netherlands; RCN, Norway; MNiSW, Poland; FCT, Portugal; MNE/IFA, Romania; MSTDI, Serbia; MSSR, Slovakia; ARIS and MVZI, Slovenia; DSI/NRF, South Africa; MICIU/AEI, Spain; SRC and Wallenberg Foundation, Sweden; SERI, SNSF and Cantons of Bern and Geneva, Switzerland; NSTC, Taipei; TENMAK, Türkiye; STFC/UKRI, United Kingdom; DOE and NSF, United States of America.

Individual groups and members have received support from BCKDF, CANARIE, CRC and DRAC, Canada; CERN-CZ, FORTE and PRIMUS, Czech Republic; COST, ERC, ERDF, Horizon 2020 and Marie Skłodowska-Curie Actions, European Union; Investissements d'Avenir Labex, Investissements d'Avenir Idex and ANR, France; DFG and AvH Foundation, Germany; Herakleitos, Thales and Aristeia programmes co-financed by EU-ESF and the Greek NSRF, Greece; BSF-NSF and MINERVA, Israel; NCN and NAWA, Poland; La Caixa Banking Foundation, CERCA Programme Generalitat de Catalunya and PROMETEO and GenT Programmes Generalitat Valenciana, Spain; Göran Gustafssons Stiftelse, Sweden; The Royal Society and Leverhulme Trust, United Kingdom.

In addition, individual members wish to acknowledge support from Chile: Agencia Nacional de Investigación y Desarrollo (FONDECYT 1230812, FONDECYT 1240864, Fondecyt 3240661, Fondecyt Regular 1240721); China: Chinese Ministry of Science and Technology (MOST-2023YFA1605700, MOST-2023YFA1609300), National Natural Science Foundation of China (NSFC - 12175119, NSFC 12275265); Czech Republic: Czech Science Foundation (GACR - 24-11373S), Ministry of Education Youth and Sports (ERC-CZ-LL2327, FORTE CZ.02.01.01/00/22_008/0004632), PRIMUS Research Programme (PRIMUS/21/SCI/017); EU: H2020 European Research Council (ERC - 101002463); European Union: European Research Council (BARD No. 101116429, ERC - 948254, ERC 101089007), European Regional Development Fund (HE COFUND GA No.101081355, ERDF), European Union, Future Artificial Intelligence Research (FAIR-NextGenerationEU PE00000013); France: Agence Nationale de la Recherche (ANR-21-CE31-0013, ANR-21-CE31-0022, ANR-22-EDIR-0002, ANR-24-CE31-0504-01); Germany: Deutsche Forschungsgemeinschaft (DFG - 469666862, DFG - CR 312/5-2); China: Research Grants Council (GRF);

Italy: Ministero dell'Università e della Ricerca (NextGenEU 153D23001490006 M4C2.1.1, NextGenEU I53D23000820006 M4C2.1.1, NextGenEU I53D23001490006 M4C2.1.1, SOE2024_0000023); Japan: Japan Society for the Promotion of Science (JSPS KAKENHI JP22H01227, JSPS KAKENHI JP22H04944, JSPS KAKENHI JP22KK0227, JSPS KAKENHI JP24K23939, JSPS KAKENHI JP24KK0251, JSPS KAKENHI JP25H00650, JSPS KAKENHI JP25H01291, JSPS KAKENHI JP25K01023); Norway: Research Council of Norway (RCN-314472); Poland: Ministry of Science and Higher Education (IDUB AGH, POB8, D4 no 9722), Polish National Science Centre (NCN 2021/42/E/ST2/00350, NCN OPUS 2023/51/B/ST2/02507, NCN UMO-2019/34/E/ST2/00393, UMO-2022/47/O/ST2/00148, UMO-2023/49/B/ST2/04085, UMO-2023/51/B/ST2/00920, UMO-2024/53/N/ST2/00869); Portugal: Foundation for Science and Technology (FCT); Spain: Generalitat Valenciana (ASFAE/2022/008), Ministry of Science and Innovation (RYC2019-028510-I, RYC2020-030254-I, RYC2021-031273-I, RYC2022-038164-I), Ministerio de Ciencia, Innovación y Universidades/Agencia Estatal de Investigación (PID2022-142604OB-C22); Sweden: Carl Trygger Foundation (Carl Trygger Foundation CTS 22:2312), Swedish Research Council (Swedish Research Council 2023-04654, VR 2021-03651, VR 2022-03845, VR 2022-04683, VR 2023-03403, VR 2024-05451), Knut and Alice Wallenberg Foundation (KAW 2018.0458, KAW 2022.0358, KAW 2023.0366); Switzerland: Swiss National Science Foundation (SNSF - PCEFP2_194658); United Kingdom: The Binks Trust, Royal Society (NIF-R1-231091); United States of America: U.S. Department of Energy (ECA DE-AC02-76SF00515), John Templeton Foundation (John Templeton Foundation 63206), Neubauer Family Foundation.

References

[1] ATLAS Collaboration, *The ATLAS Experiment at the CERN Large Hadron Collider*, JINST **3** (2008) S08003.

[2] L. Evans and P. Bryant, *LHC Machine*, JINST **3** (2008) S08001.

[3] CMS Collaboration, *Measurement of the differential dijet production cross section in proton–proton collisions at $\sqrt{s} = 7$ TeV*, Phys. Lett. B **700** (2011) 187, arXiv: 1104.1693 [hep-ex].

[4] CMS Collaboration, *Measurement of the triple-differential dijet cross section in proton–proton collisions at $\sqrt{s} = 8$ TeV and constraints on parton distribution functions*, Eur. Phys. J. C **77** (2017) 746, arXiv: 1705.02628 [hep-ex].

[5] CMS Collaboration, *Measurement of multidifferential cross sections for dijet production in proton–proton collisions at $\sqrt{s} = 13$ TeV*, Eur. Phys. J. C **85** (2025) 72, arXiv: 2312.16669 [hep-ex].

[6] ATLAS Collaboration, *Measurement of dijet cross-sections in pp collisions at 7 TeV centre-of-mass energy using the ATLAS detector*, JHEP **05** (2014) 059, arXiv: 1312.3524 [hep-ex].

[7] ATLAS Collaboration, *Measurement of inclusive jet and dijet cross-sections in proton–proton collisions at $\sqrt{s} = 13$ TeV with the ATLAS detector*, JHEP **05** (2018) 195, arXiv: 1711.02692 [hep-ex].

[8] M. Cacciari, G. P. Salam and G. Soyez, *The anti-k_t jet clustering algorithm*, JHEP **04** (2008) 063, arXiv: 0802.1189 [hep-ph].

[9] A. G.-D. Ridder, T. Gehrmann, E. W. N. Glover, A. Huss and J. Pires, *Triple Differential Dijet Cross Section at the LHC*, Phys. Rev. Lett. **123** (2019) 102001, arXiv: 1905.09047 [hep-ph].

[10] ATLAS Collaboration, *Jet energy scale and resolution measured in proton–proton collisions at $\sqrt{s}$ = 13 TeV with the ATLAS detector*, Eur. Phys. J. C **81** (2021) 689, arXiv: 2007.02645 [hep-ex].

[11] ATLAS Collaboration, *A precise measurement of the jet energy scale derived from single-particle measurements and in situ techniques in proton–proton collisions at $\sqrt{s}$ = 13 TeV with the ATLAS detector*, Eur. Phys. J. C **85** (2025) 927, arXiv: 2407.15627 [hep-ex].

[12] X. Chen, T. Gehrmann, E. W. N. Glover, A. Huss and J. Mo, *NNLO QCD corrections in full colour for jet production observables at the LHC*, JHEP **09** (2022) 025, arXiv: 2204.10173 [hep-ph].

[13] T.-J. Hou et al., *New CTEQ global analysis of quantum chromodynamics with high-precision data from the LHC*, Phys. Rev. D **103** (2021) 014013, arXiv: 1912.10053 [hep-ph].

[14] S. Bailey, T. Cridge, L. A. Harland-Lang, A. D. Martin and R. S. Thorne, *Parton distributions from LHC, HERA, Tevatron and fixed target data: MSHT20 PDFs*, Eur. Phys. J. C **81** (2021) 341, arXiv: 2012.04684 [hep-ph].

[15] NNPDF Collaboration, *Parton distributions from high-precision collider data*, Eur. Phys. J. C **77** (2017) 663, arXiv: 1706.00428 [hep-ph].

[16] NNPDF Collaboration, *The path to proton structure at 1% accuracy*, Eur. Phys. J. C **82** (2022) 428, arXiv: 2109.02653 [hep-ph].

[17] ATLAS Collaboration, *Determination of the parton distribution functions of the proton using diverse ATLAS data from pp collisions at $\sqrt{s}$ = 7, 8 and 13 TeV*, Eur. Phys. J. C **82** (2022) 438, arXiv: 2112.11266 [hep-ex].

[18] F. Ahmadova et al., *Precise Determination of the Strong Coupling Constant from Dijet Cross Sections up to the Multi-TeV Range*, Phys. Rev. Lett. **135** (2025) 031903, arXiv: 2412.21165 [hep-ph].

[19] ATLAS Collaboration, *ATLAS Insertable B-Layer: Technical Design Report*, ATLAS-TDR-19; CERN-LHCC-2010-013, 2010, URL: https://cds.cern.ch/record/1291633, Addendum: ATLAS-TDR-19-ADD-1; CERN-LHCC-2012-009, 2012, URL: https://cds.cern.ch/record/1451888.

[20] B. Abbott et al., *Production and integration of the ATLAS Insertable B-Layer*, JINST **13** (2018) T05008, arXiv: 1803.00844 [physics.ins-det].

[21] G. Avoni et al., *The new LUCID-2 detector for luminosity measurement and monitoring in ATLAS*, JINST **13** (2018) P07017.

[22] ATLAS Collaboration, *Performance of the ATLAS trigger system in 2015*, Eur. Phys. J. C **77** (2017) 317, arXiv: 1611.09661 [hep-ex].

[23] ATLAS Collaboration, *Software and computing for Run 3 of the ATLAS experiment at the LHC*, Eur. Phys. J. C **85** (2025) 234, arXiv: 2404.06335 [hep-ex], Erratum: Eur. Phys. J. C **85** (2025) 907.

[24] M. Cacciari, G. P. Salam and G. Soyez, *FastJet user manual*, Eur. Phys. J. C **72** (2012) 1896, arXiv: 1111.6097 [hep-ph].

[25] S. Frixione and G. Ridolfi, *Jet photoproduction at HERA*, Nucl. Phys. B **507** (1997) 315, arXiv: hep-ph/9707345.

[26] S. Alioli, K. Hamilton, P. Nason, C. Oleari and E. Re, *Jet pair production in POWHEG*, JHEP **04** (2011) 081, arXiv: 1012.3380 [hep-ph].

[27] ATLAS Collaboration, *ATLAS data quality operations and performance for 2015–2018 data-taking*, JINST **15** (2020) P04003, arXiv: 1911.04632 [physics.ins-det].

[28] ATLAS Collaboration, *Luminosity determination in pp collisions at $\sqrt{s} = 13$ TeV using the ATLAS detector at the LHC*, Eur. Phys. J. C **83** (2023) 982, arXiv: 2212.09379 [hep-ex].

[29] ATLAS Collaboration, *Performance of the missing transverse momentum triggers for the ATLAS detector during Run-2 data taking*, JHEP **08** (2020) 080, arXiv: 2005.09554 [hep-ex].

[30] ATLAS Collaboration, *Performance of the ATLAS Level-1 topological trigger in Run 2*, Eur. Phys. J. C **82** (2022) 7, arXiv: 2105.01416 [hep-ex].

[31] ATLAS Collaboration, *Operation of the ATLAS trigger system in Run 2*, JINST **15** (2020) P10004, arXiv: 2007.12539 [physics.ins-det].

[32] V. Lendermann et al., *Combining Triggers in HEP data analysis*, Nucl. Instrum. Meth. A **604** (2009) 707, arXiv: 0901.4118 [hep-ex].

[33] ATLAS Collaboration, *Jet reconstruction and performance using particle flow with the ATLAS Detector*, Eur. Phys. J. C **77** (2017) 466, arXiv: 1703.10485 [hep-ex].

[34] ATLAS Collaboration, *Topological cell clustering in the ATLAS calorimeters and its performance in LHC Run 1*, Eur. Phys. J. C **77** (2017) 490, arXiv: 1603.02934 [hep-ex].

[35] T. Sjöstrand et al., *An introduction to PYTHIA 8.2*, Comput. Phys. Commun. **191** (2015) 159, arXiv: 1410.3012 [hep-ph].

[36] B. Andersson, G. Gustafson, G. Ingelman and T. Sjöstrand, *Parton fragmentation and string dynamics*, Phys. Rept. **97** (1983) 31.

[37] T. Sjöstrand, *Jet fragmentation of multiparton configurations in a string framework*, Nucl. Phys. B **248** (1984) 469.

[38] T. Sjöstrand and P. Z. Skands, *Transverse-momentum-ordered showers and interleaved multiple interactions*, Eur. Phys. J. C **39** (2005) 129, arXiv: hep-ph/0408302.

[39] ATLAS Collaboration, *ATLAS Pythia 8 tunes to 7 TeV data*, ATL-PHYS-PUB-2014-021, 2014, URL: https://cds.cern.ch/record/1966419.

[40] NNPDF Collaboration, R. D. Ball et al., *Parton distributions with LHC data*, Nucl. Phys. B **867** (2013) 244, arXiv: 1207.1303 [hep-ph].

[41] D. J. Lange, *The EvtGen particle decay simulation package*, Nucl. Instrum. Meth. A **462** (2001) 152.

[42] ATLAS Collaboration, *The ATLAS Simulation Infrastructure*, Eur. Phys. J. C **70** (2010) 823, arXiv: 1005.4568 [physics.ins-det].

[43] S. Agostinelli et al., *Geant4 – a simulation toolkit*, Nucl. Instrum. Meth. A **506** (2003) 250.

[44] T. Sjöstrand, S. Mrenna and P. Skands, *A brief introduction to PYTHIA 8.1*, Comput. Phys. Commun. **178** (2008) 852, arXiv: 0710.3820 [hep-ph].

[45] ATLAS Collaboration, *Selection of jets produced in* 13 *TeV proton–proton collisions with the ATLAS detector*, ATLAS-CONF-2015-029, 2015, URL: https://cds.cern.ch/record/2037702.

[46] B. Malaescu, *An iterative, dynamically stabilized method of data unfolding*, 2009, arXiv: 0907.3791 [physics.data-an].

[47] ATLAS Collaboration, *Measurement of the energy response of the ATLAS calorimeter to charged pions from $W^\pm \to \tau^\pm(\to \pi^\pm \nu_\tau)\nu_\tau$ events in Run 2 data*, Eur. Phys. J. C **82** (2022) 223, arXiv: 2108.09043 [hep-ex].

[48] ATLAS Collaboration, *Operation and performance of the ATLAS tile calorimeter in LHC Run 2*, Eur. Phys. J. C **84** (2024) 1313, arXiv: 2401.16034 [hep-ex].

[49] ATLAS Collaboration, *Jet energy measurement with the ATLAS detector in proton–proton collisions at $\sqrt{s} = 7$ TeV*, Eur. Phys. J. C **73** (2013) 2304, arXiv: 1112.6426 [hep-ex].

[50] Z. Nagy, *Next-to-leading order calculation of three-jet observables in hadron-hadron collisions*, Phys. Rev. D **68** (2003) 094002, arXiv: hep-ph/0307268.

[51] Z. Nagy, *Three-Jet Cross Sections in Hadron-Hadron Collisions at Next-To-Leading Order*, Phys. Rev. Lett. **88** (2002) 122003, arXiv: hep-ph/0110315.

[52] A. Huss et al., *NNLOJET: a parton-level event generator for jet cross sections at NNLO QCD accuracy*, 2025, arXiv: 2503.22804 [hep-ph].

[53] J. Currie et al., *Precise Predictions for Dijet Production at the LHC*, Phys. Rev. Lett. **119** (2017) 152001, arXiv: 1705.10271 [hep-ph].

[54] M. Czakon, A. van Hameren, A. Mitov and R. Poncelet, *Single-jet inclusive rates with exact color at $O(\alpha_s^4)$*, JHEP **10** (2019) 262, arXiv: 1907.12911 [hep-ph].

[55] S. Carrazza, E. R. Nocera, C. Schwan and M. Zaro, *PineAPPL: combining EW and QCD corrections for fast evaluation of LHC processes*, JHEP **12** (2020) 108, arXiv: 2008.12789 [hep-ph].

[56] T. Carli et al., *A posteriori inclusion of parton density functions in NLO QCD final-state calculations at hadron colliders: The APPLGRID Project*, Eur. Phys. J. C **66** (2010) 503, arXiv: 0911.2985 [hep-ph].

[57] A. Buckley et al., *LHAPDF6: parton density access in the LHC precision era*, Eur. Phys. J. C **75** (2015) 132, arXiv: 1412.7420 [hep-ph].

[58] J. Pumplin et al., *New Generation of Parton Distributions with Uncertainties from Global QCD Analysis*, JHEP **07** (2002) 012, arXiv: hep-ph/0201195.

[59] R. Corke and T. Sjöstrand, *Interleaved parton showers and tuning prospects*, JHEP **03** (2011) 032, arXiv: 1011.1759 [hep-ph].

[60] ATLAS Collaboration, *Summary of ATLAS Pythia 8 tunes*, ATL-PHYS-PUB-2012-003, 2012, URL: https://cds.cern.ch/record/1474107.

[61] H.-L. Lai et al., *New parton distributions for collider physics*, Phys. Rev. D **82** (2010) 074024, arXiv: 1007.2241 [hep-ph].

[62] J. Bellm et al., *Herwig 7.2 release note*, Eur. Phys. J. C **80** (2020) 452, arXiv: 1912.06509 [hep-ph].

[63] B. R. Webber, *A QCD Model for Jet Fragmentation Including Soft Gluon Interference*, Nucl. Phys. B **238** (1984) 492.

[64] Herwig Collaboration, *Herwig 7.1 tunes*, Accessed: 2025-05-09, URL: https://herwig.hepforge.org/tutorials/mpi/tunes.html.

[65] S. Gieseke, C. Rohr and A. Siodmok, *Colour reconnections in Herwig++*, Eur. Phys. J. C **72** (2012) 2225, arXiv: 1206.0041 [hep-ph].

[66] S. Dittmaier, A. Huss and C. Speckner, *Weak radiative corrections to dijet production at hadron colliders*, JHEP **11** (2012) 095, arXiv: 1210.0438 [hep-ph].

[67] A. Gehrmann-De Ridder et al., *Jet cross sections with NNLOJET*, PoS **LL2018** (2018) 001.

[68] J. Currie et al., *Infrared sensitivity of single jet inclusive production at hadron colliders*, JHEP **10** (2018) 155, arXiv: 1807.03692 [hep-ph].

[69] T. Generet, K. Lee, I. Moult, R. Poncelet and X. Zhang, *Small radius inclusive jet production at the LHC through NNLO+NNLL*, JHEP **08** (2025) 015, arXiv: 2503.21866 [hep-ph].

[70] M. Dasgupta, L. Magnea and G. P. Salam, *Non-perturbative QCD effects in jets at hadron colliders*, JHEP **02** (2008) 055, arXiv: 0712.3014 [hep-ph].

[71] ATLAS Collaboration, *ATLAS Computing Acknowledgements*, ATL-SOFT-PUB-2025-001, 2025, URL: https://cds.cern.ch/record/2922210.

The ATLAS Collaboration

G. Aad [103], E. Aakvaag [17], B. Abbott [122], S. Abdelhameed [118a], K. Abeling [55], N.J. Abicht [49], S.H. Abidi [30], M. Aboelela [45], A. Aboulhorma [36e], H. Abramowicz [156], B.S. Acharya [69a,69b,m], A. Ackermann [63a], C. Adam Bourdarios [4], L. Adamczyk [86a], S.V. Addepalli [148], M.J. Addison [102], J. Adelman [117], A. Adiguzel [22c], T. Adye [136], A.A. Affolder [138], Y. Afik [40], M.N. Agaras [13], A. Aggarwal [101], C. Agheorghiesei [28c], F. Ahmadov [39,ad], S. Ahuja [96], S. Ahuja [168], X. Ai [142b], G. Aielli [76a,76b], A. Aikot [168], M. Ait Tamlihat [36e], B. Aitbenchikh [36a], T.P.A. Åkesson [99], D. Akiyama [173], N.N. Akolkar [25], S. Aktas [171], G.L. Alberghi [24b], J. Albert [170], U. Alberti [20], P. Albicocco [53], G.L. Albouy [60], S. Alderweireldt [52], Z.L. Alegria [123], M. Aleksa [37], I.N. Aleksandrov [39], C. Alexa [28b], T. Alexopoulos [10], F. Alfonsi [24b], M. Algren [56], M. Alhroob [172], B. Ali [134], H.M.J. Ali [92,v], S. Ali [32], S.W. Alibocus [93], M. Aliev [34c], G. Alimonti [71a], W. Alkakhi [55], C. Allaire [66], B.M.M. Allbrooke [151], D.R. Allen [123], J.S. Allen [102], J.F. Allen [52], C.S. Alley [1], A. Aloisio [72a,72b], F. Alonso [91], C. Alpigiani [141], Z.M.K. Alsolami [92], A. Alvarez Fernandez [101], M. Alves Cardoso [56], M.G. Alviggi [72a,72b], M. Aly [102], Y. Amaral Coutinho [82b], A. Ambler [105], C. Amelung[37], M. Amerl [102], T. Amezza [129], B. Amini [54], K. Amirie [160], A. Amirkhanov [39], S.P. Amor Dos Santos [132a], D. Amperiadou [157], S. An[83], C. Anastopoulos [144], T. Andeen [11], J.K. Anders [93], A.C. Anderson [59], A. Andreazza [71a,71b], S. Angelidakis [9], A. Angerami [42], A.V. Anisenkov [39], A. Annovi [74a], C. Antel [37], E. Antipov [150], M. Antonelli [53], F. Anulli [75a], M. Aoki [83], T. Aoki [158], M.A. Aparo [13], L. Aperio Bella [48], M. Apicella[31], C. Appelt [156], A. Apyan [27], M. Arampatzi [10], S.J. Arbiol Val [87], C. Arcangeletti [53], A.T.H. Arce [51], J-F. Arguin [109], S. Argyropoulos [157], J.-H. Arling [48], O. Arnaez [4], H. Arnold [150], G. Artoni [75a,75b], H. Asada [112], S. Asatryan [178], N.A. Asbah [37], R.A. Ashby Pickering [172], A.M. Aslam [96], K. Assamagan [30], R. Astalos [29a], K.S.V. Astrand [99], S. Atashi [164], R.J. Atkin [34a], H. Atmani[36f], P.A. Atmasiddha [130], K. Augsten [134], A.D. Auriol [41], V.A. Austrup [102], A.S. Avad [95], G. Avolio [37], K. Axiotis [56], A. Azzam [13], D. Babal [29b], H. Bachacou [137], K. Bachas [157,p], A. Bachiu [35], E. Bachmann [50], M.J. Backes [63a], A. Badea [40], T.M. Baer [107], M. Bahmani [19], D. Bahner [54], K. Bai [125], L. Baines [95], O.K. Baker [177], D. Bakshi Gupta [8], L.E. Balabram Filho [82b], V. Balakrishnan [122], R. Balasubramanian [4], E.M. Baldin [38], P. Balek [86a], E. Ballabene [24b,24a], F. Balli [137], L.M. Baltes [63a], W.K. Balunas [128], J. Balz [101], I. Bamwidhi [118b], E. Banas [87], M. Bandieramonte [131], A. Bandyopadhyay [25], S. Bansal [25], L. Barak [156], M. Barakat [48], E.L. Barberio [106], D. Barberis [18b], M. Barbero [103], M.Z. Barel [116], T. Barillari [111], M-S. Barisits [37], T. Barklow [148], P. Baron [135], D.A. Baron Moreno [102], A. Baroncelli [62], A.J. Barr [128], J.D. Barr [97], F. Barreiro [100], J. Barreiro Guimarães da Costa [14], M.G. Barros Teixeira [132a], S. Barsov [38], F. Bartels [63a], R. Bartoldus [148], A.E. Barton [92], P. Bartos [29a], M. Baselga [49], S. Bashiri[87], A. Bassalat [66,b], M.J. Basso [161a], S. Bataju [45], R. Bate [169], R.L. Bates [59], S. Batlamous[100], M. Battaglia [138], D. Battulga [19], M. Bauce [75a,75b], L. Bauckhage [48], P. Bauer [25], L.T. Bayer [48], L.T. Bazzano Hurrell [31], J.B. Beacham [111], T. Beau [129], J.Y. Beaucamp [91], P.H. Beauchemin [163], P. Bechtle [25], H.P. Beck [20,o], K. Becker [172], A.J. Beddall [81], V.A. Bednyakov [39], C.P. Bee [150], L.J. Beemster [16], M. Begalli [82d], M. Begel [30], J.K. Behr [48], J.F. Beirer [37], F. Beisiegel [25], M. Belfkir [118b], G. Bella [156], L. Bellagamba [24b], A. Bellerive [35], C.D. Bellgraph [68], P. Bellos [21], K. Beloborodov [38], I. Benaoumeur [21], D. Benchekroun [36a], F. Bendebba [36a], Y. Benhammou [156], K.C. Benkendorfer [61], L. Beresford [48], M. Beretta [53], E. Bergeaas Kuutmann [166], N. Berger [4], B. Bergmann [134], J. Beringer [18a], G. Bernardi [5], C. Bernius [148], F.U. Bernlochner [25],

A. Berrocal Guardia[13], T. Berry[96], P. Berta[135], A. Berti[132a], R. Bertrand[103], S. Bethke[111], A. Betti[75a,75b], A.J. Bevan[95], L. Bezio[56], N.K. Bhalla[54], S. Bharthuar[111], S. Bhatta[150], P. Bhattarai[148], Z.M. Bhatti[119], K.D. Bhide[54], V.S. Bhopatkar[123], R.M. Bianchi[131], G. Bianco[24b,24a], O. Biebel[110], M. Biglietti[77a], P. Bijl[54], C.S. Billingsley[45], Y. Bimgdi[36f], M. Bindi[55], A. Bingham[176], A. Bingul[22b], C. Bini[75a,75b], G.A. Bird[33], M. Birman[174], M. Biros[135], S. Biryukov[151], T. Bisanz[49], E. Bisceglie[24b,24a], J.P. Biswal[136], D. Biswas[146], I. Bloch[48], A. Blue[59], U. Blumenschein[95], V.S. Bobrovnikov[39], L. Boccardo[57b,57a], M. Boehler[54], B. Boehm[171], D. Bogavac[13], A.G. Bogdanchikov[38], L.S. Boggia[129], V. Boisvert[96], P. Bokan[166], T. Bold[86a], M. Bomben[5], M. Bona[95], M. Boonekamp[137], A.G. Borbély[59], I.S. Bordulev[38], G. Borissov[92], D. Bortoletto[128], D. Boscherini[24b], M. Bosman[13], K. Bouaouda[36a], L. Boudet[4], J. Boudreau[131], E.V. Bouhova-Thacker[92], D. Boumediene[41], R. Bouquet[57b,57a], A. Boveia[121], J. Boyd[37], D. Boye[30], I.R. Boyko[39], L. Bozianu[56], J. Bracinik[21], N. Brahimi[4], G. Brandt[176], O. Brandt[33], B. Brau[104], R. Brener[174], L. Brenner[116], R. Brenner[166], S. Bressler[174], G. Brianti[116], D. Britton[59], D. Britzger[111], I. Brock[25], R. Brock[108], H. Bronson[130], G. Brooijmans[42], A.J. Brooks[68], E.M. Brooks[161b], E. Brost[30], L.M. Brown[170,161a], L.E. Bruce[61], T.L. Bruckler[128], P.A. Bruckman de Renstrom[87], B. Brüers[48], A. Bruni[24b], G. Bruni[24b], D. Brunner[47a,47b], M. Bruschi[24b], N. Bruscino[75a,75b], T. Buanes[17], Q. Buat[141], D. Buchin[111], A.G. Buckley[59], M. Buhring[50], O. Bulekov[81], B.A. Bullard[148], S. Burdin[93], C.D. Burgard[49], A.M. Burger[90], B. Burghgrave[8], O. Burlayenko[54], J. Burleson[167], J.C. Burzynski[147], V. Büscher[101], P.J. Bussey[59], O. But[25], J.M. Butler[26], C.M. Buttar[59], J.M. Butterworth[97], P. Butti[37], W. Buttinger[136], C.J. Buxo Vazquez[108], A.R. Buzykaev[39], S. Cabrera Urbán[168], L. Cadamuro[66], H. Cai[37], Y. Cai[24b,113c,24a], Y. Cai[113a], V.M.M. Cairo[37], O. Cakir[3a], N. Calace[37], P. Calafiura[18a], G. Calderini[129], P. Calfayan[35], L. Calic[99], G. Callea[59], L.P. Caloba[82b], D. Calvet[41], S. Calvet[41], R. Camacho Toro[129], S. Camarda[37], D. Camarero Munoz[27], P. Camarri[76a,76b], C. Camincher[37], M. Campanelli[97], A. Camplani[43], V. Canale[72a,72b], A.C. Canbay[3a], E. Canonero[96], J. Cantero[168], Y. Cao[167], F. Capocasa[27], M. Capua[44b,44a], A. Carbone[71a,71b], R. Cardarelli[76a], J.C.J. Cardenas[8], M.P. Cardiff[27], G. Carducci[44b,44a], T. Carli[37], G. Carlino[72a], J.I. Carlotto[13], B.T. Carlson[131,q], E.M. Carlson[170], L. Carminati[71a,71b], A. Carnelli[4], M. Carnesale[37], S. Caron[115], E. Carquin[139g], I.B. Carr[106], S. Carrá[73a,73b], G. Carratta[24b,24a], C. Carrion Martinez[168], A.M. Carroll[125], M.P. Casado[13,h], P. Casolaro[72a,72b], M. Caspar[48], W.R. Castiglioni[40], F.L. Castillo[4], L. Castillo Garcia[13], V. Castillo Gimenez[168], N.F. Castro[132a,132e], A. Catinaccio[37], J.R. Catmore[127], T. Cavaliere[4], V. Cavaliere[30], L.J. Caviedes Betancourt[23b], E. Celebi[81], S. Cella[156], V. Cepaitis[56], K. Cerny[124], A.S. Cerqueira[82a], A. Cerri[74a,am], L. Cerrito[76a,76b], F. Cerutti[18a], B. Cervato[71a,71b], A. Cervelli[24b], G. Cesarini[53], S.A. Cetin[81], P.M. Chabrillat[129], R. Chakkappai[66], S. Chakraborty[172], A. Chambers[61], J. Chan[18a], W.Y. Chan[158], J.D. Chapman[33], E. Chapon[137], B. Chargeishvili[154b], D.G. Charlton[21], C. Chauhan[133], Y. Che[113a], S. Chekanov[6], G.A. Chelkov[39,a], B. Chen[170], H. Chen[30], J. Chen[143a], J. Chen[147], M. Chen[128], S. Chen[88], S.J. Chen[113a], X. Chen[143a], X. Chen[15,ah], Z. Chen[62], C.L. Cheng[175], H.C. Cheng[64a], S. Cheong[148], A. Cheplakov[39], E. Cherepanova[116], E. Cheu[7], K. Cheung[65], L. Chevalier[137], G. Chiarelli[74a], G. Chiodini[70a], A.S. Chisholm[21], A. Chitan[28b], M. Chitishvili[168], M.V. Chizhov[39,r], K. Choi[11], Y. Chou[141], E.Y.S. Chow[115], K.L. Chu[174], M.C. Chu[64a], Z. Chubinidze[53], J. Chudoba[133], J.J. Chwastowski[87], D. Cieri[111], K.M. Ciesla[86a], V. Cindro[94], A. Ciocio[18a], F. Cirotto[72a,72b], Z.H. Citron[174], M. Citterio[71a], D.A. Ciubotaru[28b], A. Clark[56], P.J. Clark[52], N. Clarke Hall[97], C. Clarry[160], S.E. Clawson[48], C. Clement[47a,47b], L. Clissa[24b,24a],

Y. Coadou [103], M. Cobal [69a,69c], A. Coccaro [57b], R.F. Coelho Barrue [132a], R. Coelho Lopes De Sa [104], S. Coelli [71a], M.M. Cohen [130], L.S. Colangeli [160], B. Cole [42], P. Collado Soto [100], J. Collot [60], R. Coluccia[70a,70b], P. Conde Muiño [132a,132g], M.P. Connell [34c], S.H. Connell [34c], E.I. Conroy [128], M. Contreras Cossio [11], F. Conventi [72a,aj], A.M. Cooper-Sarkar [128], L. Corazzina [75a,75b], F.A. Corchia [24b,24a], A. Cordeiro Oudot Choi [141], L.D. Corpe [41], M. Corradi [75a,75b], F. Corriveau [105,ab], A. Cortes-Gonzalez [158], M.J. Costa [168], F. Costanza [4], D. Costanzo [144], J. Couthures [4], G. Cowan [96], K. Cranmer [175], L. Cremer [49], D. Cremonini [24b,24a], S. Crépé-Renaudin [60], F. Crescioli [129], T. Cresta [73a,73b], M. Cristinziani [146], M. Cristoforetti [78a,78b], E. Critelli [97], A. Cueto [100], H. Cui [97], Z. Cui [7], B.M. Cunnett [151], W.R. Cunningham [59], F. Curcio [168], J.R. Curran [52], M.J. Da Cunha Sargedas De Sousa [57b,57a], J.V. Da Fonseca Pinto [82b], C. Da Via [102], W. Dabrowski [86a], T. Dado [37], S. Dahbi [153], T. Dai [107], D. Dal Santo [20], C. Dallapiccola [104], M. Dam [43], G. D'amen [30], V. D'Amico [110], J.R. Dandoy [35], M. D'Andrea [57b,57a], D. Dannheim [37], G. D'anniballe [74a,74b], M. Danninger [147], V. Dao [150], G. Darbo [57b], S.J. Das [30], F. Dattola [48], S. D'Auria [71a,71b], A. D'Avanzo [72a,72b], T. Davidek [135], J. Davidson [172], I. Dawson [95], K. De [8], C. De Almeida Rossi [160], R. De Asmundis [72a], N. De Biase [48], S. De Castro [24b,24a], N. De Groot [115], P. de Jong [116], H. De la Torre [117], A. De Maria [113a], A. De Salvo [75a], U. De Sanctis [76a,76b], F. De Santis [70a,70b], A. De Santo [151], J.B. De Vivie De Regie [60], J. Debevc [94], D.V. Dedovich[39], J. Degens [93], A.M. Deiana [45], J. Del Peso [100], L. Delagrange [129], F. Deliot [137], C.M. Delitzsch [49], M. Della Pietra [72a,72b], D. Della Volpe [56], A. Dell'Acqua [37], L. Dell'Asta [71a,71b], M. Delmastro [4], C.C. Delogu [57b,57a], P.A. Delsart [60], S. Demers [177], M. Demichev [39], S.P. Denisov [38], H. Denizli [22a,l], M.G. Depala [93], L. D'Eramo [41], D. Derendarz [87], F. Derue [129], P. Dervan [93,*], A.M. Desai [1], K. Desch [25], F.A. Di Bello [74a,74b], A. Di Ciaccio [76a,76b], L. Di Ciaccio [4], C. Di Donato [72a,72b], A. Di Girolamo [37], G. Di Gregorio [66], A. Di Luca [78a,78b], B. Di Micco [77a,77b], R. Di Nardo [77a,77b], K.F. Di Petrillo [40], M. Diamantopoulou [35], F.A. Dias [116], M.A. Diaz [139a,139b], A.R. Didenko [39], M. Didenko [168], S.D. Diefenbacher [18a], E.B. Diehl [107], S. Díez Cornell [48], C. Diez Pardos [146], C. Dimitriadi [149], A. Dimitrievska [21], A. Dimri [150], Y. Ding[62], J. Dingfelder [25], T. Dingley [128], I-M. Dinu [28b], S.J. Dittmeier [63b], F. Dittus [37], M. Divisek [135], B. Dixit [93], F. Djama [103], T. Djobava [154b], C. Doglioni [102,99], A. Dohnalova [29a], Z. Dolezal [135], K. Domijan [86a], K.M. Dona [40], M. Donadelli [82d], B. Dong [108], J. Donini [41], A. D'Onofrio [72a,72b], M. D'Onofrio [93], J. Dopke [136], A. Doria [72a], N. Dos Santos Fernandes [132a], I.A. Dos Santos Luz [82e], P. Dougan [45], M.T. Dova [91], A.T. Doyle [59], M.P. Drescher [55], E. Dreyer [174], I. Drivas-koulouris [10], M. Drnevich [119], D. Du [62], T.A. du Pree [116], Z. Duan[113a], M. Dubau [4], F. Dubinin [39], M. Dubovsky [29a], E. Duchovni [174], G. Duckeck [110], P.K. Duckett[97], O.A. Ducu [28b], D. Duda [52], A. Dudarev [37], M.M. Dudek [87], E.R. Duden [27], M. D'uffizi [102], L. Duflot [66], M. Dührssen [37], I. Duminica [28g], A.E. Dumitriu [28b], M. Dunford [63a], A. Duperrin [103], H. Duran Yildiz [3a], A. Durglishvili [154b], G.I. Dyckes [18a], M. Dyndal [86a], B.S. Dziedzic [37], Z.O. Earnshaw [151], G.H. Eberwein [128], B. Eckerova [29a], S. Eggebrecht [55], E. Egidio Purcino De Souza [82e], G. Eigen [17], K. Einsweiler [18a], T. Ekelof [166], P.A. Ekman [99], S. El Farkh [36b], Y. El Ghazali [62], H. El Jarrari [105], A. El Moussaouy [36a], I. Elbaz [156], D. Elitez [37], M. Ellert [166], F. Ellinghaus [176], T.A. Elliot [96], J. Elmsheuser [30], M. Elsawy [118a], M. Elsing [37], D. Emeliyanov [136], Y. Enari [83], S. Epari [109], D. Ernani Martins Neto [87], F. Ernst[37], M. Escalier [66], C. Escobar [168], R. Estevam De Paula [82c], E. Etzion [156], G. Evans [132a,132b], H. Evans [68], L.S. Evans [48], A. Ezhilov [38], S. Ezzarqtouni [36a], F. Fabbri [24b,24a], L. Fabbri [24b,24a], G. Facini [97], V. Fadeyev [138], R.M. Fakhrutdinov [38], D. Fakoudis [101], S. Falciano [75a], L.F. Falda Ulhoa Coelho [27], F. Fallavollita [111], G. Falsetti [44b,44a], J. Faltova [135], C. Fan [167], K.Y. Fan [64b], Y. Fan [14], Y. Fang [14,113c], M. Fanti [71a,71b], M. Faraj [69a,69c], Z. Farazpay [98],

A. Farbin[8], A. Farilla[77a], K. Farman[153], J.N. Farr[177], M.S. Farrington[61], S.M. Farrington[136,52], F. Fassi[36e], D. Fassouliotis[9], L. Fayard[66], P. Federic[135], P. Federicova[133], O.L. Fedin[38,a], M. Feickert[175], L. Feligioni[103], D.E. Fellers[18a], C. Feng[142a], Y. Feng[14], Z. Feng[66], B. Fernandez Barbadillo[92], P. Fernandez Martinez[67], M.J.V. Fernoux[103], J. Ferrando[92], A. Ferrari[166], P. Ferrari[116,115], R. Ferrari[73a], D. Ferrere[56], C. Ferretti[107], M.P. Fewell[1], D. Fiacco[75a,75b], F. Fiedler[101], P. Fiedler[134], S. Filimonov[39], M.S. Filip[28b,s], A. Filipčič[94], E.K. Filmer[161a], F. Filthaut[115], M.C.N. Fiolhais[132a,132c,c], L. Fiorini[168], W.C. Fisher[108], T. Fitschen[102], P.M. Fitzhugh[137], I. Fleck[146], P. Fleischmann[107], T. Flick[176], M. Flores[34d,ag], L.R. Flores Castillo[64a], M. Foll[127], F.M. Follega[78a,78b], N. Fomin[33], J.H. Foo[160], A. Formica[137], A.C. Forti[102], E. Fortin[150], A.W. Fortman[18a], L. Foster[18a], L. Fountas[9], H. Fox[92], P. Francavilla[74a,74b], S. Francescato[61], S. Franchellucci[56], M. Franchini[24b,24a], S. Franchino[63a], D. Francis[37], L. Franco[48], L. Franconi[48], M. Franklin[61], G. Frattari[27], Y.Y. Frid[156], J. Friend[59], N. Fritzsche[37], A. Froch[56], D. Froidevaux[37], J.A. Frost[136], Y. Fu[108], S. Fuenzalida Garrido[139g], M. Fujimoto[150], K.Y. Fung[64a], E. Furtado De Simas Filho[82e], M. Furukawa[158], M. Fuste Costa[48], J. Fuster[168], A. Gaa[55], A. Gabrielli[24b,24a], A. Gabrielli[160], P. Gadow[37], G. Gagliardi[57b,57a], L.G. Gagnon[18a], S. Gaid[84b], S. Galantzan[156], J. Gallagher[1], E.J. Gallas[128], A.L. Gallen[166], B.J. Gallop[136], K.K. Gan[121], Y. Gao[52], Z. Gao[113a], A. Garabaglu[141], F.M. Garay Walls[139a,139b], C. García[168], A. Garcia Alonso[116], A.G. Garcia Caffaro[177], J.E. García Navarro[168], M.A. Garcia Ruiz[23b], M. Garcia-Sciveres[18a], G.L. Gardner[130], R.W. Gardner[40], N. Garelli[163], R.B. Garg[148], J.M. Gargan[33], C.A. Garner[160], C.M. Garvey[34a], V.K. Gassmann[163], G. Gaudio[73a], V. Gautam[13], J. Gavranovic[94], I.L. Gavrilenko[132a], A. Gavrilyuk[38], C. Gay[169], G. Gaycken[125], A. Gekow[121], C. Gemme[57b], M.H. Genest[60], A.D. Gentry[114], S. George[96], T. Geralis[46], A.A. Gerwin[122], P. Gessinger-Befurt[37], M. Ghani[172], K. Ghorbanian[95], A. Ghosal[146], A. Ghosh[164], A. Ghosh[7], B. Giacobbe[24b], S. Giagu[75a,75b], A. Giannini[62], S.M. Gibson[96], D.T. Gil[86b], A.K. Gilbert[86a], B.J. Gilbert[42], D. Gillberg[35], G. Gilles[116], D.M. Gingrich[2,ai], M.P. Giordani[69a,69c], P.F. Giraud[137], G. Giugliarelli[69a,69c], D. Giugni[71a], F. Giuli[76a,76b], I. Gkialas[9,i], L.K. Gladilin[38], C. Glasman[100], M. Glazewska[20], R.M. Gleason[164], G. Glemža[48], M. Glisic[125], I. Gnesi[44b], Y. Go[30], M. Goblirsch-Kolb[37], B. Gocke[49], D. Godin[109], B. Gokturk[22a], S. Goldfarb[106], T. Golling[56], M.G.D. Gololo[34c], A. Golub[141], D. Golubkov[38], J.P. Gombas[108], A. Gomes[132a,132b], G. Gomes Da Silva[146], A.J. Gomez Delegido[37], R. Gonçalo[132a], A. Gongadze[154c], F. Gonnella[21], J.L. Gonski[148], R.Y. González Andana[52], S. González de la Hoz[168], M.V. Gonzalez Rodrigues[48], R. Gonzalez Suarez[166], S. Gonzalez-Sevilla[56], L. Goossens[37], B. Gorini[37], E. Gorini[70a,70b], A. Gorišek[94], T.C. Gosart[130], A.T. Goshaw[51], M.I. Gostkin[39], S. Goswami[123], C.A. Gottardo[37], S.A. Gotz[110], M. Gouighri[36b], A.G. Goussiou[141], N. Govender[34c], R.P. Grabarczyk[128], I. Grabowska-Bold[86a], K. Graham[35], E. Gramstad[127], S. Grancagnolo[70a,70b], C.M. Grant[1], P.M. Gravila[28f], F.G. Gravili[70a,70b], H.M. Gray[18a], M. Greco[111], M.J. Green[1], C. Grefe[25], A.S. Grefsrud[17], I.M. Gregor[48], K.T. Greif[164], P. Grenier[148], S.G. Grewe[111], K. Grimm[32], S. Grinstein[13,x], E. Gross[174], J. Grosse-Knetter[55], L.H. Grossman[18b], L. Guan[107], G. Guerrieri[37], R. Guevara[127], R. Gugel[101], J.A.M. Guhit[107], A. Guida[19], E. Guilloton[172], S. Guindon[37], F. Guo[14,113c], J. Guo[143a], L. Guo[48], L. Guo[113b,u], Y. Guo[107], Y. Guo[42], A. Gupta[49], R. Gupta[131], S. Gupta[27], S. Gurbuz[25], S.S. Gurdasani[48], G. Gustavino[75a,75b], P. Gutierrez[122], L.F. Gutierrez Zagazeta[130], M. Gutsche[50], C. Gutschow[97], C. Gwenlan[128], C.B. Gwilliam[93], E.S. Haaland[127], A. Haas[119], M. Habedank[59], C. Haber[18a], H.K. Hadavand[8], A. Haddad[41],

A. Hadef [50], A.I. Hagan [92], J.J. Hahn [146], M. Haleem [171], J. Haley [123], G.D. Hallewell [103], J.A. Hallford [48], K. Hamano [170], H. Hamdaoui [166], M. Hamer [25], S.E.D. Hammoud [66], E.J. Hampshire [96], L. Han [113a], L. Han [62], S. Han [14], K. Hanagaki [83], M. Hance [138], D.A. Hangal [42], H. Hanif [147], M.D. Hank [130], J.B. Hansen [43], P.H. Hansen [43], T. Harenberg [176], S. Harkusha [178], M.L. Harris [104], Y.T. Harris [25], J. Harrison [13], P.F. Harrison[172], M.L.E. Hart [97], N.M. Hartman [111], N.M. Hartmann [110], R.Z. Hasan [96,136], Y. Hasegawa [145], D. Hashimoto [112], F. Haslbeck [37], S. Hassan [17], R. Hauser [108], M. Haviernik [135], C.M. Hawkes [21], R.J. Hawkings [37], Y. Hayashi [158], D. Hayden [108], R.L. Hayes [116], C.P. Hays [128], J.M. Hays [95], H.S. Hayward [93], M. He [14,113c], Y. He [48], Y. He [97], N.B. Heatley [95], V. Hedberg [99], J. Heilman [35], S. Heim [48], T. Heim [18a], J.J. Heinrich [125], L. Heinrich [111], J. Hejbal [133], M. Helbig [50], A. Held [175], S. Hellesund [17], C.M. Helling [169], H. Herde [99], Y. Hernández Jiménez [150], L.M. Herrmann [25], G. Herten [54], R. Hertenberger [110], L. Hervas [37], M.E. Hesping [101], N.P. Hessey [161a], J. Hessler [111], M. Hidaoui [36b], N. Hidic [135], E. Hill [160], T.S. Hillersoy [17], S.J. Hillier [21], J.R. Hinds [108], F. Hinterkeuser [25], M. Hirose [126], S. Hirose [162], D. Hirschbuehl [176], T.G. Hitchings [102], B. Hiti [94], J. Hobbs [150], R. Hobincu [28e], N. Hod [174], A.M. Hodges [167], M.C. Hodgkinson [144], B.H. Hodkinson [128], A. Hoecker [37], D.D. Hofer [107], J. Hofer [168], J. Hofner [101], M. Holzbock [37], L.B.A.H. Hommels [33], V. Homsak [128], J.J. Hong [68], T.M. Hong [131], B.H. Hooberman [167], W.H. Hopkins [6], M.C. Hoppesch [167], Y. Horii [112], M.E. Horstmann [111], S. Hou [153], M.R. Housenga [167], J. Howarth [59], J. Hoya [6], M. Hrabovsky [124], T. Hryn'ova [4], P.J. Hsu [65], S.-C. Hsu [141], T. Hsu [66], M. Hu [18a], Q. Hu [62], S. Huang [33], X. Huang [14,113c], Y. Huang [135], Y. Huang [113b], Y. Huang [14], Z. Huang [66], Z. Hubacek [134], F. Huegging [25], T.B. Huffman [128], M. Hufnagel Maranha De Faria [82a], C.A. Hugli [48], M. Huhtinen [37], S.K. Huiberts [127], R. Hulsken [105], C.E. Hultquist [18a], D.L. Humphreys [104], N. Huseynov [12], A. Huss [37], J. Huston [108], B. Huth [37], J. Huth [61], L. Huth [48], R. Hyneman [7], G. Iacobucci [56], G. Iakovidis [30], L. Iconomidou-Fayard [66], J.P. Iddon [37], P. Iengo [72a,72b], Y. Iiyama [158], T. Iizawa [158], Y. Ikegami [83], D. Iliadis [157], N. Ilic [160], H. Imam [36a], G. Inacio Goncalves [82d], S.A. Infante Cabanas [139c], T. Ingebretsen Carlson [47a,47b], J.M. Inglis [95], G. Introzzi [73a,73b], M. Iodice [77a], V. Ippolito [75a,75b], R.K. Irwin [93], M. Ishino [158], W. Islam [175], C. Issever [19], S. Istin [22a,ao], K. Itabashi [126], H. Ito [173], R. Iuppa [78a,78b], A. Ivina [174], S. Izumiyama [112], V. Izzo [72a], P. Jacka [134], P. Jackson [1], P.R. Jacobson [51], P. Jain [48], K. Jakobs [54], T. Jakoubek [174], J. Jamieson [59], W. Jang [158], S. Jankovych [116], M. Javurkova [104], P. Jawahar [102], L. Jeanty [125], J. Jejelava [154a,ae], P. Jenni [54,f], C.E. Jessiman [35], H. Jia [169], J. Jia [150], X. Jia [111,113c], Z. Jia [113a], C. Jiang [52], Q. Jiang [64b], S. Jiggins [48], M. Jimenez Ortega [168], J. Jimenez Pena [13], S. Jin [113a], A. Jinaru [28b], O. Jinnouchi [140], P. Johansson [144], K.A. Johns [7], J.W. Johnson [138], F.A. Jolly [48], D.M. Jones [151], E. Jones [48], K.S. Jones[8], P. Jones [33], R.W.L. Jones [92], T.J. Jones [93], H.L. Joos [55], R. Joshi [121], J. Jovicevic [16], X. Ju [18a], J.J. Junggeburth [37], T. Junkermann [63a], A. Juste Rozas [13,x], M.K. Juzek [87], S. Kabana [139f], A. Kaczmarska [87], S.A. Kadir[148], M. Kado [111], H. Kagan [121], M. Kagan [148], A. Kahn [130], C. Kahra [101], T. Kaji [158], E. Kajomovitz [155], N. Kakati [174], N. Kakoty [13], S. Kandel [8], N. Kanellos [10], N.J. Kang [138], D. Kar [34j], E. Karentzos [25], K. Karki [8], O. Karkout [116], S.N. Karpov [39], Z.M. Karpova [39], V. Kartvelishvili [92,154b], A.N. Karyukhin [38], E. Kasimi [157], J. Katzy [48], S. Kaur [35], K. Kawade [145], M.P. Kawale [122], C. Kawamoto [88], E.F. Kay [37], S. Kazakos [108], K. Kazakova [103], V.F. Kazanin [38], J.M. Keaveney [34a], R. Keeler [170], G.V. Kehris [61], J.S. Keller [35], J.M. Kelly [170], J.J. Kempster [151], O. Kepka [133], J. Kerr [161b], B.P. Kerridge [136], B.P. Kerševan [94], L. Keszeghova [29a], R.A. Khan [131], A. Khanov [123], A.G. Kharlamov [38], T. Kharlamova [38], M. Kholodenko [132a], T.J. Khoo [19], G. Khoriauli [171], Y. Khoulaki [36a], Y.A.R. Khwaira [129], D. Kim [6], D.W. Kim [18b], Y.K. Kim [40], N. Kimura [97], M.K. Kingston [55], C. Kirfel [25], F. Kirfel [25], J. Kirk [136], A.E. Kiryunin [111], S. Kita [162], O. Kivernyk [25], M. Klassen [163], C. Klein [35], L. Klein [171], M.H. Klein [45], S.B. Klein [56], U. Klein [93], A. Klimentov [30], P. Kluit [116], S. Kluth [111], E. Kneringer [79], T.M. Knight [160], A. Knue [49], M. Kobel [50], D. Kobylianskii [174], S.F. Koch [37], M. Kocian [148], P. Kodyš [135], D.M. Koeck [125], T. Koffas [35], O. Kolay [50], I. Koletsou [4], T. Komarek [87], K. Köneke [55], A.X.Y. Kong [1], T. Kono [120], N. Konstantinidis [97], P. Kontaxakis [56], B. Konya [99], R. Kopeliansky [42], S. Koperny [86a], R. Koppenhofer [54], K. Korcyl [87], K. Kordas [157,d], A. Korn [97], S. Korn [55], I. Korolkov [13], N. Korotkova [38], B. Kortman [116], O. Kortner [111], S. Kortner [111], W.H. Kostecka [117], M. Kostov [29a], V.V. Kostyukhin [146], A. Kotsokechagia [37], A. Kotwal [51], A. Koulouris [37], A. Kourkoumeli-Charalampidi [73a,73b], E. Kourlitis [111], O. Kovanda [125], R. Kowalewski [170], W. Kozanecki [125], A.S. Kozhin [38], V.A. Kramarenko [38], G. Kramberger [94], P. Kramer [25], A. Krasznahorkay [104], A.C. Kraus [117], J.W. Kraus [176], J.A. Kremer [48], N.B. Krengel [146], T. Kresse [50], L. Kretschmann [176], J. Kretzschmar [93], P. Krieger [160], K. Krizka [21], K. Kroeninger [49], H. Kroha [111], J. Kroll [133], J. Kroll [130], K.S. Krowpman [108], U. Kruchonak [39], H. Krüger [25], N. Krumnack[80], M.C. Kruse [51], O. Kuchinskaia [39], S. Kuday [3a], S. Kuehn [37], R. Kuesters [54], T. Kuhl [48], V. Kukhtin [39], Y. Kulchitsky [39], S. Kuleshov [139d,139b], J. Kull [1], E.V. Kumar [110], M. Kumar [34j], N. Kumari [48], P. Kumari [161b], A. Kupco [133], A. Kupich [38], O. Kuprash [54], H. Kurashige [85], L.L. Kurchaninov [161a], O. Kurdysh [4], A. Kurova [38], M. Kuze [140], A.K. Kvam [104], J. Kvita [124], N.G. Kyriacou [141], M. Laassiri [30], C. Lacasta [168], H. Lacker [19], D. Lacour [129], E. Ladygin [39], A. Lafarge [41], B. Laforge [129], T. Lagouri [177], F.Z. Lahbabi [36a], S. Lai [55], W.S. Lai [97], I.K. Lakomiec [55], J.E. Lambert [170], S. Lammers [68], W. Lampl [7], C. Lampoudis [157], G. Lamprinoudis [171], A.N. Lancaster [117], U. Landgraf [54], M.P.J. Landon [95], V.S. Lang [54], A.J. Lankford [164], F. Lanni [37], C.S. Lantz[167], K. Lantzsch [25], A. Lanza [73a], M. Lanzac Berrocal [168], T. Lari [71a], D. Larsen [17], L. Larson [11], F. Lasagni Manghi [24b], M. Lassnig [37], S.D. Lawlor [144], R. Lazaridou[164], M. Lazzaroni [71a,71b], E.T.T. Le [164], H.D.M. Le [108], E.M. Le Boulicaut [177], L.T. Le Pottier [18a], B. Leban [24b,24a], F. Ledroit-Guillon [60], T.F. Lee [161b], L.L. Leeuw [34h], M. Lefebvre [170], C. Leggett [18a], G. Lehmann Miotto [37], M. Leigh [56], W.A. Leight [104], W. Leinonen [115], A. Leisos [157,t], M.A.L. Leite [82c], C.E. Leitgeb [19], R. Leitner [135], K.J.C. Leney [45], T. Lenz [25], S. Leone [74a], C. Leonidopoulos [52], A. Leopold [149], J. LePage Bourbonnais [35], R. Les [108], C.G. Lester [33], M. Levchenko [38], J. Levêque [4], L.J. Levinson [174], G. Levrini [24b,24a], M.P. Lewicki [87], C. Lewis [141], D.J. Lewis [4], L. Lewitt [144], A. Li [30], B. Li [142a], C. Li[107], C-Q. Li [111], H. Li [142a], H. Li [102], H. Li [15], H. Li[62], H. Li [142a], J. Li [143a], L. Li [143a], R. Li [177], S. Li [143b,143a], T. Li [5], Y. Li[14], Z. Li [14,113c], Z. Li [62], S. Liang [14,113c], Z. Liang [14], M. Liberatore [137], B. Liberti [76a], G.B. Libotte [82d], K. Lie [64c], J. Lieber Marin [82e], H. Lien [68], H. Lin [107], S.F. Lin [150], L. Linden [110], R.E. Lindley [7], J.H. Lindon [37], J. Ling [61], E. Lipeles [130], A. Lipniacka [17], A. Lister [169], J.D. Little [68], B. Liu [14], B.X. Liu [113b], D. Liu [155], D. Liu [138], E.H.L. Liu [21], J.K.K. Liu [119], K. Liu [143b], K. Liu [143b], M. Liu [62], M.Y. Liu [62], P. Liu [142a], Q. Liu [148], S. Liu [150], X. Liu [142a], Y. Liu [113b,113c], Y. Liu [167], Y.L. Liu [142a], Y.W. Liu [62], Z. Liu [66,j], S.L. Lloyd [95], E.M. Lobodzinska [48], P. Loch [7], E. Lodhi [160], K. Lohwasser [144], E. Loiacono [48], J.D. Lomas [21], I. Longarini [164], R. Longo [167], A. Lopez Solis [13], N.A. Lopez-canelas [7], N. Lorenzo Martinez [4], A.M. Lory [110], M. Losada [118a], G. Löschcke Centeno [4], X. Lou [14,113c], P.A. Love [92], M. Lu [66], S. Lu [130], Y.J. Lu [153], H.J. Lubatti [141], C. Luci [75a,75b], F.L. Lucio Alves [113a], F. Luehring [68], B.S. Lunday [130], O. Lundberg [149], J. Lunde [37], N.A. Luongo [6], M.S. Lutz [170], A.B. Lux [26], D. Lynn [30], R. Lysak [133], V. Lysenko [134], E. Lytken [99], V. Lyubushkin [39], T. Lyubushkina [39], M.M. Lyukova [150], H. Ma [30], K. Ma [62], L.L. Ma [142a], W. Ma [62], Y. Ma [123], J.C. MacDonald [101], P.C. Machado De Abreu Farias [82e], D. Macina [37], R. Madar [41], T. Madula [97], J. Maeda [85], T. Maeno [30], P.T. Mafa [34f], H. Maguire [144], M. Maheshwari [33], V. Maiboroda [66], A. Maio [132a,132b,132d], K. Maj [86a], O. Majersky [48], S. Majewski [125], R. Makhmanazarov [38], N. Makovec [66], V. Maksimovic [16], B. Malaescu [129], J. Malamant[127], Pa. Malecki [87], V.P. Maleev [38], F. Malek [60,n], M. Mali [94], D. Malito [96], A. Maloizel [5], A. Malvezzi Lopes [82d], S. Malyukov[39], J. Mamuzic [94], G. Mancini [53], M.N. Mancini [27], G. Manco [73a,73b], S.S. Mandarry [151], I. Mandić [94], L. Manhaes de Andrade Filho [82a], I.M. Maniatis [174], J. Manjarres Ramos [90], D.C. Mankad [174], A. Mann [110], T. Manoussos [37], M.N. Mantinan [40], S. Manzoni [37], L. Mao [143a], X. Mapekula [34c], A. Marantis [157], R.R. Marcelo Gregorio [1], G. Marchiori [5], C. Marcon [71a], E. Maricic [16], M. Marinescu [48], S. Marium [48], M. Marjanovic [122], A. Markhoos [54], M. Markovitch [66], M.K. Maroun [104], M.C. Marr [147], G.T. Marsden[102], E.J. Marshall [92], Z. Marshall [18a], S. Marti-Garcia [168], J. Martin [97], T.A. Martin [136], V.J. Martin [52], B. Martin dit Latour [17], L. Martinelli [75a,75b], P. Martinez Agullo [168], V.I. Martinez Outschoorn [104], P. Martinez Suarez [37], S. Martin-Haugh [136], G. Martinovicova [135], V.S. Martoiu [28b], A.C. Martyniuk [97], A. Marzin [37], D. Mascione [78a,78b], L. Masetti [101], J. Masik [102], A.L. Maslennikov [39], S.L. Mason [42], P. Massarotti [72a,72b], P. Mastrandrea [74a,74b], A. Mastroberardino [44b,44a], T. Masubuchi [126], T.T. Mathew [125], J. Matousek [135], D.M. Mattern [49], K. Mauer [48], J. Maurer [28b], T. Maurin [59], A.J. Maury [66], B. Maček [94], C. Mavungu Tsava [103], D.A. Maximov [38], A.E. May [102], E. Mayer [41], R. Mazini [34j], S.M. Mazza [138], E. Mazzeo [37], J.P. Mc Gowan [170], S.P. Mc Kee [107], C.A. Mc Lean [6], C.C. McCracken [169], E.F. McDonald [106], L.F. Mcelhinney [92], J.A. Mcfayden [151], R.P. McGovern [130], R.P. Mckenzie [34j], D.J. Mclaughlin [97], S.J. McMahon [136], C.M. Mcpartland [93], R.A. McPherson [170,ab], S. Mehlhase [110], A. Mehta [93], D. Melini [168], B.R. Mellado Garcia [34j], A.H. Melo [55], F. Meloni [48], A.M. Mendes Jacques Da Costa [102], L. Meng [92], S. Menke [111], M. Mentink [37], E. Meoni [44b,44a], G. Mercado [117], S. Merianos [157], C. Merlassino [69a,69c], C. Meroni [71a,71b], J. Metcalfe [6], A.S. Mete [6], E. Meuser [101], C. Meyer [68], J-P. Meyer [137], Y. Miao[113a], R.P. Middleton [136], M. Mihovilovic [66], L. Mijović [52], G. Mikenberg [174], M. Mikestikova [133], M. Mikuž [94], H. Mildner [101], A. Milic [37], D.W. Miller [40], E.H. Miller [148], A. Milov [174], D.A. Milstead[47a,47b], T. Min[113a], A.A. Minaenko [38], I.A. Minashvili [154b], A.I. Mincer [119], B. Mindur [86a], M. Mineev [39], Y. Mino [88], L.M. Mir [13], M. Miralles Lopez [59], M. Mironova [18a], M. Missio [41], A. Mitra [172], V.A. Mitsou [168], Y. Mitsumori [112], P.S. Miyagawa [95], T. Mkrtchyan [37], M. Mlinarevic [97], T. Mlinarevic [97], M. Mlynarikova [135], L. Mlynarska [86a], C. Mo [143a], S. Mobius [20], M.H. Mohamed Farook [114], S. Mohapatra [42], M.F. Mohd Soberi [52], S. Mohiuddin [123], G. Mokgatitswane [34j], L. Moleri [174], U. Molinatti [128], L.G. Mollier [20], B. Mondal [133], S. Mondal [135], K. Mönig [48], E. Monnier [103], L. Monsonis Romero[168], A. Montella [47a,47b], M. Montella [121], F. Montereali [77a,77b], F. Monticelli [91], S. Monzani [69a,69c], A. Morancho Tarda [43], N. Morange [66], M. Moreno Llácer [168], C. Moreno Martinez [56], J.M. Moreno Perez[23b], P. Morettini [57b], S. Morgenstern [63a], M. Morii [61], M. Morinaga [158], F. Morodei [75a,75b], P. Moschovakos [37], B. Moser [54], M. Mosidze [154b], T. Moskalets [45], P. Moskvitina [115], J. Moss [32], T. Motta Quirino [82d], A. Moussa [36d], Y. Moyal [174,k], H. Moyano Gomez [13], E.J.W. Moyse [104], T.G. Mroz [87], S. Muanza [103], M. Mucha [25], J. Mueller [131], G.A. Mullier [166], A.J. Mullin[33], J.J. Mullin[51], A.C. Mullins[45], A.E. Mulski [61], D.P. Mungo [160], D. Munoz Perez [168], F.J. Munoz Sanchez [102], W.J. Murray [172,136], E. Musajan [62], M. Muškinja [94], C. Mwewa [48], A.G. Myagkov [38,a], A.J. Myers [8], G. Myers [107], M. Myska [134], B.P. Nachman [148], K. Nagai [128], K. Nagano [83], R. Nagasaka[158], J.L. Nagle [30,al], E. Nagy [103], A.M. Nairz [37], Y. Nakahama [83], K. Nakamura [83], K. Nakkalil [5], A. Nandi [63b],

H. Nanjo [126], E.A. Narayanan [45], Y. Narukawa [158], I. Naryshkin [38], L. Nasella [71a,71b], S. Nasri [118b], C. Nass [25], G. Navarro [23a], A. Nayaz [19], P.Y. Nechaeva [38], S. Nechaeva [24b,24a], F. Nechansky [133], L. Nedic [128], A. Negri [73a,73b], M. Negrini [24b], C. Nellist [116], C. Nelson [105], K. Nelson [107], S. Nemecek [133], M. Nessi [37,g], M.S. Neubauer [167], J. Newell [93], P.R. Newman [21], Y.W.Y. Ng [167], B. Ngair [118a], H.D.N. Nguyen [109], J.D. Nichols [122], R. Nicolaidou [137], J. Nielsen [138], M. Niemeyer [55], J. Niermann [37], N. Nikiforou [37], V. Nikolaenko [38,a], I. Nikolic-Audit [129], P. Nilsson [30], G. Ninio [156], A. Nisati [75a], R. Nisius [111], N. Nitika [174], E.K. Nkadimeng [34b], T. Nobe [158], D. Noll [148], T. Nommensen [152], M.B. Norfolk [144], B.J. Norman [35], L.C. Nosler[18a], M. Noury [36a], J. Novak [94], T. Novak [94], P. Novotny [174], R. Novotny [134], L. Nozka [124], K. Ntekas [37], D. Ntounis [148], N.M.J. Nunes De Moura Junior [82b], J. Ocariz [129], I. Ochoa [132a], A. Odella Rodriguez [13], S. Oerdek [48,y], J.T. Offermann [40], A. Ogrodnik [87], A. Oh [102], C.C. Ohm [149], H. Oide [83], M.L. Ojeda [37], Y. Okumura [158], L.F. Oleiro Seabra [132a], I. Oleksiyuk [56], G. Oliveira Correa [13], D. Oliveira Damazio [30], J.L. Oliver [1], R. Omar [68], A.P. O'Neill [20], Y. Onoda[140], A. Onofre [132a,132e,e], P.U.E. Onyisi [11], M.J. Oreglia [40], D. Orestano [77a,77b], R. Orlandini [77a,77b], R.S. Orr [160], L.M. Osojnak [42], Y. Osumi [112], G. Otero y Garzon [31], H. Otono [89], M. Ouchrif [36d], F. Ould-Saada [127], T. Ovsiannikova [141], M. Owen [59], R.E. Owen [136], V.E. Ozcan [22a], F. Ozturk [87], N. Ozturk [8], S. Ozturk [81], H.A. Pacey [128], K. Pachal [161a], A. Pacheco Pages [13], C. Padilla Aranda [13], G. Padovano [75a,75b], S. Pagan Griso [18a], L. Pagani [76a,76b], J. Pampel [25], J. Pan [177], D.K. Panchal [11], C.E. Pandini [60], J.G. Panduro Vazquez [136], H.D. Pandya [1], H. Pang [137], P. Pani [48], G. Panizzo [69a,69c], L. Panwar [129,w], L. Paolozzi [56], S. Parajuli [167], A. Paramonov [6], C. Paraskevopoulos [53], D. Paredes Hernandez [64b], S.R. Paredes Saenz [52], A. Pareti [73a,73b], K.R. Park [42], T.H. Park [111], F. Parodi [57b,57a], J.A. Parsons [42], U. Parzefall [54], B. Pascual Dias [41], L. Pascual Dominguez [100], E. Pasqualucci [75a], S. Passaggio [57b], F. Pastore [96], P. Patel [87], U.M. Patel [51], J.R. Pater [102], T. Pauly [37], F. Pauwels [135], C.I. Pazos [163], M. Pedersen [127], R. Pedro [132a], S.V. Peleganchuk [38], O. Penc [133], S. Peng [15], G.D. Penn [177], K.E. Penski [110], M. Penzin [38], B.S. Peralva [82d], A.P. Pereira Peixoto [141], L. Pereira Sanchez [148], D.V. Perepelitsa [30,al], G. Perera [104], E. Perez Codina [37], M. Perganti [10], H. Pernegger [37], S. Perrella [75a,75b], K. Peters [48], R.F.Y. Peters [102], B.A. Petersen [37], T.C. Petersen [43], E. Petit [103], V. Petousis [134], A.R. Petri [71a,71b], T. Petru [135], M. Pettee [18a], A. Petukhov [81], K. Petukhova [37], R. Pezoa [139g], L. Pezzotti [24b,24a], G. Pezzullo [177], L. Pfaffenbichler [37], A.J. Pfleger [79], T.M. Pham [175], T. Pham [106], P.W. Phillips [136], G. Piacquadio [150], E. Pianori [18a], F. Piazza [125], R. Piegaia [31], D. Pietreanu [28b], A.D. Pilkington [102], M. Pinamonti [69a,69c], J.L. Pinfold [2], G. Pinheiro Matos [42], B.C. Pinheiro Pereira [132a], J. Pinol Bel [13], A.E. Pinto Pinoargote [129], L. Pintucci [69a,69c], A. Pirttikoski [56], D.A. Pizzi [35], L. Pizzimento [64b], A. Plebani [33], M.-A. Pleier [30], V. Pleskot [135], E. Plotnikova[39], G. Poddar [95], R. Poettgen [99], L. Poggioli [129], S. Polacek [135], G. Polesello [73a], A. Poley [147], A. Polini [24b], C.S. Pollard [172], Z.B. Pollock [121], E. Pompa Pacchi [122], N.I. Pond [97], D. Ponomarenko [68], L. Pontecorvo [37], S. Popa [28a], G.A. Popeneciu [28d], A. Poreba [63a], D.M. Portillo Quintero [161a], S. Pospisil [134], M.A. Postill [144], P. Postolache [28c], K. Potamianos [172], P.A. Potepa [86a], I.N. Potrap [39], C.J. Potter [33], H. Potti [152], J. Poveda [168], M.E. Pozo Astigarraga [37], R. Pozzi [37], A. Prades Ibanez [76a,76b], S.R. Pradhan [144], J. Pretel [170], D. Price [102], M. Primavera [70a], L. Primomo [69a,69c], M.A. Principe Martin [100], R. Privara [124], T. Procter [86b], M.L. Proffitt [141], N. Proklova [130], K. Prokofiev [64c], G. Proto [111], J. Proudfoot [6], M. Przybycien [86a], W.W. Przygoda [86b], A. Psallidas [46], J.E. Puddefoot [144], D. Pudzha [53], P. Puhl [58], H.I. Purnell [1], D. Pyatiizbyantseva [115], J. Qian [107], R. Qian [108], D. Qichen [128], Y. Qin [13], T. Qiu [52], A. Quadt [55], M. Queitsch-Maitland [102], G. Quetant [56], R.P. Quinn [169], G. Rabanal Bolanos [61], D. Rafanoharana [111], F. Raffaeli [76a,76b], J.L. Rainbolt [40],

S. Rajagopalan [30], E. Ramakoti [39], L. Rambelli [57b,57a], I.A. Ramirez-Berend [35], K. Ran [107,113c], D.S. Rankin [130], N.P. Rapheeha [34j], H. Rasheed [28b], A. Rastogi [18a], S. Rave [101], S. Ravera [57b,57a], B. Ravina [37], I. Ravinovich [174], M. Raymond [37], A.L. Read [127], N.P. Readioff [144], D.M. Rebuzzi [73a,73b], A.S. Reed [59], K. Reeves [27], D. Reikher [37], A. Rej [49], C. Rembser [37], H. Ren [62], M. Renda [28b], F. Renner [48], A.G. Rennie [59], M. Repik [56], A.L. Rescia [57b,57a], S. Resconi [71a], M. Ressegotti [57b,57a], S. Rettie [116], W.F. Rettie [35], M.M. Revering [33], O.L. Rezanova [39], P. Reznicek [135], H. Riani [36d], N. Ribaric [51], B. Ricci [69a,69c], E. Ricci [78a,78b], R. Richter [111], S. Richter [47a,47b], E. Richter-Was [86b], M. Ridel [129], S. Ridouani [36d], P. Rieck [119], P. Riedler [37], E.M. Riefel [47a,47b], J.O. Rieger [116], M. Rimoldi [34c], L. Rinaldi [24b,24a], P. Rincke [166,55], G. Ripellino [166], I. Riu [13], J.C. Rivera Vergara [170], F. Rizatdinova [123], E. Rizvi [95], B.R. Roberts [40], S.S. Roberts [138], D. Robinson [33], A. Robson [59], A. Rocchi [76a,76b], C. Roda [74a,74b], F.A. Rodriguez [117], S. Rodriguez Bosca [37], Y. Rodriguez Garcia [23a], A.M. Rodríguez Vera [117], S. Roe[37], J.T. Roemer [37], O. Røhne [127], R.A. Rojas [37], C.P.A. Roland [129], A. Romaniouk [79], E. Romano [73a,73b], M. Romano [24b], N. Rompotis [93], L. Roos [129], S. Rosati [75a], B.J. Rosser [40], E. Rossi [128], E. Rossi [72a,72b], L.P. Rossi [61], L. Rossini [54], R. Rosten [121], M. Rotaru [28b], R. Roth [37], D. Rousseau [66], D. Rousso [48], S. Roy-Garand [160], A. Rozanov [103], Z.M.A. Rozario [59], Y. Rozen [155], A. Rubio Jimenez [168], V.H. Ruelas Rivera [19], T.A. Ruggeri [1], A. Ruggiero [128], A. Ruiz-Martinez [168], A. Rummler [37], G.B. Rupnik Boero [37], Z. Rurikova [54], N.A. Rusakovich [39], S. Ruscelli [49], H.L. Russell [170], G. Russo [138], J.P. Rutherfoord [7], S. Rutherford Colmenares [119], M. Rybar [135], P. Rybczynski [86a], A. Ryzhov [45], F. Safai Tehrani [75a], S. Saha [1], B. Sahoo [174], A. Saibel [168], B.T. Saifuddin [122], M. Saimpert [137], G.T. Saito [82c], M. Saito [158], T. Saito [158], A. Sala [71a,71b], A. Salnikov [148], J. Salt [168], A. Salvador Salas [156], F. Salvatore [151], A. Salzburger [37], D. Sammel [54], E. Sampson [92], D. Sampsonidis [157,d], D. Sampsonidou [125], M.A.A. Samy [59], J. Sánchez [168], V. Sanchez Sebastian [168], H. Sandaker [127], C.O. Sander [48], J.A. Sandesara [175], M. Sandhoff [176], C. Sandoval [23b], L. Sanfilippo [63a], D.P.C. Sankey [136], T. Sano [88], A. Sansoni [53], M. Santana Queiroz [18b], L. Santi [37], C. Santoni [41], H. Santos [132a,132b], L. Santos Pereira Trigo [48], E. Sanzani [24b,24a], K.A. Saoucha [84b], J.G. Saraiva [132a,132d], J. Sardain [7], O. Sasaki [83], K. Sato [162], C. Sauer[37], E. Sauvan [4], P. Savard [160,ai], R. Sawada [158], C. Sawyer [136], L. Sawyer [98], A.M. Sayed [27], C. Sbarra [24b], A. Sbrizzi [24b,24a], T. Scanlon [97], J. Schaarschmidt [141], U. Schäfer [101], A.C. Schaffer [66,45], D. Schaile [110], R.D. Schamberger [150], C. Scharf [19], M.M. Schefer [20], V.A. Schegelsky [38], D. Scheirich [135], M. Schernau [139f], C. Scheulen [56], C. Schiavi [57b,57a], M. Schioppa [44b,44a], S. Schlenker [37], J. Schmeing [176], E. Schmidt [111], M.A. Schmidt [176], K. Schmieden [25], C. Schmitt [101], N. Schmitt [101], S. Schmitt [48], N.A. Schneider [110], L. Schoeffel [137], A. Schoening [63b], P.G. Scholer [35], E. Schopf [146], M. Schott [25], S. Schramm [56], T. Schroer [56], H-C. Schultz-Coulon [63a], M. Schumacher [54], B.A. Schumm [138], Ph. Schune [137], H.R. Schwartz [7], A. Schwartzman [148], T.A. Schwarz [107], Ph. Schwemling [137], R. Schwienhorst [108], F.G. Sciacca [20], A. Sciandra [30], G. Sciolla [27], S.A. Scoville [131], F. Scuri [74a], C.D. Sebastiani [37], K. Sedlaczek [117], S.C. Seidel [114], B.D. Seidlitz [42], C. Seitz [48], J.M. Seixas [82b], G. Sekhniaidze [72a], L. Selem [129], N. Semprini-Cesari [24b,24a], A. Semushin [178], D. Sengupta [56], V. Senthilkumar [116], L. Serin [66], M. Sessa [72a,72b], H. Severini [122], F. Sforza [57b,57a], A. Sfyrla [56], Q. Sha [14], H. Shaddix [117], A.H. Shah [33], R. Shaheen [149], J.D. Shahinian [130], M. Shamim [37], L.Y. Shan [14], M. Shapiro [18a], A. Sharma [37], A.S. Sharma [169], P. Sharma [30], P.B. Shatalov [38], K. Shaw [151], S.M. Shaw [102], Q. Shen [14], D.J. Sheppard [147], P. Sherwood [97], L. Shi [113b], X. Shi [14], S. Shimizu [83], S. Shirabe [89], M. Shiyakova [39,z], M.J. Shochet [40], D.R. Shope [127], B. Shrestha [122],

S. Shrestha[121,an], I. Shreyber[39], M.J. Shroff[105], P. Sicho[133], A.M. Sickles[167], E. Sideras Haddad[34j,165], A.C. Sidley[116], A. Sidoti[24b], F. Siegert[50], Dj. Sijacki[16], F. Sili[62], J.M. Silva[52], I. Silva Ferreira[82b], M.V. Silva Oliveira[30], S.B. Silverstein[47a], S. Simion[66], R. Simoniello[37], E.L. Simpson[102], H. Simpson[151], L.R. Simpson[6], S. Simsek[81], S. Sindhu[55], S.N. Singh[27], S. Singh[30], S. Sinha[48], S. Sinha[102], M. Sioli[24b,24a], K. Sioulas[9], I. Siral[37], E. Sitnikova[48], J. Sjölin[47a,47b], A. Skaf[55], E. Skorda[21], P. Skubic[122], M. Slawinska[87], I. Slazyk[17], I. Sliusar[127], V. Smakhtin[174], B.H. Smart[136], S.Yu. Smirnov[139b], Y. Smirnov[34c], L.N. Smirnova[38,a], O. Smirnova[99], A.C. Smith[42], J.L. Smith[102], M.B. Smith[35], R. Smith[148], H. Smitmanns[101], M. Smizanska[92], K. Smolek[134], P. Smolyanskiy[134], A.A. Snesarev[39], H.L. Snoek[116], R.M. Snyder[51], S. Snyder[30], R. Sobie[170,ab], A. Soffer[156], C.A. Solans Sanchez[37], E.Yu. Soldatov[39], U. Soldevila[168], A.A. Solodkov[34j], S. Solomon[27], A. Soloshenko[39], K. Solovieva[54], O.V. Solovyanov[41], P. Sommer[50], A. Sonay[13], A. Sopczak[134], A.L. Sopio[52], F. Sopkova[29b], J.D. Sorenson[114], I.R. Sotarriva Alvarez[140], V. Sothilingam[63a], O.J. Soto Sandoval[139c,139b], S. Sottocornola[68], R. Soualah[84a], Z. Soumaimi[36e], D. South[48], N. Soybelman[174], S. Spagnolo[70a,70b], A.S. Spellman[125], D. Sperlich[54], B. Spisso[72a,72b], L. Splendori[103], M. Spousta[135], E.J. Staats[35], R. Stamen[63a], E. Stanecka[87], W. Stanek-Maslouska[48], M.V. Stange[50], B. Stanislaus[18a], M.M. Stanitzki[48], E.A. Starchenko[38], G.H. Stark[138], J. Stark[90], P. Staroba[133], P. Starovoitov[84b], R. Staszewski[87], C. Stauch[110], G. Stavropoulos[46], A. Stefl[37], A. Stein[101], P. Steinberg[30], B. Stelzer[147,161a], H.J. Stelzer[131], O. Stelzer[161a], H. Stenzel[58], T.J. Stevenson[151], G.A. Stewart[48], G. Stoicea[28b], M. Stolarski[132a], S. Stonjek[111], A. Straessner[50], J. Strandberg[149], S. Strandberg[47a,47b], M. Stratmann[176], M. Strauss[122], T. Strebler[103], P. Strizenec[29b], R. Ströhmer[171], D.M. Strom[125], R. Stroynowski[45], A. Strubig[47a,47b], S.A. Stucci[30], B. Stugu[17], J. Stupak[122], N.A. Styles[48], D. Su[148], S. Su[62], X. Su[62], D. Suchy[29a], A.D. Sudhakar Ponnu[55], L. Sudit[174], Y. Sue[83], K. Sugizaki[130], V.V. Sulin[38], D.M.S. Sultan[128], L. Sultanaliyeva[25], S. Sultansoy[3b], S. Sun[175], W. Sun[14], S. Sundar Raman[169], N. Sur[99], N. Suri Jr[177], M.R. Sutton[151], M. Svatos[133], P.N. Swallow[33], M. Swiatlowski[161a], A. Swoboda[37], I. Sykora[29a], M. Sykora[135], T. Sykora[135], D. Ta[101], K. Tackmann[48,y], A. Taffard[164], R. Tafirout[161a], Y. Takubo[83], M. Talby[103], A.A. Talyshev[38], N.M. Tamir[156], A. Tanaka[158], J. Tanaka[158], R. Tanaka[66], M. Tanasini[150], Z. Tao[169], S. Tapia Araya[139g], S. Tapprogge[101], A. Tarek Abouelfadl Mohamed[37], S. Tarem[155], K. Tariq[14], G. Tarna[37], G.F. Tartarelli[71a], M.J. Tartarin[90], P. Tas[135], M. Tasevsky[133], E. Tassi[44b,44a], A.C. Tate[167], Y. Tayalati[36e,aa], G.N. Taylor[106], W. Taylor[161b], R.J. Taylor Vara[168], A.S. Tegetmeier[90], P. Teixeira-Dias[96], J.J. Teoh[160], K. Terashi[158], J. Terron[100], S. Terzo[13], M. Testa[53], R.J. Teuscher[160,ab], A. Thaler[79], O. Theiner[56], T. Theveneaux-Pelzer[103], J.P. Thomas[21], E.A. Thompson[18a], P.D. Thompson[21], E. Thomson[130], R.E. Thornberry[45], C. Tian[62], Y. Tian[56], V. Tikhomirov[81], Yu.A. Tikhonov[39], S. Timoshenko[38], D. Timoshyn[135], E.X.L. Ting[1], P. Tipton[177], A. Tishelman-Charny[30], K. Todome[140], S. Todorova-Nova[135], L. Toffolin[69a,69c], M. Togawa[83], J. Tojo[89], S. Tokár[29a], O. Toldaiev[68], G. Tolkachev[103], M. Tomoto[83], L. Tompkins[148], E. Torrence[125], H. Torres[90], D.I. Torres Arza[139g], E. Torró Pastor[168], M. Toscani[31], C. Tosciri[40], M. Tost[11], D.R. Tovey[144], T. Trefzger[171], P.M. Tricarico[13], A. Tricoli[30], I.M. Trigger[161a], S. Trincaz-Duvoid[129], D.A. Trischuk[170], A. Tropina[39], D. Truncali[76a,76b], L. Truong[34c], M. Trzebinski[87], A. Trzupek[87], F. Tsai[150], M. Tsai[107], A. Tsiamis[157], P.V. Tsiareshka[39], S. Tsigaridas[161a], A. Tsirigotis[157,t], V. Tsiskaridze[154a], E.G. Tskhadadze[154a], Y. Tsujikawa[88], I.I. Tsukerman[38], V. Tsulaia[18a], K. Tsuri[120], D. Tsybychev[150], Y. Tu[64b], A. Tudorache[28b], V. Tudorache[28b], S.B. Tuncay[128],

S. Turchikhin [57b,57a], I. Turk Cakir [3a], R. Turra [71a], T. Turtuvshin [39,ac], P.M. Tuts [42], Y. Uematsu [83], F. Ukegawa [162], P.A. Ulloa Poblete [139c,139b], G. Unal [37], A. Undrus [30], J. Urban [29b], P. Urrejola [139e], G. Usai [8], R. Ushioda [159], M. Usman [109], F. Ustuner [52], Z. Uysal [81], V. Vacek [134], B. Vachon [105], T. Vafeiadis [37], A. Vaitkus [97], C. Valderanis [110], E. Valdes Santurio [47a,47b], M. Valente [37], S. Valentinetti [24b,24a], A. Valero [168], E. Valiente Moreno [168], A. Vallier [90], J.A. Valls Ferrer [168], D.R. Van Arneman [116], R. Van Den Broucke [129], A. Van Der Graaf [49], H.Z. Van Der Schyf [34j], P. Van Gemmeren [6], M. Van Rijnbach [37], S. Van Stroud [97], I. Van Vulpen [116], P. Vana [135], M. Vanadia [76a,76b], U.M. Vande Voorde [149], W. Vandelli [37], E.R. Vandewall [148], D. Vannicola [156], L. Vannoli [53], R. Vari [75a], M. Varma [177], E.W. Varnes [7], C. Varni [79], D. Varouchas [66], L. Varriale [168], K.E. Varvell [152], M.E. Vasile [28b], L. Vaslin[83], M.D. Vassilev [148], A. Vasyukov [39], L.M. Vaughan [123], R. Vavricka[135], T. Vazquez Schroeder [13], J. Veatch [32], V. Vecchio [102], M.J. Veen [104], I. Veliscek [30], I. Velkovska [94], L.M. Veloce [160], F. Veloso [132a,132c], A.G. Veltman [52], S.H. Venetianer [163], S. Veneziano [75a], A. Ventura [70a,70b], A. Verbytskyi [111], M. Verducci [74a,74b], C. Vergis [95], M. Verissimo De Araujo [82b], W. Verkerke [116], J.C. Vermeulen [116], C. Vernieri [148], M. Vessella [164], M.C. Vetterli [147,ai], A. Vgenopoulos [101], N. Viaux Maira [139g,af], T. Vickey [144], O.E. Vickey Boeriu [144], G.H.A. Viehhauser [128], L. Vigani [63b], M. Vigl [111], M. Villa [24b,24a], M. Villaplana Perez [168], E.M. Villhauer[40], E. Vilucchi [53], M. Vincent [168], M.G. Vincter [35], A. Visibile [116], A. Visive [116], C. Vittori [37], I. Vivarelli [24b,24a], M.I. Vivas Albornoz [48], E. Voevodina [111], F. Vogel [110], J.C. Voigt [50], P. Vokac [134], Yu. Volkotrub [86b], L. Vomberg [25], E. Von Toerne [25], B. Vormwald [37], K. Vorobev [51], M. Vos [168], K. Voss [146], M. Vozak [37], L. Vozdecky [122], N. Vranjes [16], M. Vranjes Milosavljevic [16], M. Vreeswijk [116], N.K. Vu [143b,143a], R. Vuillermet [37], O. Vujinovic [101], I. Vukotic [40], I.K. Vyas [35], J.F. Wack [33], A. Wada [112], S. Wada [162], C. Wagner[148], J.M. Wagner [18a], W. Wagner [176], S. Wahdan [176], H. Wahlberg [91], C.H. Waits [122], J. Walder [136], R. Walker [110], K. Walkingshaw Pass [59], W. Walkowiak [146], A. Wall [130], E.J. Wallin [99], T. Wamorkar [148], K. Wandall-Christensen [168], A. Wang [62], A.Z. Wang [138], C. Wang [48], C. Wang [11], H. Wang [18a], J. Wang [64c], P. Wang [102], P. Wang [97], R. Wang [61], R. Wang [107], R. Wang [6], S.M. Wang [153], S. Wang [14], T. Wang [115], T. Wang [62], W.T. Wang [128], X. Wang [167], X. Wang [143a], X. Wang [48], Y. Wang [150], Y. Wang [114], Z. Wang [107], Z. Wang [143b], Z. Wang [107], C. Wanotayaroj [83], A. Warburton [105], A.L. Warnerbring [146], S. Waterhouse [96], A.T. Watson [21], H. Watson [52], M.F. Watson [21], E. Watton [37], G. Watts [141], B.M. Waugh [97], J.M. Webb [54], C. Weber [30], M.S. Weber [20], C. Wei [62], Y. Wei [54], A.R. Weidberg [128], E.J. Weik [119], J. Weingarten [49], C. Weiser [54], C.J. Wells [48], T. Wenaus [30], T. Wengler [37], N.S. Wenke[111], N. Wermes [25], M. Wessels [63a], A.M. Wharton [92], A.S. White [37], A. White [8], M.J. White [1], D. Whiteson [164], L. Wickremasinghe [126], W. Wiedenmann [175], M. Wielers [136], R. Wierda [149], C. Wiglesworth [43], H.G. Wilkens [37], J.J.H. Wilkinson [33], S. Williams [33], S. Willocq [104], D.J. Wilson [102], P.J. Windischhofer [40], F.I. Winkel [31], F. Winklmeier [125], B.T. Winter [54], M. Wittgen[148], M. Wobisch [98], T. Wojtkowski[60], Z. Wolffs [116], J. Wollrath[37], M.W. Wolter [87], H. Wolters [132a,132c], M.C. Wong[138], E.L. Woodward [42], S.D. Worm [48], B.K. Wosiek [87], K.W. Woźniak [87], S. Wozniewski [55], K. Wraight [59], C. Wu [160], C. Wu [21], J. Wu [158], M. Wu [113b], M. Wu [115], S.L. Wu [175], S. Wu [14,ak], X. Wu [62], Y.Q. Wu [160], Y. Wu [62], Z. Wu [4], Z. Wu [113a], J. Wuerzinger [111], T.R. Wyatt [102], B.M. Wynne [52], S. Xella [43], L. Xia [113a], M. Xie [62], A. Xiong [125], D. Xu [14], H. Xu [62], L. Xu [62], R. Xu [130], T. Xu [107], W. Xu[113a], Y. Xu [141], Z. Xu [52], R. Xue [131], B. Yabsley [152], S. Yacoob [11], Y. Yamaguchi [83], E. Yamashita [158], H. Yamauchi [162], T. Yamazaki [18a], Y. Yamazaki [85], S. Yan [59], Z. Yan [104], H.J. Yang [143a], H.T. Yang [62], S. Yang [62], X. Yang [37],

X. Yang[14], Y. Yang[158], Y. Yang[62], W-M. Yao[18a], C.L. Yardley[151], J. Ye[14], S. Ye[30], X. Ye[62], Y. Yeh[97], I. Yeletskikh[39], B. Yeo[18b], M.R. Yexley[97], T.P. Yildirim[128], K. Yorita[173], C.J.S. Young[37], C. Young[148], I.N.L. Young[59], N.D. Young[125], Y. Yu[62], J. Yuan[14,113c,ak], M. Yuan[107], R. Yuan[143b], L. Yue[97], M. Zaazoua[62], B. Zabinski[87], I. Zahir[36a], A. Zaio[57b,57a], Z.K. Zak[87], T. Zakareishvili[168], S. Zambito[56], J.A. Zamora Saa[139d], J. Zang[158], R. Zanzottera[71a,71b], O. Zaplatilek[134], C. Zeitnitz[176], H. Zeng[14], D.T. Zenger Jr[27], O. Zenin[38], T. Ženiš[29a], S. Zenz[95], D. Zerwas[66], B. Zhang[172], D.F. Zhang[144], G. Zhang[14,ak], J. Zhang[142a], J. Zhang[6], L. Zhang[62], L. Zhang[113a], P. Zhang[14,113c], R. Zhang[113a], S. Zhang[90], Y. Zhang[141], Y. Zhang[97], Y. Zhang[62], Y. Zhang[113a], Z. Zhang[18a], Z. Zhang[142a], Z. Zhang[66], H. Zhao[141], T. Zhao[142a], Y. Zhao[35], Z. Zhao[62], Z. Zhao[62], A. Zhemchugov[39], J. Zheng[113a], K. Zheng[167], L. Zheng[142a], X. Zheng[62], Z. Zheng[148], D. Zhong[167], B. Zhou[107], B. Zhou[143b,143a], H. Zhou[7], N. Zhou[143a], Y. Zhou[15], Y. Zhou[113a], Y. Zhou[7], J. Zhu[107], X. Zhu[143b], Y. Zhu[143a], X. Zhuang[14], K. Zhukov[68], N.I. Zimine[39], J. Zinsser[63b], M. Ziolkowski[146], L. Živković[16], A. Zoccoli[24b,24a], K. Zoch[61], A. Zografos[37], T.G. Zorbas[144], O. Zormpa[46], L. Zwalinski[37].

[1]Department of Physics, University of Adelaide, Adelaide; Australia.
[2]Department of Physics, University of Alberta, Edmonton AB; Canada.
[3](a)Department of Physics, Ankara University, Ankara;(b)Division of Physics, TOBB University of Economics and Technology, Ankara; Türkiye.
[4]LAPP, Université Savoie Mont Blanc, CNRS/IN2P3, Annecy; France.
[5]APC, Université Paris Cité, CNRS/IN2P3, Paris; France.
[6]High Energy Physics Division, Argonne National Laboratory, Argonne IL; United States of America.
[7]Department of Physics, University of Arizona, Tucson AZ; United States of America.
[8]Department of Physics, University of Texas at Arlington, Arlington TX; United States of America.
[9]Physics Department, National and Kapodistrian University of Athens, Athens; Greece.
[10]Physics Department, National Technical University of Athens, Zografou; Greece.
[11]Department of Physics, University of Texas at Austin, Austin TX; United States of America.
[12]Institute of Physics, Azerbaijan Academy of Sciences, Baku; Azerbaijan.
[13]Institut de Física d'Altes Energies (IFAE), Barcelona Institute of Science and Technology, Barcelona; Spain.
[14]Institute of High Energy Physics, Chinese Academy of Sciences, Beijing; China.
[15]Physics Department, Tsinghua University, Beijing; China.
[16]Institute of Physics, University of Belgrade, Belgrade; Serbia.
[17]Department for Physics and Technology, University of Bergen, Bergen; Norway.
[18](a)Physics Division, Lawrence Berkeley National Laboratory, Berkeley CA;(b)University of California, Berkeley CA; United States of America.
[19]Institut für Physik, Humboldt Universität zu Berlin, Berlin; Germany.
[20]Albert Einstein Center for Fundamental Physics and Laboratory for High Energy Physics, University of Bern, Bern; Switzerland.
[21]School of Physics and Astronomy, University of Birmingham, Birmingham; United Kingdom.
[22](a)Department of Physics, Bogazici University, Istanbul;(b)Department of Physics Engineering, Gaziantep University, Gaziantep;(c)Department of Physics, Istanbul University, Istanbul; Türkiye.
[23](a)Facultad de Ciencias y Centro de Investigaciónes, Universidad Antonio Nariño, Bogotá;(b)Departamento de Física, Universidad Nacional de Colombia, Bogotá; Colombia.
[24](a)Dipartimento di Fisica e Astronomia A. Righi, Università di Bologna, Bologna;(b)INFN Sezione di Bologna; Italy.

[25]Physikalisches Institut, Universität Bonn, Bonn; Germany.
[26]Department of Physics, Boston University, Boston MA; United States of America.
[27]Department of Physics, Brandeis University, Waltham MA; United States of America.
[28][(a)]Transilvania University of Brasov, Brasov;[(b)]Horia Hulubei National Institute of Physics and Nuclear Engineering, Bucharest;[(c)]Department of Physics, Alexandru Ioan Cuza University of Iasi, Iasi;[(d)]National Institute for Research and Development of Isotopic and Molecular Technologies, Physics Department, Cluj-Napoca;[(e)]National University of Science and Technology Politechnica, Bucharest;[(f)]West University in Timisoara, Timisoara;[(g)]Faculty of Physics, University of Bucharest, Bucharest; Romania.
[29][(a)]Faculty of Mathematics, Physics and Informatics, Comenius University, Bratislava;[(b)]Department of Subnuclear Physics, Institute of Experimental Physics of the Slovak Academy of Sciences, Kosice; Slovak Republic.
[30]Physics Department, Brookhaven National Laboratory, Upton NY; United States of America.
[31]Universidad de Buenos Aires, Facultad de Ciencias Exactas y Naturales, Departamento de Física, y CONICET, Instituto de Física de Buenos Aires (IFIBA), Buenos Aires; Argentina.
[32]California State University, CA; United States of America.
[33]Cavendish Laboratory, University of Cambridge, Cambridge; United Kingdom.
[34][(a)]Department of Physics, University of Cape Town, Cape Town;[(b)]iThemba Labs, Western Cape;[(c)]Department of Mechanical Engineering Science, University of Johannesburg, Johannesburg;[(d)]National Institute of Physics, University of the Philippines Diliman (Philippines);[(e)]Department of Physics, Stellenbosch University, Matieland;[(f)]University of KwaZulu-Natal, School of Agriculture and Science, Mathematics, Westville;[(g)]University of South Africa, Department of Physics, Pretoria;[(h)]University of Pretoria, Department of Mechanical and Aeronautical Engineering, Pretoria;[(i)]University of Zululand, KwaDlangezwa;[(j)]School of Physics, University of the Witwatersrand, Johannesburg; South Africa.
[35]Department of Physics, Carleton University, Ottawa ON; Canada.
[36][(a)]Faculté des Sciences Ain Chock, Université Hassan II de Casablanca;[(b)]Faculté des Sciences, Université Ibn-Tofail, Kénitra;[(c)]Faculté des Sciences Semlalia, Université Cadi Ayyad, LPHEA-Marrakech;[(d)]LPMR, Faculté des Sciences, Université Mohamed Premier, Oujda;[(e)]Faculté des sciences, Université Mohammed V, Rabat;[(f)]Institute of Applied Physics, Mohammed VI Polytechnic University, Ben Guerir; Morocco.
[37]CERN, Geneva; Switzerland.
[38]Affiliated with an institute formerly covered by a cooperation agreement with CERN.
[39]Affiliated with an international laboratory covered by a cooperation agreement with CERN.
[40]Enrico Fermi Institute, University of Chicago, Chicago IL; United States of America.
[41]LPC, Université Clermont Auvergne, CNRS/IN2P3, Clermont-Ferrand; France.
[42]Nevis Laboratory, Columbia University, Irvington NY; United States of America.
[43]Niels Bohr Institute, University of Copenhagen, Copenhagen; Denmark.
[44][(a)]Dipartimento di Fisica, Università della Calabria, Rende;[(b)]INFN Gruppo Collegato di Cosenza, Laboratori Nazionali di Frascati; Italy.
[45]Physics Department, Southern Methodist University, Dallas TX; United States of America.
[46]National Centre for Scientific Research "Demokritos", Agia Paraskevi; Greece.
[47][(a)]Department of Physics, Stockholm University;[(b)]Oskar Klein Centre, Stockholm; Sweden.
[48]Deutsches Elektronen-Synchrotron DESY, Hamburg and Zeuthen; Germany.
[49]Fakultät Physik, Technische Universität Dortmund, Dortmund; Germany.
[50]Institut für Kern- und Teilchenphysik, Technische Universität Dresden, Dresden; Germany.
[51]Department of Physics, Duke University, Durham NC; United States of America.
[52]SUPA - School of Physics and Astronomy, University of Edinburgh, Edinburgh; United Kingdom.

[53]INFN e Laboratori Nazionali di Frascati, Frascati; Italy.
[54]Physikalisches Institut, Albert-Ludwigs-Universität Freiburg, Freiburg; Germany.
[55]II. Physikalisches Institut, Georg-August-Universität Göttingen, Göttingen; Germany.
[56]Département de Physique Nucléaire et Corpusculaire, Université de Genève, Genève; Switzerland.
[57(a)]Dipartimento di Fisica, Università di Genova, Genova;[(b)]INFN Sezione di Genova; Italy.
[58]II. Physikalisches Institut, Justus-Liebig-Universität Giessen, Giessen; Germany.
[59]SUPA - School of Physics and Astronomy, University of Glasgow, Glasgow; United Kingdom.
[60]LPSC, Université Grenoble Alpes, CNRS/IN2P3, Grenoble INP, Grenoble; France.
[61]Laboratory for Particle Physics and Cosmology, Harvard University, Cambridge MA; United States of America.
[62]Department of Modern Physics and State Key Laboratory of Particle Detection and Electronics, University of Science and Technology of China, Hefei; China.
[63(a)]Kirchhoff-Institut für Physik, Ruprecht-Karls-Universität Heidelberg, Heidelberg;[(b)]Physikalisches Institut, Ruprecht-Karls-Universität Heidelberg, Heidelberg; Germany.
[64(a)]Department of Physics, Chinese University of Hong Kong, Shatin, N.T., Hong Kong;[(b)]Department of Physics, University of Hong Kong, Hong Kong;[(c)]Department of Physics and Institute for Advanced Study, Hong Kong University of Science and Technology, Clear Water Bay, Kowloon, Hong Kong; China.
[65]Department of Physics, National Tsing Hua University, Hsinchu; Taiwan.
[66]IJCLab, Université Paris-Saclay, CNRS/IN2P3, 91405, Orsay; France.
[67]Centro Nacional de Microelectrónica (IMB-CNM-CSIC), Barcelona; Spain.
[68]Department of Physics, Indiana University, Bloomington IN; United States of America.
[69(a)]INFN Gruppo Collegato di Udine, Sezione di Trieste, Udine;[(b)]ICTP, Trieste;[(c)]Dipartimento Politecnico di Ingegneria e Architettura, Università di Udine, Udine; Italy.
[70(a)]INFN Sezione di Lecce;[(b)]Dipartimento di Matematica e Fisica, Università del Salento, Lecce; Italy.
[71(a)]INFN Sezione di Milano;[(b)]Dipartimento di Fisica, Università di Milano, Milano; Italy.
[72(a)]INFN Sezione di Napoli;[(b)]Dipartimento di Fisica, Università di Napoli, Napoli; Italy.
[73(a)]INFN Sezione di Pavia;[(b)]Dipartimento di Fisica, Università di Pavia, Pavia; Italy.
[74(a)]INFN Sezione di Pisa;[(b)]Dipartimento di Fisica E. Fermi, Università di Pisa, Pisa; Italy.
[75(a)]INFN Sezione di Roma;[(b)]Dipartimento di Fisica, Sapienza Università di Roma, Roma; Italy.
[76(a)]INFN Sezione di Roma Tor Vergata;[(b)]Dipartimento di Fisica, Università di Roma Tor Vergata, Roma; Italy.
[77(a)]INFN Sezione di Roma Tre;[(b)]Dipartimento di Matematica e Fisica, Università Roma Tre, Roma; Italy.
[78(a)]INFN-TIFPA;[(b)]Università degli Studi di Trento, Trento; Italy.
[79]Universität Innsbruck, Department of Astro and Particle Physics, Innsbruck; Austria.
[80]Department of Physics and Astronomy, Iowa State University, Ames IA; United States of America.
[81]Istinye University, Sariyer, Istanbul; Türkiye.
[82(a)]Departamento de Engenharia Elétrica, Universidade Federal de Juiz de Fora (UFJF), Juiz de Fora;[(b)]Universidade Federal do Rio De Janeiro COPPE/EE/IF, Rio de Janeiro;[(c)]Instituto de Física, Universidade de São Paulo, São Paulo;[(d)]Rio de Janeiro State University, Rio de Janeiro;[(e)]Federal University of Bahia, Bahia; Brazil.
[83]KEK, High Energy Accelerator Research Organization, Tsukuba; Japan.
[84(a)]Khalifa University of Science and Technology, Abu Dhabi;[(b)]University of Sharjah, Sharjah; United Arab Emirates.
[85]Graduate School of Science, Kobe University, Kobe; Japan.
[86(a)]AGH University of Krakow, Faculty of Physics and Applied Computer Science, Krakow;[(b)]Marian Smoluchowski Institute of Physics, Jagiellonian University, Krakow; Poland.

[87]Institute of Nuclear Physics Polish Academy of Sciences, Krakow; Poland.
[88]Faculty of Science, Kyoto University, Kyoto; Japan.
[89]Research Center for Advanced Particle Physics and Department of Physics, Kyushu University, Fukuoka ; Japan.
[90]L2IT, Université de Toulouse, CNRS/IN2P3, UPS, Toulouse; France.
[91]Instituto de Física La Plata, Universidad Nacional de La Plata and CONICET, La Plata; Argentina.
[92]Physics Department, Lancaster University, Lancaster; United Kingdom.
[93]Oliver Lodge Laboratory, University of Liverpool, Liverpool; United Kingdom.
[94]Department of Experimental Particle Physics, Jožef Stefan Institute and Department of Physics, University of Ljubljana, Ljubljana; Slovenia.
[95]Department of Physics and Astronomy, Queen Mary University of London, London; United Kingdom.
[96]Department of Physics, Royal Holloway University of London, Egham; United Kingdom.
[97]Department of Physics and Astronomy, University College London, London; United Kingdom.
[98]Louisiana Tech University, Ruston LA; United States of America.
[99]Fysiska institutionen, Lunds universitet, Lund; Sweden.
[100]Departamento de Física Teorica C-15 and CIAFF, Universidad Autónoma de Madrid, Madrid; Spain.
[101]Institut für Physik, Universität Mainz, Mainz; Germany.
[102]School of Physics and Astronomy, University of Manchester, Manchester; United Kingdom.
[103]CPPM, Aix-Marseille Université, CNRS/IN2P3, Marseille; France.
[104]Department of Physics, University of Massachusetts, Amherst MA; United States of America.
[105]Department of Physics, McGill University, Montreal QC; Canada.
[106]School of Physics, University of Melbourne, Victoria; Australia.
[107]Department of Physics, University of Michigan, Ann Arbor MI; United States of America.
[108]Department of Physics and Astronomy, Michigan State University, East Lansing MI; United States of America.
[109]Group of Particle Physics, University of Montreal, Montreal QC; Canada.
[110]Fakultät für Physik, Ludwig-Maximilians-Universität München, München; Germany.
[111]Max-Planck-Institut für Physik (Werner-Heisenberg-Institut), München; Germany.
[112]Graduate School of Science and Kobayashi-Maskawa Institute, Nagoya University, Nagoya; Japan.
[113][(a)]Department of Physics, Nanjing University, Nanjing;[(b)]School of Science, Shenzhen Campus of Sun Yat-sen University;[(c)]University of Chinese Academy of Science (UCAS), Beijing; China.
[114]Department of Physics and Astronomy, University of New Mexico, Albuquerque NM; United States of America.
[115]Institute for Mathematics, Astrophysics and Particle Physics, Radboud University/Nikhef, Nijmegen; Netherlands.
[116]Nikhef National Institute for Subatomic Physics and University of Amsterdam, Amsterdam; Netherlands.
[117]Department of Physics, Northern Illinois University, DeKalb IL; United States of America.
[118][(a)]New York University Abu Dhabi, Abu Dhabi;[(b)]United Arab Emirates University, Al Ain; United Arab Emirates.
[119]Department of Physics, New York University, New York NY; United States of America.
[120]Ochanomizu University, Otsuka, Bunkyo-ku, Tokyo; Japan.
[121]Ohio State University, Columbus OH; United States of America.
[122]Homer L. Dodge Department of Physics and Astronomy, University of Oklahoma, Norman OK; United States of America.
[123]Department of Physics, Oklahoma State University, Stillwater OK; United States of America.
[124]Palacký University, Joint Laboratory of Optics, Olomouc; Czech Republic.

[125]Institute for Fundamental Science, University of Oregon, Eugene, OR; United States of America.
[126]Graduate School of Science, University of Osaka, Osaka; Japan.
[127]Department of Physics, University of Oslo, Oslo; Norway.
[128]Department of Physics, Oxford University, Oxford; United Kingdom.
[129]LPNHE, Sorbonne Université, Université Paris Cité, CNRS/IN2P3, Paris; France.
[130]Department of Physics, University of Pennsylvania, Philadelphia PA; United States of America.
[131]Department of Physics and Astronomy, University of Pittsburgh, Pittsburgh PA; United States of America.
[132(a)]Laboratório de Instrumentação e Física Experimental de Partículas - LIP, Lisboa;[(b)]Departamento de Física, Faculdade de Ciências, Universidade de Lisboa, Lisboa;[(c)]Departamento de Física, Universidade de Coimbra, Coimbra;[(d)]Centro de Física Nuclear da Universidade de Lisboa, Lisboa;[(e)]Departamento de Física, Escola de Ciências, Universidade do Minho, Braga;[(f)]Departamento de Física Teórica y del Cosmos, Universidad de Granada, Granada (Spain);[(g)]Departamento de Física, Instituto Superior Técnico, Universidade de Lisboa, Lisboa; Portugal.
[133]Institute of Physics of the Czech Academy of Sciences, Prague; Czech Republic.
[134]Czech Technical University in Prague, Prague; Czech Republic.
[135]Charles University, Faculty of Mathematics and Physics, Prague; Czech Republic.
[136]Particle Physics Department, Rutherford Appleton Laboratory, Didcot; United Kingdom.
[137]IRFU, CEA, Université Paris-Saclay, Gif-sur-Yvette; France.
[138]Santa Cruz Institute for Particle Physics, University of California Santa Cruz, Santa Cruz CA; United States of America.
[139(a)]Departamento de Física, Pontificia Universidad Católica de Chile, Santiago;[(b)]Millennium Institute for Subatomic physics at high energy frontier (SAPHIR), Santiago;[(c)]Instituto de Investigación Multidisciplinario en Ciencia y Tecnología, y Departamento de Física, Universidad de La Serena;[(d)]Universidad Andres Bello, Department of Physics, Santiago;[(e)]Universidad San Sebastian, Recoleta;[(f)]Instituto de Alta Investigación, Universidad de Tarapacá, Arica;[(g)]Departamento de Física, Universidad Técnica Federico Santa María, Valparaíso; Chile.
[140]Department of Physics, Institute of Science, Tokyo; Japan.
[141]Department of Physics, University of Washington, Seattle WA; United States of America.
[142(a)]Institute of Frontier and Interdisciplinary Science and Key Laboratory of Particle Physics and Particle Irradiation (MOE), Shandong University, Qingdao;[(b)]School of Physics, Zhengzhou University; China.
[143(a)]State Key Laboratory of Dark Matter Physics, School of Physics and Astronomy, Shanghai Jiao Tong University, Key Laboratory for Particle Astrophysics and Cosmology (MOE), SKLPPC, Shanghai;[(b)]State Key Laboratory of Dark Matter Physics, Tsung-Dao Lee Institute, Shanghai Jiao Tong University, Shanghai; China.
[144]Department of Physics and Astronomy, University of Sheffield, Sheffield; United Kingdom.
[145]Department of Physics, Shinshu University, Nagano; Japan.
[146]Department Physik, Universität Siegen, Siegen; Germany.
[147]Department of Physics, Simon Fraser University, Burnaby BC; Canada.
[148]SLAC National Accelerator Laboratory, Stanford CA; United States of America.
[149]Department of Physics, Royal Institute of Technology, Stockholm; Sweden.
[150]Departments of Physics and Astronomy, Stony Brook University, Stony Brook NY; United States of America.
[151]Department of Physics and Astronomy, University of Sussex, Brighton; United Kingdom.
[152]School of Physics, University of Sydney, Sydney; Australia.
[153]Institute of Physics, Academia Sinica, Taipei; Taiwan.
[154(a)]E. Andronikashvili Institute of Physics, Iv. Javakhishvili Tbilisi State University, Tbilisi;[(b)]High

Energy Physics Institute, Tbilisi State University, Tbilisi;[(c)]University of Georgia, Tbilisi; Georgia.
[155]Department of Physics, Technion, Israel Institute of Technology, Haifa; Israel.
[156]Raymond and Beverly Sackler School of Physics and Astronomy, Tel Aviv University, Tel Aviv; Israel.
[157]Department of Physics, Aristotle University of Thessaloniki, Thessaloniki; Greece.
[158]International Center for Elementary Particle Physics and Department of Physics, University of Tokyo, Tokyo; Japan.
[159]Graduate School of Science and Technology, Tokyo Metropolitan University, Tokyo; Japan.
[160]Department of Physics, University of Toronto, Toronto ON; Canada.
[161(a)]TRIUMF, Vancouver BC;[(b)]Department of Physics and Astronomy, York University, Toronto ON; Canada.
[162]Division of Physics and Tomonaga Center for the History of the Universe, Faculty of Pure and Applied Sciences, University of Tsukuba, Tsukuba; Japan.
[163]Department of Physics and Astronomy, Tufts University, Medford MA; United States of America.
[164]Department of Physics and Astronomy, University of California Irvine, Irvine CA; United States of America.
[165]University of West Attica, Athens; Greece.
[166]Department of Physics and Astronomy, University of Uppsala, Uppsala; Sweden.
[167]Department of Physics, University of Illinois, Urbana IL; United States of America.
[168]Instituto de Física Corpuscular (IFIC), Centro Mixto Universidad de Valencia - CSIC, Valencia; Spain.
[169]Department of Physics, University of British Columbia, Vancouver BC; Canada.
[170]Department of Physics and Astronomy, University of Victoria, Victoria BC; Canada.
[171]Fakultät für Physik und Astronomie, Julius-Maximilians-Universität Würzburg, Würzburg; Germany.
[172]Department of Physics, University of Warwick, Coventry; United Kingdom.
[173]Waseda University, Tokyo; Japan.
[174]Department of Particle Physics and Astrophysics, Weizmann Institute of Science, Rehovot; Israel.
[175]Department of Physics, University of Wisconsin, Madison WI; United States of America.
[176]Fakultät für Mathematik und Naturwissenschaften, Fachgruppe Physik, Bergische Universität Wuppertal, Wuppertal; Germany.
[177]Department of Physics, Yale University, New Haven CT; United States of America.
[178]Yerevan Physics Institute, Yerevan; Armenia.
[a] Also at Affiliated with an institute formerly covered by a cooperation agreement with CERN.
[b] Also at An-Najah National University, Nablus; Palestine.
[c] Also at Borough of Manhattan Community College, City University of New York, New York NY; United States of America.
[d] Also at Center for Interdisciplinary Research and Innovation (CIRI-AUTH), Thessaloniki; Greece.
[e] Also at Centre of Physics of the Universities of Minho and Porto (CF-UM-UP); Portugal.
[f] Also at CERN, Geneva; Switzerland.
[g] Also at Département de Physique Nucléaire et Corpusculaire, Université de Genève, Genève; Switzerland.
[h] Also at Departament de Fisica de la Universitat Autonoma de Barcelona, Barcelona; Spain.
[i] Also at Department of Financial and Management Engineering, University of the Aegean, Chios; Greece.
[j] Also at Department of Modern Physics and State Key Laboratory of Particle Detection and Electronics, University of Science and Technology of China, Hefei; China.
[k] Also at Department of Physics, Ben Gurion University of the Negev, Beer Sheva; Israel.
[l] Also at Department of Physics, Bolu Abant Izzet Baysal University, Bolu; Türkiye.
[m] Also at Department of Physics, King's College London, London; United Kingdom.
[n] Also at Department of Physics, Stellenbosch University; South Africa.

[o] Also at Department of Physics, University of Fribourg, Fribourg; Switzerland.
[p] Also at Department of Physics, University of Thessaly; Greece.
[q] Also at Department of Physics, Westmont College, Santa Barbara; United States of America.
[r] Also at Faculty of Physics, Sofia University, 'St. Kliment Ohridski', Sofia; Bulgaria.
[s] Also at Faculty of Physics, University of Bucharest; Romania.
[t] Also at Hellenic Open University, Patras; Greece.
[u] Also at Henan University; China.
[v] Also at Imam Mohammad Ibn Saud Islamic University; Saudi Arabia.
[w] Also at Indian Institute of Technology (IIT), Jodhpur; India.
[x] Also at Institucio Catalana de Recerca i Estudis Avancats, ICREA, Barcelona; Spain.
[y] Also at Institut für Experimentalphysik, Universität Hamburg, Hamburg; Germany.
[z] Also at Institute for Nuclear Research and Nuclear Energy (INRNE) of the Bulgarian Academy of Sciences, Sofia; Bulgaria.
[aa] Also at Institute of Applied Physics, Mohammed VI Polytechnic University, Ben Guerir; Morocco.
[ab] Also at Institute of Particle Physics (IPP); Canada.
[ac] Also at Institute of Physics and Technology, Mongolian Academy of Sciences, Ulaanbaatar; Mongolia.
[ad] Also at Institute of Physics, Azerbaijan Academy of Sciences, Baku; Azerbaijan.
[ae] Also at Institute of Theoretical Physics, Ilia State University, Tbilisi; Georgia.
[af] Also at Millennium Institute for Subatomic physics at high energy frontier (SAPHIR), Santiago; Chile.
[ag] Also at National Institute of Physics, University of the Philippines Diliman (Philippines); Philippines.
[ah] Also at The Collaborative Innovation Center of Quantum Matter (CICQM), Beijing; China.
[ai] Also at TRIUMF, Vancouver BC; Canada.
[aj] Also at Università di Napoli Parthenope, Napoli; Italy.
[ak] Also at University of Chinese Academy of Sciences (UCAS), Beijing; China.
[al] Also at University of Colorado Boulder, Department of Physics, Colorado; United States of America.
[am] Also at University of Siena; Italy.
[an] Also at Washington College, Chestertown, MD; United States of America.
[ao] Also at Yeditepe University, Physics Department, Istanbul; Türkiye.
[*] Deceased